

Material Recovery from Dutch Wind Energy

A dynamic material flow analysis on Dutch wind turbines towards 2050 including recycling approaches for recovery of key materials.

MSc thesis Industrial Ecology

B.M. Roelofs



Material Recovery from Dutch Wind Energy

A dynamic material flow analysis of Dutch wind turbines towards 2050 including recycling approaches for recovery of key materials.

by

B.M. (Bas) Roelofs

Thesis MSc Industrial Ecology

Leiden, August 2020

in partial fulfilment of the requirements for the degree of

Master of Science
in Industrial Ecology

at Delft University of Technology and Leiden University

Student number TU Delft: 4291638

Student number Leiden: s2328097

Graduation committee: dr. E. van der Voet
dr. Y. Yang



Universiteit
Leiden

 **TU**Delft

TABLE OF CONTENTS

Abbreviations.....	ii
Glossary.....	iii
Preface.....	iv
Executive summary.....	v
1 Introduction.....	2
1.1 Background.....	2
1.2 Objectives and research questions.....	3
1.3 Report structure.....	4
2 Methods and Data.....	5
2.1 Dynamic Material Flow Analysis.....	5
2.2 Modelling structure.....	6
2.3 Data requirements.....	7
2.4 Environmental and economic context.....	8
3 Results.....	10
3.1 Stock analysis.....	10
3.2 Material compositions.....	15
3.3 Future developments.....	20
3.4 Inflows, stocks and outflows.....	25
3.5 Material recovery.....	36
4 Discussion.....	49
4.1 Reflection on methodology.....	49
4.2 Reflection on Results.....	50
4.3 Broader context.....	51
5 Conclusions & recommendations.....	52
5.1 Recommendations.....	55
References.....	58
Appendices.....	66
A. Stock analysis.....	1
B. Material composition.....	4
C. Future installed capacity.....	30
D. Sensitivity checks.....	37
E. Stacked results.....	41
F. Additional results.....	44
G. Python model.....	48
H. Background material recovery.....	49

ABBREVIATIONS

(d)MFA	-	(dynamic) Material Flow Analysis
a	-	annum, yearly
AG	-	Asynchronous generator
CFRP	-	Carbon fibre reinforced plastic/polymer
DD	-	Direct Drive
DFIG	-	Doubly Fed Induction Generator
DSM	-	Dynamic Stock Model (Python module)
EESG	-	Electrically Excited Synchronous Generator
EOL	-	End Of Life
GFRP	-	Glass fibre reinforced plastic
HTS	-	High Temperature Superconductor
LCA	-	Life Cycle Assessment
LCI	-	Life Cycle Inventory
PM	-	Permanent Magnet
PMSG	-	Permanent Magnet Synchronous Generator
REE	-	Rare Earth Element
SCIG	-	Squirrel Cage Induction Generator
SG	-	Siemens Gamesa
SG-iron	-	Spheroidal Graphite cast iron
t	-	Tonne (metric), prefixes k (kilo), M (Mega)
TRL	-	Technology Readiness Level
W	-	Watt, prefixes k (kilo), M (mega), G (giga)
WT	-	Wind Turbine (abbreviation in figures)

GLOSSARY

Circularity	- Responsible resource use through multiple use lifecycles of products and materials.
Collection rate	- Efficiency of material collection
Decommissioning	- Removing from active status, removing from stock.
Nacelle	- Top part of the wind turbine that houses the drive train and yaw mechanism.
Pitch	- Turning of the blades around their axes to adjust aerodynamics, influencing rotor speed.
Processing rate	- Efficiency of material liberation and separation processes
Recovery rate	- Yield of material after collection, separation and recycling
Rotor	- Assembly containing the wind turbine blades, hub, nose cone and pitch mechanisms. Or in the context of drivetrains, rotating part of electric motors and generators.
Yaw	- Rotation of the nacelle to move the rotor into the wind.

PREFACE

This research, in context of my master thesis, is the result of an inspiring time as a student Industrial Ecology and a collaborative effort with TNO - wind energy as research intern. Therefore, I owe a lot of people my gratitude as they inspired and supported me.

In particular, I am very thankful for all the help and feedback I received from my academic supervisors, Ester van der Voet, Yongxiang Yang and Janneke van Oorschot and TNO supervisors Novita Saraswati and Iana Bakhmet. The regular meetings and your expertise were much appreciated.

Secondly, to all the experts that have taken part in discussions and were available for questions at TNO, CML future resource hub, TU Delft, Equinor, LM, Jumbo and Lagerwey.

Finally, my friends and family for their support and distraction through some unusual times.

Bedankt!

Bas

The transition to a renewable electricity system requires more intensive material use, causing problem shifting in environmental impacts. To conserve resources for the future and mitigate environmental impact, circular economy principles are needed. This entails more responsible resource use through multiple use lifecycles of products and materials. This study analyses material flows in Dutch wind energy towards 2050 to identify the potential for material recovery. This reveals material demand, stock, secondary material supply and required recycling infrastructure within environmental and economic context.

Current stock of wind turbines in the Netherlands is composed of a wide variety of turbines ranging from kilowatt up to multi-megawatt scale. Trends for increasing rated capacity and hub heights can be observed. Drivetrain technologies vary and are mostly specific to manufacturers along with other characterizing technologies. The current Dutch market is dominated by Enercon, Vestas and Siemens Gamesa. Current onshore installed capacity is roughly 6 GW. Offshore installed capacity is roughly 1 GW with strong expected growth. Analysis of wind turbine decommissioning, which is steadily increasing after 2010, reveals a mean lifespan of 18 years.

Material compositions of wind turbines are determined, leading to estimations on component mass and material shares. Linear and non-linear approximations are used based mainly on rated capacity and hub height. Future installed capacity scenarios are generated for a minimum and maximum expected development based on different policy scenarios and a prognosis based on current policy. Technological development is considered based on increasing rated capacity, increasing hub height, drivetrain technology and blade material compositions. Combined, the material compositions, current stock and future installed capacity result in inflow, stock and outflow of materials in Dutch wind energy. This leads to two general observations for the development of material flows in Dutch wind energy:

- Inflows or demand for materials is increasing rapidly due to strong expected growth in the near future (2023), additional inflows are required after 2030 for stock maintenance.
- Outflows fluctuate, partly due to an early peak in onshore decommissioning and late peak in offshore decommissioning caused by a more mature stock of onshore wind turbines and currently developing stock of offshore wind turbines.

The outflow of scrap materials is used to determine secondary materials through various recycling routes. Conventional recycling routes are used for structural steel, copper and aluminium, leading to high-quality secondary materials with low losses. Clean aggregate recycling is considered for concrete, which yields secondary cement, roadbed material and aggregate that can be used in new concrete. Alloy steel and iron can be recycled through primary or secondary steelmaking, but this would cause non-functional recycling of alloying elements. Selective recycling can provide functional recycling of these valuable and critical alloying elements. Critical rare earth elements (REE) in permanent magnets can also be recovered. Permanent magnets recycling is currently at pilot scale and can be distinguished by magnet-to-magnet or magnet-to-REE recycling. Composite recycling is considered on various levels of material recovery. First, repurposing of blades can provide sheet and beam segments for construction with low processing efforts. Alternatively cement co-processing can be used to recover energy and cement clinker, which can be used to replace cement production. Mechanical recycling can provide a fibre rich powder that can be used as reinforcement in thermoplastics. Fibre recovery through pyrolysis can yield secondary fibres with lower mechanical properties, that can be used to make new composites.

Through collection-, processing- and recycling rates under current practice the following observations can be made.

- For steel, iron, aluminium and copper minor processing losses occur as materials oxidize or get lost to slag.
- Due to partial removal of monopiles, a hibernating stock is expected for structural steel that increases towards 0.5 Mt in 2050.
- Current steel and iron recycling results in dilution and therefore loss of function of valuable and critical alloying elements.

These observations lead to the following policy-related areas of inquiry:

- Full monopile removal is under development, but challenged by cost-effectiveness. Regulation and economic incentive could stimulate full monopile removal and avoid large hibernating stocks.
- Selective recycling of iron and steel alloys allows functional recovery of valuable and critical alloying elements.

Composite waste management in wind energy is a major challenge as closed-loop recycling of composites is not feasible. The cascading effect of material quality results in low-value materials, with varying potential demand. Key findings and implications for composite recycling are presented here:

- Repurposing of blade segments requires minimal processing and could be implemented at present, provided that there is enough demand for composite sheet and beam segments.
- Cement co-processing uses existing cement production infrastructure and could be implemented at present, with ample demand for cement clinker.
- Dutch wind energy could exclusively provide sufficient composite scrap material to run industrial-scale mechanical grinding after 2030 and pyrolysis facilities after 2040.

These findings and implications on composite scrap lead to the following policy-related areas of inquiry.

- International collaboration can be realized with several neighbouring countries. Denmark has the oldest stock of wind turbines and Germany the largest, making them interesting sources or destinations for scrap composites material. Furthermore, opportunities for a North Sea regional recycling facility provide advantages in logistics. This region will become an increasingly important source of scrap composite material in the future due to UK, Dutch, Belgian, German and Danish offshore developments.
- Cross-sector collaborations with, most importantly, the aviation sector could increase scrap material availability. However, this will cause a less homogenous scrap source and hence likely lower quality secondary materials.
- Additional markets for various recycled materials (e.g. sheet material, thermoplastics reinforced by fibrous fraction, recovered fibres) need to be identified as full closed-loop or recycling within wind turbines is currently not feasible.

Technology related areas for further research include:

- Effect on secondary material quality of combined recycling of wind turbine blades and composites in aviation.
- Recycling rates and minimum (break-even) throughput for composite recycling facilities for all recycling routes.

Critical materials include vanadium in gear steel alloys, magnesium in cast iron and rare earth elements neodymium, dysprosium, praseodymium and terbium in permanent magnets. Potentially yttrium will be used in new drivetrain innovations as well. These critical materials are subject to high economic importance and supply risk. Secondary supply through recycling can mitigate this criticality. Key findings and implications are listed below:

- Vanadium in gearbox steel and magnesium in cast iron can be functionally recycled by selective collection within existing recycling infrastructure for specialty steels.
- It is estimated that with maximum recycling efforts, secondary supply of critical materials can meet up to ~15% of REE, ~30% of V and ~25% of Mg demand by 2050.
- Dutch wind energy will not provide sufficient scrap magnet material for an industrial size recycling facility dedicated to magnet or REE recovery before 2050.

This leads to the following policy related areas of inquiry:

- Cross-sector collaboration with, most importantly, the automotive sector (EV) could increase scrap material availability. However, this will cause a less homogenous scrap source and hence likely lower quality secondary materials.
- International collaboration is most advisable on a European Union scale as REE criticality requires increased supply from within the EU to mitigate its criticality through secondary supply.

Technology related areas for further research include:

- Recycling rates and minimum throughput for novel recycling technologies.
- Effect on secondary material quality of combined recycling of permanent magnets from EV and wind turbines.

The results of this study rely on several key assumptions, leading to varying degrees of uncertainty. Naturally, the future developments in installed capacity and technology are uncertain and could lead to strong variations in results. Several other assumptions are made in this study. To summarize, key assumptions include:

- ♦ The mean lifespan of wind turbines is 18 years, increasing towards maximum of 25 years as technology matures.
- ♦ Offshore wind turbines have a longer intended lifespan than onshore due to costly installation and removal.
- ♦ Horizontal axis wind turbines are used until 2050
- ♦ Material compositions as determined in this study are correct estimations and remain true until 2050.
- ♦ Exclusively monopiles are used for offshore foundations due to consistent North Sea water depth.
- ♦ Minimum (break-even) throughputs for mechanical recycling and pyrolysis are 4 kt/a and 9 kt/a respectively.
- ♦ Minimum throughputs for permanent magnet recycling are in the order of magnitude of several kt/a.

By determining the potential for material recovery from Dutch wind energy, a timeline is created for potential implementation of domestic recycling and secondary material availability. This is a first step towards circularity goals in 2050 and is intended to provide a sense of scale and timing for material demand, secondary supply and required recycling infrastructure for Dutch wind energy.

Glossary

To construct a basic understanding of wind turbine components, a visual glossary is provided here.

Source: OneEnergy (2020)

BLADE

Long composite structures that convert incoming wind to a rotating motion.

BLADES + HUB = ROTOR

Assembly of blades and hub that converts the wind energy to a rotating motion

NACELLE

Top section of a wind turbine that houses drivetrain components

HUB

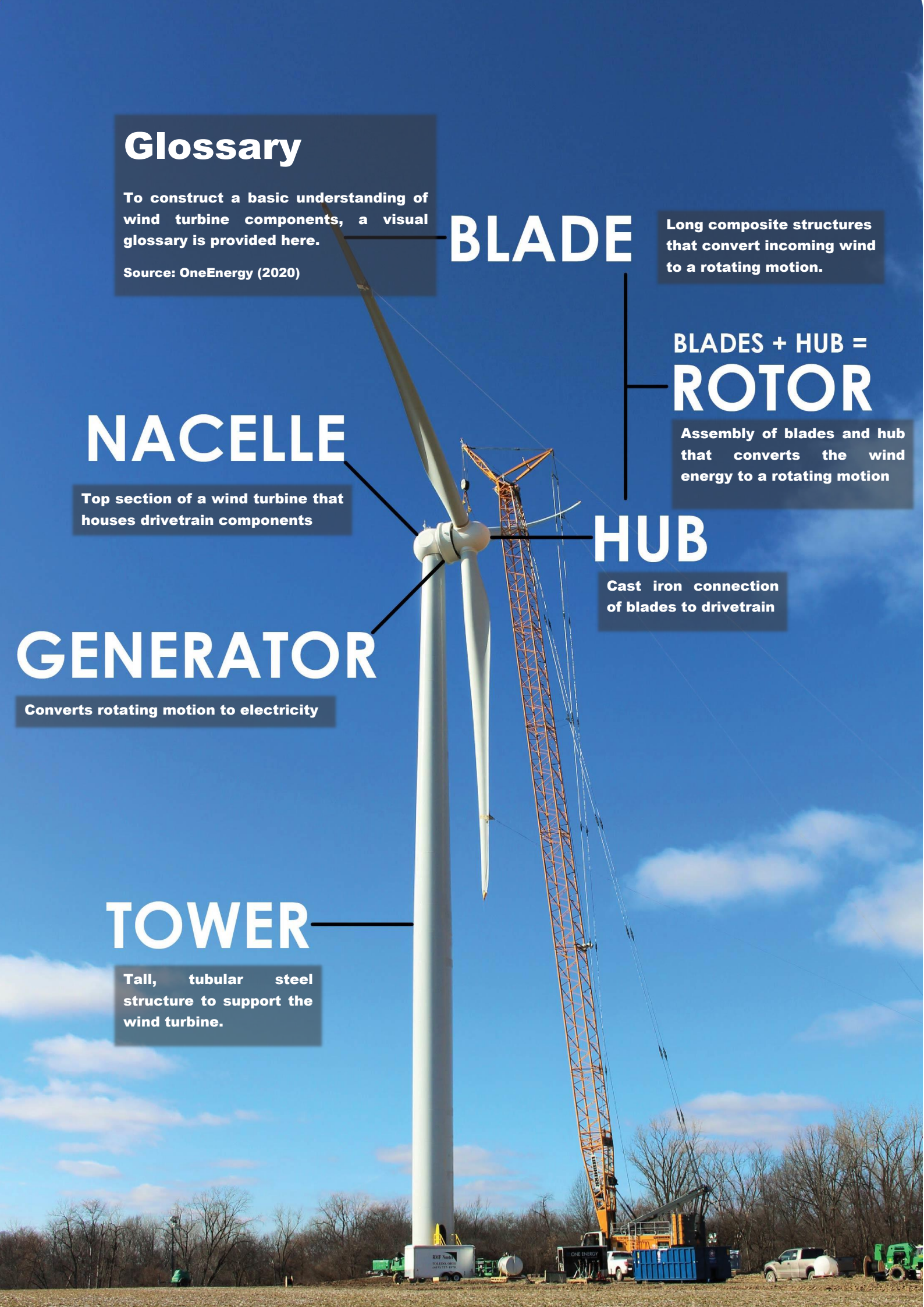
Cast iron connection of blades to drivetrain

GENERATOR

Converts rotating motion to electricity

TOWER

Tall, tubular steel structure to support the wind turbine.



1 INTRODUCTION

1.1 BACKGROUND

In the transition to a more sustainable society, the electricity system is required to shift from fossil-based to low-carbon and renewable energy to mitigate global warming (Teske, 2019; Klimaatakkoord, 2019). However, renewable energy generation requires more materials, causing problem shifting to other environmental impacts (Hertwich et al., 2015; Kleijn et al., 2011; World Bank, 2017). To conserve resources for the future and mitigate environmental impact from renewable electricity generation and many other societal activities, circular economy principles are needed (MacArthur, 2013; Peck et al., 2019; Rijksoverheid, 2016; PBL, 2019). This entails more responsible resource use through multiple use lifecycles of products and materials.

For the implementation of a circular economy, prospects of available materials are needed. Van Oorschot et al. (2020) examined the Dutch energy system and identified what aspects should be added to the stock inventory and roughly estimated potential future outflows according to a single scenario. Given the various available technologies in wind energy, issues concerning critical materials¹ (Blagoeva et al., 2016) and end-of-life management of blade waste (Liu & Barlow, 2017), various scenarios can be imagined that could strongly influence future material availability. Van Oorschot et al. mention that to further secondary production, more specific material compositions (e.g. specific alloys used, trace elements) and the material composition on component level are required.

In general, studies on material flows focus on global bulk materials or critical materials². These studies aim to identify the amount of material needed for- or disposed of due to specific societal developments. Focus in these studies lies on supply issues for critical raw materials or waste issues, resulting in flows of scrap or waste material. While that latter is interesting from a recycling perspective, Reuter et al. (2019) argue that a product centric approach is needed to move towards improved recycling rates. The product centric approach to recycling sees complex products as inputs, opposing the conventional material centric approach where the focus is on recovering a single material. The reasoning behind this approach is that modern products are complex in their design, meaning they contain many different materials, joined or mixed in various intricate ways. A recycling approach that takes this complexity into account can deal with this in a more appropriate than a recycling approach focussed on individual materials. Furthermore, a product centric approach includes design for recycling where the aim is to reduce product complexity. Having scrap materials available for recycling is only one aspect of recovering materials. The essential aspect of recycling technology in material recovery is often not discussed in much detail in material flow analysis studies. The recycling route determines to large extent the amount and quality of secondary materials. Collection, processing and refining of scrap materials in the end provide the secondary materials. Recycling of blades and magnets remain the most debated issues in literature on materials and wind energy³, due to composite waste management and critical rare earth elements (REE). Some studies focussed on wind turbine decommissioning exist⁴ that touch upon the recycling aspect, but not specifically apply this to material flows. In these studies, the economic aspect of recycling is also highlighted.

¹ Materials with high economic importance and supply risk.

² e.g. Månberger & Stenqvist (2018), Deetman et al. (2018), Zimmerman et al. (2013a), Cao et al. (2019)

³ e.g. Skelton (2017); Liu & Barlow (2017), Rademaker et al. (2013)

⁴ e.g. Topham et al. (2019), Topham & McMillan, (2017)

1.2 OBJECTIVES AND RESEARCH QUESTIONS

This research aims to identify the potential for material recovery from Dutch wind energy towards 2050. This includes the current stock of materials in wind turbines, various scenarios of future stock developments according to technological developments and material recovery through recycling. On a practical level this research serves as explorative case study for necessary recycling infrastructure development. In an academic context it can be used as framework for product centric dynamic material flow analysis for material recovery. Reuse and repair/refurbishment of components are recognized as an important aspect of the circular economy but are covered to a limited extent.

To allow for an increased level of detail on material compositions and end-of-life options, a relatively small scope is considered. The Netherlands is an interesting case study as it has a maturing stock of onshore wind energy and a strong expected growth in offshore wind energy. The scope of a national economy also increases the applicability of the results for local actors that are needed to implement the ideals set out by circular economy targets for 2050 (Rijksoverheid, 2016). A detailed description of material compositions requires extensive research. This includes rough data from similar studies on a lower level of detail, but also bottom-up engineering data from design studies and manufacturer data. Meanwhile remaining the focus on material recovery by considering the materials that will be the input for recycling processes and its constituents (e.g. blade material instead of glass fibre). Therefore, the geographical scope for this project is the Netherlands and its territorial North Sea waters. The temporal scope includes the 1980's when the first wind turbines were implemented up to 2050 as this would include the end of life for new innovations and wind turbine designs. Additionally, this fits the Dutch government ambition to be circular in 2050. The technological scope includes various existing and emerging technologies as this strongly affects specific material flows. The boundary of the wind turbine system is set at the physical boundary of the wind turbine, meaning that transmission cables and transformer stations are excluded from the analysis.

The main objective of this research is to gain insight in what materials can be recovered from decommissioned wind turbines. This leads to the following research question:

What materials can be recovered from decommissioned wind turbines in the Netherlands until 2050?

To answer the research question, six sub-questions are formulated. First, it is necessary to know what types of wind turbines are installed in the Netherlands. This results in an understanding of involved manufacturers, rated capacity and lifespans of currently installed wind turbines.

1. What is the current stock of wind turbines in the Netherlands?

Next, the material composition of the various wind turbine technologies needs to be described. Each manufacturer produces wind turbines with different material compositions due to varying designs and technologies that are used. Estimations in literature are supplemented to increase accuracy and new estimations for future technologies are created.

2. What is the material composition of various wind turbines currently in use and under development?

The goals of implementing more than triple the current amount of wind power can be achieved in many ways. These could be influenced by supply chain disruptions (Blagoeva et al., 2016), share of onshore versus offshore or dominant technologies (e.g. permanent magnet or induction generators). Therefore, multiple scenarios are needed on how installed capacity and technological trends develop in the Dutch wind energy sector.

3. *What would be plausible and relevant scenarios for implementation of goals for Dutch wind energy and the resulting inflows of materials in wind turbines towards 2050?*

These results contribute to the next step, where estimations of material outflows from decommissioned wind turbines is estimated. This step requires dynamic modelling, which will be discussed further in chapter 2: Methods and Data.

4. *What is the material requirement (inflow) and what materials will become available (outflow) from stock until 2050?*

This concludes the analysis of scrap material outflow. Further analysis determines the recovered or secondary materials available in society after recycling. For each material, recycling options are identified. These include established processes, but also new innovations in recycling technology. The best available technologies are considered here, economic aspects are covered to limited extent.

5. *What opportunities and challenges exist for recycling the bulk, valuable and critical materials from decommissioned wind turbines?*

The combined results provide an estimation on materials that will be available on the market. This could lead to oversupply of downgraded materials and/or alleviation of material criticality.

6. *How much secondary material can be recovered from decommissioned wind turbines and when is this expected to be available on the market?*

With goals to increase resource efficiency and reduce environmental impacts, environmental impact assessment on various steps (technological development, material demand and recycling approaches) are relevant aspects. However, full life cycle assessments (LCA) on each of these aspects is too extensive for the time and resources available for this research. Environmental impacts are broadly assessed using available LCA studies and data on material environmental impact. This includes mostly impacts from resource use and related emissions. Further impacts of wind turbines on the environment during its operational life (Lindeboom et al., 2011; Slavik et al., 2019) are neglected. Furthermore, additional attention is paid to critical and cross-cutting (key) metals. These materials are of high economic importance and in the case of critical metals are associated with supply risk. Cross-cutting means the materials are used in a wide variety of technologies essential for low-carbon energy generation and high demand and competition for these resources (Sheldon, 2020). These aspects provide some indication of impacts from material demand and waste and are used to provide context for recommendations on further, more specific, research.

1.3 REPORT STRUCTURE

This report is structured as follows. First, in chapter 2, Methods and Data are discussed to introduce dynamic material flow analysis, outline the modelling structure, outline data requirements and introduce the environmental and economic context. Next, in chapter 3, Results from research steps are discussed including an analysis of current Dutch wind turbine stock, material compositions, future development in Dutch wind energy, the inflows, outflows and stocks of materials as result of the dynamic material flow analysis and a description of material recovery routes and resulting secondary materials. The results are further discussed in chapter 4, Discussion, where a reflection on method, results and the broader context is given. Finally, in chapter 5, conclusions and recommendations are discussed. The appendices supplement the report with additional information and details. The Python model created for this study is also included here. Additional background- and modelling data is included in *Input_data.xlsx* and *Mat_comp_data.xlsx*.

2 METHODS AND DATA

The research is divided in three stages, namely *stock analysis* (determining what materials are used in wind turbines in the Netherlands), *dynamic material flow analysis* (assessing in- and outflows of materials according to various scenarios) and *recycling approach* (determining best suited recycling approaches and extending the model accordingly). First, the current stock of wind turbines in the Netherlands is analysed using installation and decommissioning data. Data for this step is retrieved from online databases, government plans and literature and can be described as data analysis. This results in installed capacity and number of turbines per manufacturer, number of turbines per rated capacity, lifespan, location of wind turbines, historic installation and decommissioning (inflows and outflows) and current stock. Once clear what type of turbines are currently installed, material compositions are used to translate the installation (inflows) and decommissioning (outflows) to material flows. This involves desk research, using academic- and grey literature and expert validation. Categorisation of turbines is based on literature and insights from analysing historic data. Next, scenarios are created for technology implementation. This involves a prognosis, minimum and maximum for installed capacity and technological developments that can influence material compositions. Desk study is used to determine future scenarios for installed capacity, which are validated by expert opinion.

With these inputs a dynamic stock model can be created, resulting in stocks and outflows for the various materials under multiple scenarios. The resulting outflows of scrap material lead to potential secondary materials. In the recycling approach, the means with which these secondary materials can be recovered are identified and analysed. Multiple established and conceptual recycling routes are considered for steel/iron, composites, permanent magnets, copper, aluminium and concrete. This analysis is then used to determine potential recovery rates for the various materials, leading to an extended model that includes recycling approaches.

Throughout, environmental and economic aspects are discussed for various results to quantify environmental impact for various scenarios, potential reduction through recycling, potential trade-offs and economic feasibility of dedicated recycling infrastructure.

The following subsections describe dynamic material flow analysis as a methodology, the model computational structure, data requirements for the dynamic stock model and the application of environmental and economic context in this study.

2.1 DYNAMIC MATERIAL FLOW ANALYSIS

Material Flow Analysis (MFA) is a core Industrial Ecology tool to quantify the metabolism of modern society. It is commonly based on three methodological steps, including goal and systems definition, quantification and interpretation of results. When time is included as a modelling variable the system is considered dynamic and hence called a dynamic material flow analysis (dMFA), which can be used to determine stocks and development of stocks and flows over time (Graedel, 2019). The principal goal of this dMFA is to calculate material outflows and consequential secondary materials using historic- and projected inflows in the context of circularity. The results also show stock dynamics and demand for materials (inflows), which provides additional insights. The following section further elaborates on the system definition. The quantification involves the sections on inflow, stock, outflow and material recovery sections in chapter 3: Results. The interpretation step results in placing these flows in context with recycling approaches, discussing results and the conclusion.

The system is quantified using a dynamic stock model. Here, inflow of materials, in this case installation of wind turbines containing various materials, accumulate in society and form the societal

stock. These wind turbines, or alternatively the materials in the wind turbines, remain in the societal stock for the duration of the lifespan of the wind turbine. When these materials leave the stock - the wind turbine is decommissioned - it becomes an outflow. A stock model is visualised in Figure 2-1.

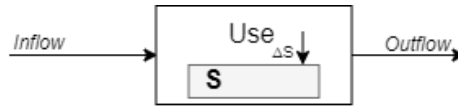


Figure 2-1: Stock model, where the balance of inflow and outflow determine the stock (S) and stock change (ΔS).

An inflow driven stock is dependent on inflow and outflow and can be described according to equation [2-1].

$$S(t) = \sum F_{in}(t) - F_{out}(t) \quad [2-1]$$

In this case, outflows occur as a delayed function of the inflow, the lifespan of the wind turbine $L(t)$. This can be written as equation [2-2].

$$F_{out} = F_{in}(t - L(t)) \quad [2-2]$$

The lifespan $L(t)$ is a distributed function [2-3] and is time dependent as it is assumed to increase as wind turbine technology matures. The specific distribution is determined by a normally distributed probability density function. Here, μ is the mean lifespan and σ is the standard deviation. Choices for lifespan modelling are further discussed in section: 3.1.4 Lifespan.

$$f(x) = \frac{1}{\sigma\sqrt{2\pi}} e^{-\frac{1}{2}\left(\frac{x-\mu}{\sigma}\right)^2} \quad [2-3]$$

2.2 MODELLING STRUCTURE

The dynamic model is created in Python and involves combining and manipulating the inflow datasets, the Dynamic_Stock_Model (DSM) Python module (Pauliuk, 2014) and further processing of the output data to include recovery and recycling rates and visualize the results. The use of Python and the DSM module provides several advantages over other software (e.g. Vensim, Ventity, Excel) as it is open-source, flexible and better equipped to handle various scenarios and large numbers of variables. The system definition and therefore the structure of the model can be visualised as shown in Figure 2-2.

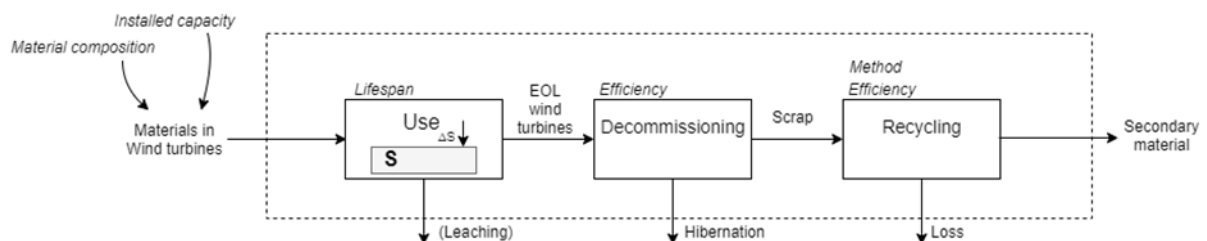


Figure 2-2: System definition and model structure for material flows, describing the steps to calculate inflows (materials in wind turbines), stock (Use), outflow (EOL wind turbines), lifespan, collection efficiency (Decommissioning) and recycling efficiency (depending on the recycling method), leading to a secondary material flow. Leaching is identified as potential loss through corrosion and erosion during operation, but not further discussed. Hibernation is stock that is not collected and therefore accumulates as 'hibernating stock'.

To create the input data *Installed capacity*, the raw data from online databases is first processed, meaning its values are stripped from quotes and other redundant information. Next, the data frame is sorted on date, creating a consecutive list of wind turbine installations or inflows. The next step is to add the future scenario data frame, which contains similar data to describe technological development. This process creates a data frame for past and future inflows, allowing for various manipulations to obtain material flows.

Implementing the *material compositions* for a variety of wind turbines requires categorizing to deal with the complexity and variety of wind turbine material compositions. A rough categorisation leads to lack of detail, whereas a division into individual wind turbines would not be feasible due to a lack of exact data on material composition. Considering various indicators, such as manufacturer, age, rated capacity and location, a sensible categorisation is made that is implemented through conditional statements⁵ in the model. The estimation on materials per installation is attached to the data frame.

From the updated data frame, lists containing inflow in capacity and any material inflow of interest (e.g. blade waste, glass fibre in blade waste, etc.) can be extracted. These lists are then used as input, *Materials in Wind turbines* for the DSM as shown in the model structure in Figure 2-2. The resulting outflows can then be used to determine the potentially recovered materials, using the data on recycling processes⁶. Decommissioning covers the collection rate, whereas processing- and recycling rates are covered by the recycling process. This process can be described by equation [2-4], where recovery rate of material in component *i* is the result of collection-, processing- and refining rates.

$$m_{recovered,i} = collection_i \cdot processing_i \cdot refining_i \quad [2-4]$$

2.3 DATA REQUIREMENTS

To model the material recovery potential of Dutch wind energy, several datasets are needed. First, historically installed capacity data is needed. This data is obtained from WindStats and contains information on individual turbines, among others manufacturer, hub height, rotor diameter, rated capacity, location (province), start - and end date (of operation). Therefore, this dataset can be used to determine historic inflow, -stock and -outflow of materials by using the additional information as indicators for turbine type and therefore material composition.

The WindStats dataset is also used for the stock analysis. The results from the analysis of current installed capacity in the Netherlands is discussed in section 3.1. This includes information on wind turbine characteristics such as rated capacity, manufacturer characterizing technologies, historic installed capacity and lifespan.

Next, material compositions are needed to determine material demand for each wind turbine. Assembly- and component mass and material compositions are obtained from wind-turbine-models.com and various other sources such as manufacturer brochures and academic literature. This data is used to determine equations for component and material mass. A summary of material compositions is provided in section 3.2, which is further discussed in *Appendix B*.

⁵ For example; **if** the manufacturer is **a**, **then** the component material intensity is **x** t/MW for material **b** and **if** the rated capacity exceeds a certain rated capacity **and** the wind turbine is installed after a certain year, **then** the component material intensity is **c** t/MW for material **d**.

⁶ The structure can be formulated as process **z**, being a *decommissioning* and *recycling* process for material **x**, leads to a material **x** recovery rate through collection rate **x** * processing rate **x** * recycling rate **x**.

Future developments in installed capacity and wind turbine technology are needed to determine installed capacity and type of wind turbines. The installed capacity scenarios are compiled from various existing scenarios in government documents and research. This aspect summarized and discussed in section 3.3. As described in Methods, these provide the necessary data for the dynamic stock model. Therefore, inflows, stock and outflows are presented in section 3.4.

These results serve as input for material recovery in section 3.5, which requires material recovery rates for various recycling routes and results in potentially recovered materials. This data is obtained principally from literature and expert opinion.

An overview of data requirements is presented in Table 2-1.

Table 2-1: Data requirements for historic and future stocks and flows.

Historic stocks and flows	Future stocks and flows
Material composition for various types of turbines	Material compositions for various (future) turbines
Types of turbines installed	Technological development
Capacity and number of turbines installed	Scenarios for wind energy capacity
	Lifespan of turbines
	Inflow (stock maintenance + increase)
	Material recovery rates (recovered material flows)

2.4 ENVIRONMENTAL AND ECONOMIC CONTEXT

The environmental impact of inflows and stocks is estimated by multiplication of material environmental extensions from literature and the flows [t/a] or stocks [t]. For this assessment cradle-to-gate LCA/LCI studies⁷, cradle-to-grave LCA (Schreiber et al., 2019) and process information⁸ is used. Relevant sources are described where used and their system boundaries explained. By omitting important life cycle steps, such as transport and manufacturing no exact results can be obtained. The assessment does provide an indication of the environmental impact for the use of alternative technologies that use different materials when used in a comparative way. It supplements this research by providing context by considering not only resource use, but also other impact categories that are vulnerable for trade-offs. Recycling is considered to substitute the need for primary materials. Therefore, this can be considered positive impact. Which material can be substituted is dependent on the quality of the secondary material. Ideally, closed loop recycling⁹ is achieved, but this is not always possible due to losses and lower grade secondary materials.

Economic context is provided where relevant and entails information on criticality, material quality and value. These factors can strongly influence the incentive for recycling and are therefore important to consider.

⁷ e.g. Haque & Norgate (2013), Liu & Barlow (2016), Sprecher et al. (2014).

⁸ e.g. Hasanbeigi et al. (2016), Epri (2020).

⁹ No losses in material quality, therefore material to same material or materials that can be used for identical purposes as the primary material.

Results

Onshore and offshore wind turbines in the Netherlands at wind park Noordoostpolder. Enercon E-126 onshore and Siemens 3.0 DD-108 offshore with a combined capacity of 429 MW provide 1.4 TWh of electricity annually, enough for 400.000 households.

Source: Windparknoordoostpolder (2020)



3 RESULTS

This chapter covers the main results obtained in this study. First, the results from the analysis of current installed capacity in the Netherlands is discussed in section 3.1. This includes information on wind turbine characteristics such as rated capacity, manufacturer characterizing technologies, historic installed capacity and lifespan. Next, a summary of material compositions is provided in section 3.2, which is further discussed in *Appendix B*. Then, future developments in installed capacity and wind turbine technology are summarized in section 3.3. As described in Methods, these provide the necessary data for the dynamic stock model. Therefore, inflows, stock and outflows are presented in section 3.4 .

3.1 STOCK ANALYSIS

The current stock of wind turbines in the Netherlands is analysed using data from WindStats (2020). This provides a basis for understanding material compositions and material flows as the data includes turbine rated capacity, manufacturer, number of turbines and location. The total installed capacity from WindStats amounts to roughly 4.5 GW after removing decommissioned turbines. As most sources report on approximately 5.7 GW currently installed (RVO, 2020a,b), the data is likely incomplete. Although the data for offshore wind capacity is reliable (confirmed by other sources e.g. RVO, 2020a), this indicates that the ~1 GW discrepancy between WindStats data and other sources is in onshore capacity. This is likely due to a delay in administration as installations occur in a short timeframe¹⁰. Although the data is incomplete, it is assumed the observations made on manufacturer and capacity categorization and shares are a good approximation. Further use of this data includes a compensation for this discrepancy.

3.1.1 Rated capacity

The average rated capacity for a wind turbine is currently 1.23 MW, with a minimum of 50 kW (1994 Lagerwey turbines) and a maximum of 12 MW (2019 GE Haliade X). This range is indicative for the rapid development of wind turbines over the past decades (Wiser et al., 2018), but also complicates categorizing wind turbines on their rated capacity. An overview of wind turbines installed per rated capacity category (with a range of 250kW) is shown in Figure 3-1.

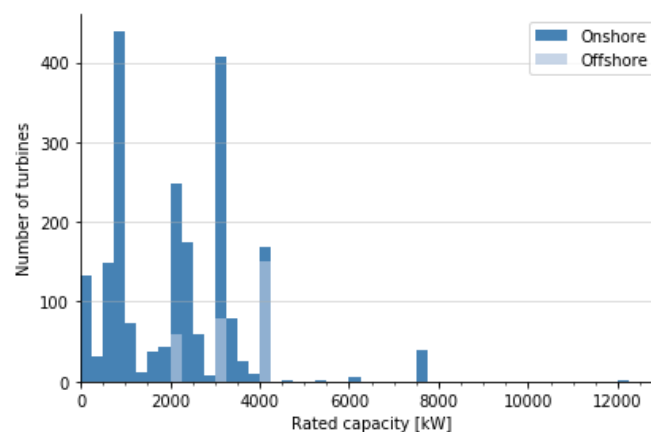


Figure 3-1: Number of turbines per rated turbine capacity category [kW]. Offshore wind turbines are highlighted in light blue.

¹⁰ At the end of 2018 3.38 GW was installed onshore and at the end of 2020 4.73 GW is almost certain to be expected (RVO, 2020b).

An outlier, the 12 MW GE Haliade X barely visible here as it only consists of a single (test) turbine (Port of Rotterdam, 2020). The peak in amount at 7500 kW is composed exclusively of Enercon E126 turbines (See cover page of this chapter). In the 6 MW category four Servion and one 2-B Energy turbine are present. The 4 MW category is composed almost exclusively of offshore turbines from Siemens Gamesa (SG). Offshore turbines in the 2MW and 3MW categories are composed of (MHI-)Vestas wind turbines. The difference in rated capacity is not related to the manufacturer however, as the SG turbines are more recent. It can be noted that most onshore turbines fall in the categories 3 MW, 2 MW and 1 MW. The 0-250 kW category is largely composed of turbines from Lagerwey, Micon, Bonus, NedWind, Nordtank from before the year 2000.

3.1.2 Manufacturers

Globally, the wind turbine market is currently dominated by a few large manufacturers, with strong regional differences in manufacturer presence¹¹. In Europe, Vestas (Danish), Siemens Gamesa (German/Spanish) and Enercon (German) are the top three manufacturers (BloombergNEF, 2020). Although all wind turbine manufacturers have experienced a rapid technological development of wind energy, many rely on characteristic technologies that set them apart from the competition. These characteristic technologies mostly include drivetrain innovations, e.g. direct drive and geared concepts, but also hybrid concrete towers and blade design. These technologies influence material composition and therefore relationships can be identified between material composition and manufacturer. Wind energy in the Netherlands has seen a lot of small-scale manufacturers in the early days of wind energy but is currently dominated by three major manufacturers: Enercon, Vestas and Siemens Gamesa (Figure 3-2). As Enercon focuses on onshore wind turbines, offshore consists exclusively of Vestas and SG turbines (*Appendix A Stock analysis*, Figure A-1). Further characterizing technologies and information are presented in *Appendix A*.

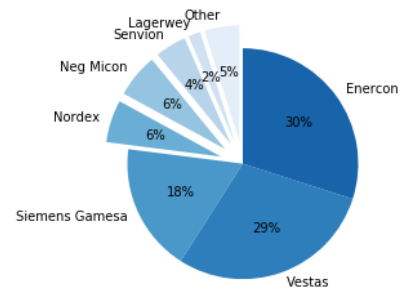


Figure 3-2: Shares of wind turbine manufacturers in the Netherlands for installed capacity.

3.1.3 Historic installed capacity

Using the installation and decommissioning data, the current stock of wind turbines can be determined. The data is compensated for the gap in installed capacity by adding 21% capacity to each inflow. The inflows and outflows are shown in Figure 3-3, resulting in the stock visualised in Figure 3-4. The sum of historically decommissioned wind turbine capacity amounts to 548 MW.

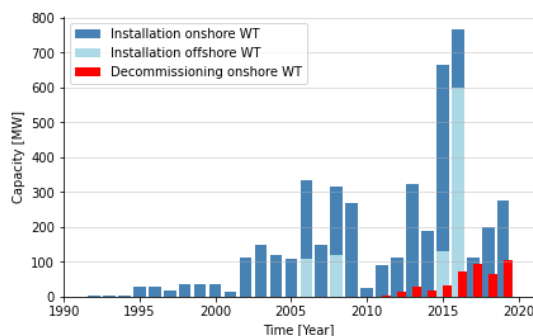


Figure 3-3: In- and outflows of onshore (blue) and offshore (light blue) wind turbines and decommissioning (red) in the Netherlands in [MW]. Data discrepancy is compensated.

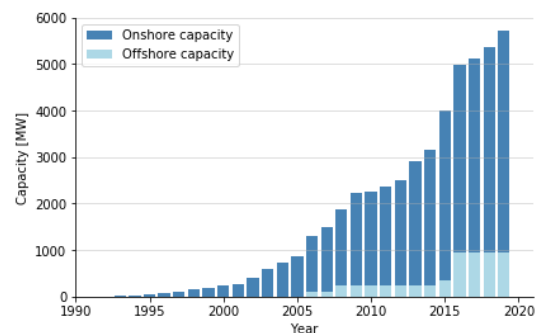


Figure 3-4: Stock of onshore (blue) and offshore (light blue) wind turbines in the Netherlands. Data discrepancy is compensated.

¹¹ Asian manufacturers Goldwind, Envision, Ming Yang, Dongfang and Windey are dominant on the Asian market, whereas European Vestas, SG, Nordex and Enercon are mostly present in the European market. The American General Electric (GE) is most dominant on the American market. (BloombergNEF, 2020).

As rated capacity of turbines has increased over the years, the in- and outflow in capacity tell little about the number of turbines that are installed and decommissioned. Therefore, in *Appendix A*, the number of turbines is visualised in the same way to compare these results for in- and outflows (Figure A-3) and stock (Figure A-4). The sum of historically decommissioned wind turbines amounts to 445 turbines. Comparing these figures leads to confirmation of the assumption that older turbines have a lower rated capacity as inflows in number of turbines are relatively larger before 2005 compared to capacity in- and outflows.

Based on the analysis of the current stock in the Netherlands, various indicators have been identified that determine the type of wind turbine and therefore its material composition. First, distinction is made on location: onshore or offshore. Onshore turbines require steel reinforced concrete foundations, have a longer history, include a wider variety of manufacturers, are often smaller and have lower rated capacity on average. Offshore wind turbines in the Netherlands use monopile foundations, are around since 2006, currently only consist of Siemens and Vestas turbines, only include larger turbines with a rated capacity of 2 MW or more. Next, a distinction can be made based on rated capacity, which is shown in Table 3-1.

Table 3-1: Categorisation of Dutch wind turbines based on stock analysis. Major manufacturers include Enercon, Vestas and SG. Peak or single years for a certain category are indicated with square brackets []. Expected installations are indicated with normal brackets ().

Rated capacity [MW]	Period [Year]	Manufacturer(s)	Note
< 0.25	1990-2000	Lagerwey	Two-blade rotor
0.25 < 0.75	1990-2005	Various ¹²	
0.75 < 2	>2000 [2005]	Major	Most from 2005
2 < 3	>2000	Major	
3 < 4	>2005 [2015]	Major	Most from 2015
4 < 6	[2016]	4 MW SG offshore	
6 < 8	[2015]	7.5 MW Enercon	Only onshore
8 < 10	(2020-2023)	SG/Vestas	Expected
10 < 12	(2020-2023)	SG/Vestas	Expected ¹³
12 < 15	2019	GE Haliade X	Test turbine
15 < 20	-	-	Future turbines

3.1.4 Lifespan

The lifespan of a wind turbine is an essential parameter in modelling the dynamic aspect of this study. Overall, literature seems to attribute a 20 – 25-year lifespan for wind turbines, but it is also acknowledged that in reality this number is currently lower (Market analysis DECOM Tools, 2019; Liu & Barlow, 2017; Lefevre et al., 2019). Liu & Barlow also discuss a theoretical maximum lifespan of 27 years due to fatigue issues in blades. Furthermore, manufacturer warranties and planned obsolescence could influence the life span of a wind turbine in various ways. First, warranties can eliminate the very short life spans by decreasing the extremes in shorter lifespan, creating a positively skewed distribution. Secondly, planned obsolescence often occurs as technology rapidly improves and newer turbines have achieved significant improvements that make replacement an economically

¹² Variety of manufacturers, many of which do not exist anymore or have merged with and/or acquired by larger manufacturers.

¹³ Currently no turbines are registered in the 8 - <10 MW or 10 - <12 MW categories, but will be in the near future due to offshore projects involving 8, 9.5 and 10 MW Siemens and Vestas turbines (RVO, 2020a; Vattenfal, 2020; Ørsted, 2020).

attractive option. This could decrease extremes on longer life spans and create a negatively skewed distribution¹⁴.

Being a relatively new technology, with first notable applications between 1990 and 2000, many wind turbines have yet to reach their end of life. Therefore, historical data on actual life spans of wind turbines is not often used to determine lifespans. Furthermore, onshore wind turbines have a longer history and are implemented in smaller numbers. ‘Offshore’ wind parks (these include near-shore and experimental) that have been decommissioned are limited to Yttre Stengrund (Sweden), Vindeby (Denmark), Windfloat I (Portugal), Hoostiel (Germany), Lely (Netherlands) and Utgrunden I (Sweden). The oldest offshore wind park, Tunoe Knob (Denmark), is still operational. With only five cases of decommissioning, little can be said about their lifespan distribution as data is limited.

Using data from WindStats, a lifespan distribution for onshore wind turbines in the Netherlands is created (Figure 3-5). Here, a histogram is shown, containing 151 decommissioning projects for a total of 445 wind turbines. Through the mean and standard deviation of this histogram, a normal distribution is plotted. Alternatively, a Weibull distribution could be used, but based on Sacchi et al. (2019) a normal distribution is assumed. This results in a mean lifespan of 16.3 years with a standard deviation of 5.3 years, but It can be observed that there is a poor fit to the existing dataset. It must be noted here that turbines that have reached this life span have been built around 2004 and therefore in the early days of wind energy in the Netherlands. Furthermore, much older turbines, dating back to the 1980s and ‘90s are still operational and not represented by this data as they are still operational, meaning that longer lifespans than average are for the most part not represented. Finally, this analysis considers exclusively onshore wind turbines (if near-shore wind turbines (e.g. Lely wind park) are considered onshore). It is often discussed offshore turbines have longer designed lifespan of 25 up to 30 years (Market analysis DECOM Tools, 2019). Therefore, it could be more realistic to assume a longer life span (20-year mean) as indicated by the dashed line. A more complete analysis of decommissioned wind turbines has been done by Sacchi et al. (2019) on Danish wind energy. They conclude on an 18.4-year mean life span with a standard deviation of 4 years. Again, this study considers mostly older onshore turbines as it looks at historically decommissioned wind turbines.

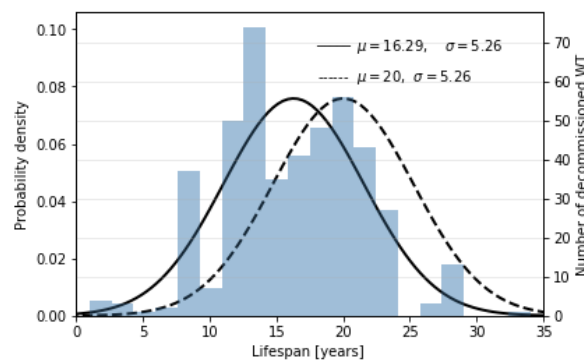
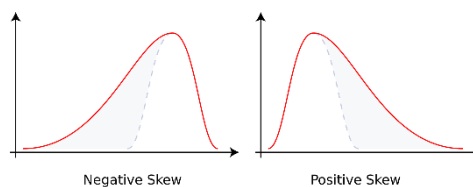


Figure 3-5: Life span distribution for wind turbines (WT) in the Netherlands based on decommissioning data from WindStats. The histogram shows number of turbines decommissioned (right y-axis) with their lifespan category (x-axis). Probability is for the normal distribution is shown on the left y-axis. The $\mu = 16.29$, $\sigma = 5.26$ distribution is created based on the mean and standard deviation from the histogram. The $\mu = 20$, $\sigma = 5.26$ distribution (dashed) is estimated to potentially be a better fit.

¹⁴ Negative (right) and positive (left) skewness, potentially present as a result of either planned obsolescence or manufacturer warranties. Image obtained from Macrosammon (2020).



Another approach that can be taken to determine the lifespan uses the dynamic stock model (Pauliuk, 2014) to estimate a good fit for modelled- and historic outflow. Figure 3-6 shows this exercise indicates the mean lifespan should be 18 years, based on a standard deviation of 5.3 years. However, the 18, std 4 years as assumed by Sacchi et al. (2019) and 16-year mean, 4 years standard deviation seem plausible as well. The 16-year, 5.3 standard deviation as determined in Figure 3-5 seems to agree with maxima of decommissioning in 2017/2018/2019, but is largely overestimating outflows in other years. The opposite can be said for the 20-year mean lifespans where underestimations can be observed after 2011.

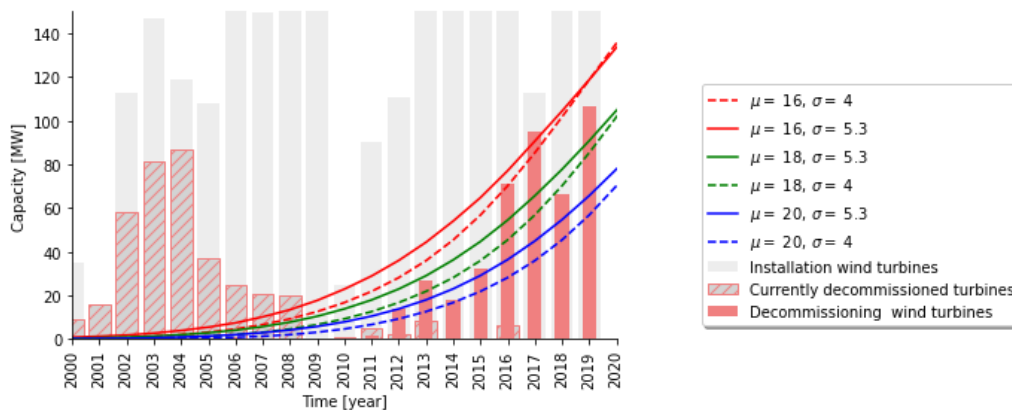


Figure 3-6: Modelled versus actual decommissioning of wind turbines in the Netherlands. Historic installations of wind turbines are shown in grey. The hatched red installations are currently decommissioned i.e. show up in the red bars as decommissioning of wind turbines. The lines indicate modelled decommissioning based on historic installation data. The $\mu = 18, \sigma = 5.3$ distribution approximates historic decommissioning data most accurately.

It must therefore be concluded that the lifespan of 20-25 years is optimistic for currently installed wind turbines in the Netherlands. However, it must also be noted that current data is from a rapidly developing wind energy sector and mostly represents small scale onshore wind turbines. Although weather conditions are more demanding in offshore applications, manufacturers and exploiters of wind parks aim for a life span of 25 years (Siemens Gamesa, 2020). Variations in life span occur due to technological development and intended location of the turbine (offshore and onshore) and a skewness could be assumed due to manufacturer warranty, but this might be counteracted by planned obsolescence. How the actual life spans of wind turbines will develop remains to be seen, but these observations lead to several assumptions for the stock model:

- A distinction should be made between offshore and onshore wind turbines lifespan.
- Mean lifespan should be dynamic as it likely increases over time due to technological development.
- For historic installations an 18 year mean lifespan is assumed with a standard deviation of 5.3.

The development of mean lifespan for future wind turbines is further discussed in section 3.3 Future development.

3.2 MATERIAL COMPOSITIONS

The material composition of a wind turbine varies depending on multiple variables, such as location, capacity and specific technologies used for in for example the drivetrain. These variations are sometimes large for bulk materials, but also include small but important variations in the use of critical materials. Due to the complexity and diversity of material compositions, categorisation indicators are determined based on the stock analysis that enable generalized yet detailed enough material compositions. These indicators determine the specifics for (sub)components (Table 3-2) used. This section summarizes the results from *Appendix B Material compositions*.

3.2.1 Components

For a typical modern 2 MW wind turbine, a 36-tonne rotor weight, 106 tonne top head weight and 5.8 tonne blades are common (Schubel & Crossley, 2012). It can be derived from this that a nacelle would weigh approximately 70 tonne and the rotor hub, pitch mechanisms and nose cone would weigh approximately 18.6 tonne. Further description of the typical 2 MW includes a 67-100m tower weighing 153-255 tonnes, a three-stage gearbox and a doubly fed induction generator (DFIG). Although these values are useful as default values, many variations exist. To describe the material composition of wind turbines, various simplifications must be made to deal with its complexity and variation. Modern wind turbines can consist of more than 8000 parts (Busby, 2012) and therefore a division in sub-assemblies is commonly made. This division is shown Table 3-2.

Table 3-2: Wind turbine component and assembly breakdown. *Italic indicates components are not always present as described.*

Assembly	Sub-assembly/component	Sub-sub-assembly/component
Rotor	Hub	
	Nose cone	frame and cover
	Pitch system	pitch drive, bearings and gears
	Blades	blade root connection, <i>shells</i> , <i>shear web</i>
Nacelle	Bed plate	
	Cover	
	<i>Mechanical brake</i>	<i>calliper and disc</i>
	Yaw system	yaw drive, bearing and gears
	Drive train	<i>gearbox</i>
		shaft
		generator
bearings		
Other	e.g. measuring equipment, transformer	
Tower	Tower sections	tower internals: power cables, ladders
Foundation	<i>Concrete or Monopile</i>	
Other	e.g. power electronics, cables	

To determine the mass of these components, relationships with rated capacity and hub height are determined based on literature and empirically. For roughly 60 specific wind turbines blade-, hub, rotor, nacelle, and tower mass are obtained from wind-turbine-models.com. Furthermore, Schubel & Crossley (2012) give nacelle and rotor weights for various wind turbines. Wind turbine reference

models¹⁵ are included and provide a valuable estimation for current and future turbines. A wind turbine scaling study (Smith, 2001) identified component masses dependent on rotor diameter. These scaling results supplement the data for 0.75 MW to 5 MW wind turbines. Further specific data on components is obtained through dedicated literature and personal communication with experts (TNO) and involved companies (Jumbo, Lagerwey, LM). The process of deriving the mass equations for each component is reported in more detail in *Appendix B Material composition*. The underlying data is presented in *Mat_comp_data.xlsx*, which is provided in the supplementary information.

Hub, nose cone, blades, bed plate, transformer, shaft, cover, pitch- and yaw mechanisms are be described linearly using a t/MW approximation in the form of Equation [3-1] where $m_{component,i}$ is the mass of a component or material/element in a component in tonne, c_i is the share of the individual material or element in the component, I_c is the derived mass intensity in [t/MW] and P_{rated} is the rated capacity in MW. An overview of mass intensities is presented in Table 3-3 a) and other relationships in Table 3-3 b).

$$m_{component,i} = c_i \cdot I_c \cdot P_{rated} \quad [3-1]$$

Table 3-3: Mass estimation summary tables. Linear relationships with capacity are shown in a), including their mass intensity value. Other relationships are described in b) and further explained in this section.

a)		b)	
Component	Mass intensity [t/MW]	Component	Mass equation
Blades *	12.022	Generator	Polynomials - P
Hub	11.522	Tower steel	Polynomial - h
Nose cone	0.649	Tower hybrid	Linear - h
Transformer	4.85	Tower internals	Linear - h
Shaft geared	3.13	Onshore foundation	Average/turbine
Shaft DD	1.05	Offshore foundation	Average/turbine
Bed plate	5		
Cover	2.424		
Pitch mechanism	2.979		
Yaw mechanism	4		

*Blade materials use categorized mass intensities.

Blade materials

Blade mass is derived using a single linear approximation factor as well but are further specified according to rated capacity based on Liu & Barlow (2017) as blades for turbines with a lower rated capacity have a roughly 30% lower mass intensity. Reasons for this variation could include two-bladed designs. The categorized mass intensities are shown Table 3-4.

Table 3-4: Mass intensities for blades categorised by rated turbine capacity. Based on Liu & Barlow (2017)

	< 1 MW	1-1.5 MW	1.5 – 2.5 MW	2.5 – 5 MW	>5 MW
Material intensity [t/MW]	8.43	12.37	13.34	13.41	12.58

Another distinction is made based on estimates for carbon fibre content in blades (Lefevre et al., 2019). Carbon fibre use in blades varies, therefore Lefevre et al. estimate that on average blades

¹⁵ Including a 5, 8, 10 and 15 MW turbine described in Jonkman et al. (2009) from the National Renewable Energy Laboratory (NREL), Desmond et al. (2016) from the EU LEANWIND project, Bak et al. (2013) from Technical University of Denmark (DTU) and Gaertner et al. (2020) (NREL) respectively.

after 2010 and above a turbine rated capacity of 2 MW contain 6% carbon fibre. This leads to equations [3-2] and [3-3] for blades below 2MW and before 2010:

$$m_{blades,GF} = 0.604 \cdot I_c \cdot P_{rated} \quad [3-2]$$

And above 2MW after 2010:

$$m_{blades,GF} = 0.544 \cdot I_c \cdot P_{rated} \text{ and } m_{blades,CF} = 0.06 \cdot I_c \cdot P_{rated} \quad [3-3]$$

Generator materials

The generator converts rotational motion to electricity through electromagnetic principles. For this a permanent magnet or electromagnet are needed to create a changing magnetic field and consequentially electric current. Therefore, large amounts of copper and/or permanent (NdFeB) magnets are needed. These materials are considered cross-cutting (copper) and critical (REEs). Figure 3-7 shows various drivetrain configurations, leading to different generator types.

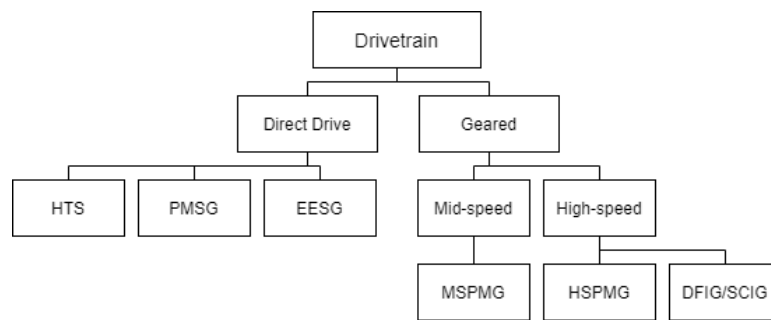


Figure 3-7: Drivetrain configurations. HTS: high temperature super conductor, PMSG(DDPMG): permanent magnet synchronous generator, EESG: electrically excited synchronous generator, MSPMG: mid-speed permanent magnet generator, HSPMG: high-speed permanent magnet generator, DFIG/SCIG (AG): doubly fed induction generator or squirrel cage induction generator. Based on Manberger and Stenqvist (2018).

Although literature (e.g. Viebahn et al., 2015; Lacal-Aránategui, 2015) often use a linear approximation for generator materials, generator design studies (Polinder et al., 2006; Bang et al. 2008a,b, Bang et al., 2009; Shammugam et al., 2017) show a non-linear mass scaling for generators. Appendix B Material compositions describes the discrepancies (>33%) that can occur by linearizing this and further elaborate the decision to use a polynomial on rated capacity for generator mass.

For DFIG and SCIG very similar mass equations are derived and therefore they are both described by Asynchronous Generator (AG) mass equations for total generator [3.4], iron [3.5] and copper [3.6]. Here P refers to the rated capacity of the wind turbine.

$$m_{AG} = 0.3 \cdot P^2 + 3.65 \cdot P \quad [3-4]$$

$$m_{AG,iron} = 0.29 \cdot P^2 + 3.19 \cdot P \quad [3-5]$$

$$m_{AG,copper} = 0.1834 \cdot P \quad [3-6]$$

For PMG it is derived from Polinder (2006) that an HSPMG is a factor 0.125 in materials and HSPMG a factor 0.25 of DDPMG, which is determined for iron [3.7], copper [3.8] and magnet [3.9].

$$m_{PMG,iron} = 1.0682 \cdot P^2 + 11.655 \cdot P \quad [3-7]$$

$$m_{PMG,copper} = -0.0329 \cdot P^2 + 1.4249 \cdot P \quad [3-8]$$

$$m_{PMG,magnet} = 0.0358 \cdot P^2 + 0.269 \cdot P \quad [3-9]$$

EESG mass is described for iron [3.10] and copper [3.11].

$$m_{ESG,iron} = 2.1402 \cdot P^2 + 13.131 \cdot P \quad [3-10]$$

$$m_{ESG,copper} = -0.0825 \cdot P^2 + 4.4692 \cdot P \quad [3-11]$$

Tower materials

Although most components show strong or some correlation with rated capacity, it is shown in *Appendix B Material composition* that tower mass can be better described by tower height. Therefore, tower mass is estimated based on a polynomial trend for hub height from 61 turbines [3.12].

$$M_{tower,steel} = 0.048h^2 - 2.0235h + 28.068 \quad [3-12]$$

The tower types are generalized into steel and hybrid(concrete) as modular concepts are assumed not to be required in the Netherlands. For concrete towers less data is available, and it cannot be said with certainty if steel or concrete is being used. Therefore, concrete and reinforcement in the concrete tower are approximated linearly by equations [3.13-3.15].

$$m_{hybrid\ tower} = 20.872 \cdot h \quad [3-13]$$

$$m_{hybrid\ tower, concrete} = 0.885 \cdot 20.872 \cdot h \quad [3-14]$$

$$m_{hybrid\ tower, steel} = 0.115 \cdot 20.872 \cdot h \quad [3-15]$$

Tower internals include among others lighting, ladders and the power cable. However, all but power cables are considered to be too detailed and are left out of the analysis. The power cable likely scales with height and is therefore estimated as by equations [3.16-3.17].

$$m_{cable\ copper} = 3.175 \cdot 10^{-3} h \quad [3-16]$$

$$m_{cable\ aluminium} = 9 \cdot 10^{-3} \cdot h \quad [3-17]$$

Foundation materials

For foundations or support structures a clear distinction between onshore and offshore can be made. Onshore wind turbines use concrete foundations whereas in the Netherlands offshore exclusively uses monopiles (other foundations include gravity-based, jackets and floating) due to shallow sea depth.

Onshore foundation mass is based on total turbine weight according to two estimates from Busby (2012). *Appendix B Material compositions* shows how wind turbines with a steel tower have a foundation that is heavier in relation to the turbine than concrete towers. Therefore, using the general equation [3.18], steel tower foundations can be described by equation [3.19] and concrete tower foundations by equation [3.20]

$$m_{foundation} = W * \frac{m_{rotor} + m_{nacelle} + m_{tower}}{1 - W} \quad [3-18]$$

$$m_{foundation,steel\ tower} = 2.33 * (68.566 P + 0.048h^2 - 2.0235h + 28.068) \quad [3-19]$$

$$m_{foundation,concrete\ tower} = 0.818 * (68.566P + 20.872 h) \quad [3-20]$$

For offshore foundations (monopile and transition piece) averaged mass per turbine as this is largely depth dependent). Therefore, a monopile mass of 850 t per turbine and transition piece mass of 300 t per turbine is assumed based on data from offshore foundation manufacturers and transporters. This leads to equations [3.21-3.22] for monopile and transition piece mass.

$$m_{monopile} = 850 \cdot t \quad [3-21]$$

$$m_{transition\ piece} = 300 \cdot t \quad [3-22]$$

Future development

Designated areas for wind energy development in the North Sea show ambitions goals for Dutch offshore wind energy in the near future.

Source: RVO (2020c)

IJmuiden Ver
4.000 MW
tenders
2023 - 2025



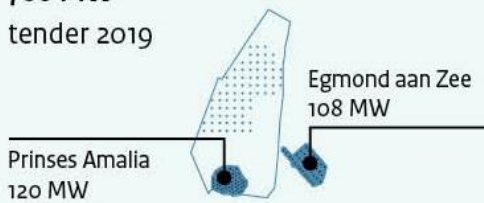
Ten Noorden van de
Waddeneilanden
700 MW
tender 2022



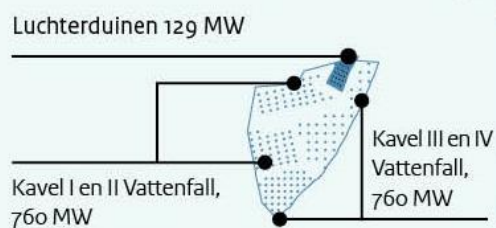
Hollandse Kust (west)
1.400 MW
tenders 2021



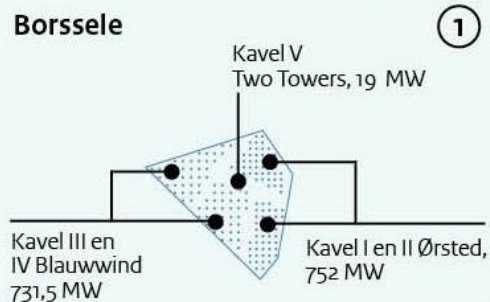
Hollandse Kust (noord)
700 MW
tender 2019



Hollandse Kust (zuid)



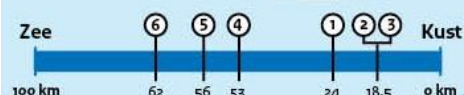
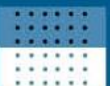
Borssele



Legenda

Bestaande windparken: ~1 GW

Toekomstige windparken: ~10 GW



3.3 FUTURE DEVELOPMENTS

To determine scenarios for future wind energy development, two aspects must be considered: installed capacity and technological development. First, the future installed capacity is discussed, resulting in a prognosis-, minimum- and maximum scenario. Secondly, the technological development will cover various trends and disruptive technologies that impact wind energy and its material use.

3.3.1 Future installed capacity

For material flows it is interesting to know what the range of expected materials is. This shows the minimum and maximum amount of materials that is potentially required, needs to be processed and becomes available as secondary materials. Various existing scenarios, prognoses and goals are analysed and compiled (*Appendix C Future installed capacity*) to form a prognosis- minimum- and maximum scenario (Figure 3-8). The minimum and maximum correspond with scenarios from a CE Delft & Netbeheer NL (Alfman & Rooijers, 2018) and Berenschot (Den Ouden et al., 2020). As these are the only known studies that consider different policies, these scenarios form the outer bounds for expected development. The prognosis under current policy also has a maximum and minimum range, this is shown to indicate how much the various studies under current policy agree. For the prognosis, the National Energy Exploration study (Nationale Energie Verkenning, 2017) from ECN and PBL is used. Finally, the dashed-dotted line indicates the average from all the examined studies combined.

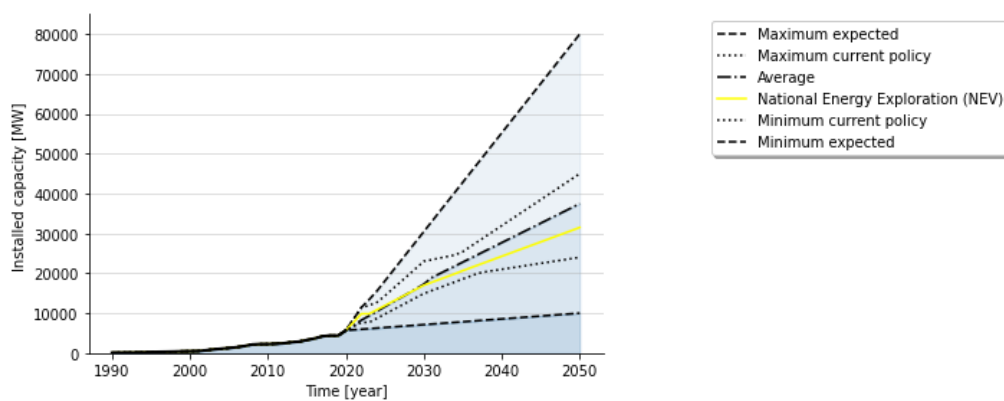


Figure 3-8: Future installed capacity scenarios. Dashed lines indicate minimum and maximum expected installed capacity under different policy scenarios. Under the current policy, a range is indicated by the dotted lines. Within this range the average from the examined studies is shown as dashed-dotted line and the predictions based on the National Energy Exploration (NEV) study is shown in yellow. The NEV is used as prognosis and minimum and maximum expected as range.

For offshore wind energy the National Energy Exploration (NEV) prognosis is close to the average, but onshore the NEV prognosis is closer to the minimum expected (Figure 3-9). This is under the assumption that onshore wind is considered to either grow significantly or remain relatively stable, depending on government policy and public opinion (TNC, personal communication, 2020).

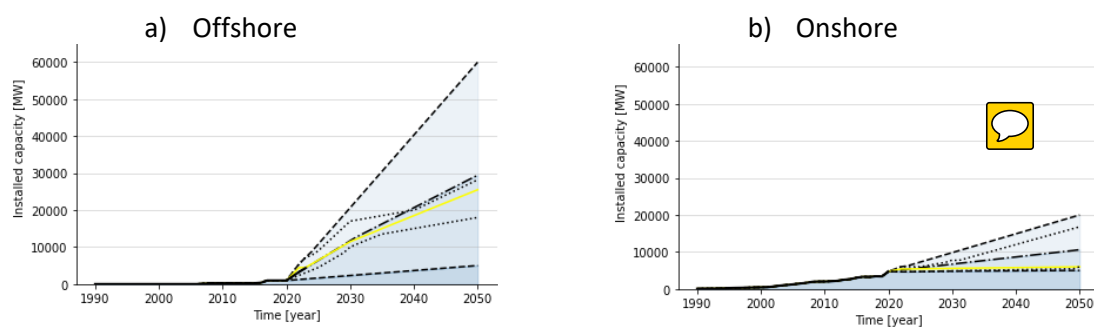


Figure 3-9: Future installed capacity scenarios for a) offshore and b) onshore wind energy. Colour indications are as described for the total installed capacity scenarios.

3.3.2 Technological developments

Technological innovation requires new designs involving variations in wind turbine properties, size and material compositions. First, trends in increasing rated capacity and hub height are analysed. Next, the increasing lifespan of wind turbines is discussed. Then, the use of different steel alloys and several variations in blade design are discussed. This is followed by various generator technologies and their development. Finally, composite towers and other wind energy converter designs are briefly touched upon.

Rated capacity & hub height

A general trend in wind energy can be described by an increase in hub-height and rated capacity (Figure 3-10). This can be observed in historical data, but likely develops differently for onshore and offshore wind energy.

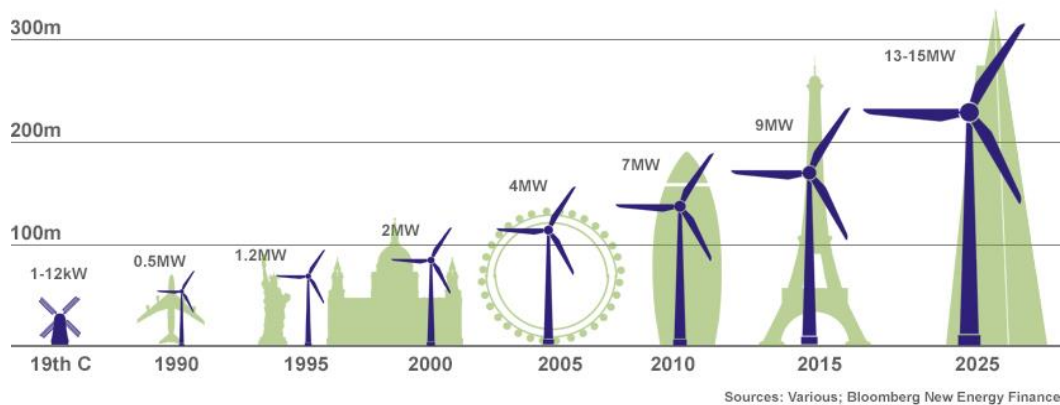


Figure 3-10: technological developments for wind turbines in rated capacity and hub height. Image obtained from Sustainability-soapbox (2020).

The maximum rated capacities for individual turbines are shown in Figure 3-11. It follows the expected developments in increase in rated capacity. However, Figure 3-12 indicates the mean rated capacity of new installations is generally much lower. Reasons for this include that available wind on location determines the rated capacity that is best suited. Therefore, the development of average rated capacity as shown in Figure 3-12 is assumed. Due to offshore locations having more wind available, higher average rated capacities are assumed here. Offshore wind parks under development also reveal much higher rated capacities will be used (RVO, 2020a; Vattenfal, 2020; Ørsted, 2020).

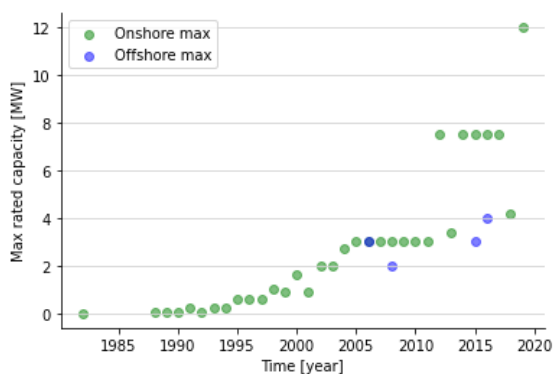


Figure 3-11: Increase in rated capacity. Maximum rated capacity of wind turbine installations in the Netherlands per year for onshore (green) and offshore (blue).

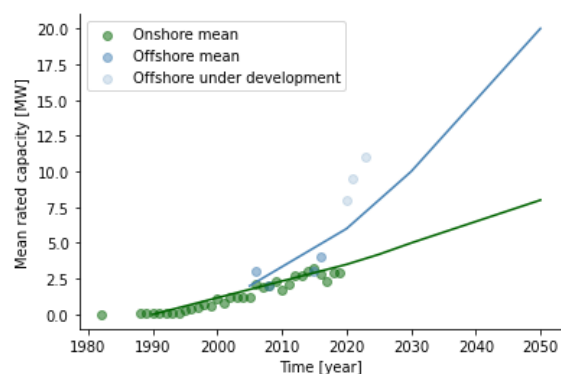


Figure 3-12: Increase in rated capacity. Mean values for onshore (green) and offshore with future estimations (blue)

For hub heights, generally associated with rated capacity, the development is shown in Figure 3-13. It is assumed onshore hub heights will be limited due to the logistics and aesthetic reasons. Offshore average hub heights are assumed to increase but might see limitations due to cost effectiveness and structural limitations. These projections for rated capacity and hub height will be used to determine the properties for future wind turbines. Similar trends in the USA validate these observations (Wiser et al., 2019).

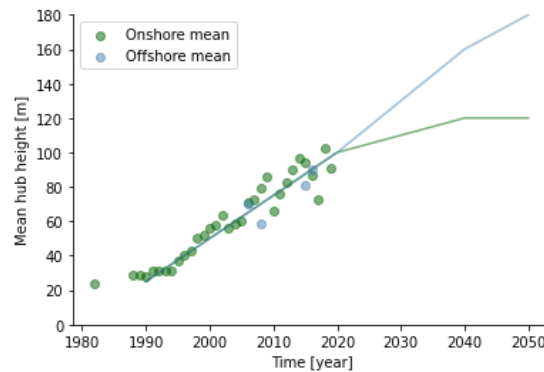


Figure 3-13: Increase in average hub height for onshore (green) and offshore (blue).


Lifespan

As discussed in section 3.1 Stock analysis, lifespan is expected to increase. For this it is assumed that offshore wind turbines require longer lifespans due to costly installation and dismantling. Starting from a current mean lifespan until 2020 of 18 years the onshore mean lifespan is expected to develop towards 24 years in 2040 and offshore 25 years from 2030 as shown in Table 3-5.

Table 3-5: Assumed increasing mean lifespans of onshore and offshore wind turbines towards 2050.

	> 2020	2020 – 2025	2025 - 2030	2030-2040	2040-2050
Onshore	18	20	22	23	24
Offshore	18	24	24	25	25

Material compositions

Structural steel in wind turbines is currently mainly S355 (potentially S235 for older turbines), but it could be needed for higher hub heights that higher steel grades are used. Van Wingerde (2015) estimates that S460 will be more common, but even higher grades (S690) would not be economical. This influences the elemental composition of the steel, requiring a higher purity (less tramp elements) and more specific alloying elements .

Blade material compositions could change incrementally or be replaced with different composite materials. Advances in blade manufacturing (e.g. automated fibre placement) could further reduce blade weight¹⁶ (Mishnaevsky et al., 2017). Mishnaevsky et al. further mention the increasing length of blades requires more integrated designs and potentially stronger and stiffer fibres. For future blades an increased CF content is possible (LM, personal communication, June 8, 2020; TNO, personal communication, March 17, 2020), leading to an alternative scenario where an increasing CF content is used. Liu & Barlow (2016) discuss up to 50% of fibres being replaced by carbon fibres by 2025, however this development is currently not observed and lower values are expected. It is therefore assumed the average CF content increases from 6% in 2020 to 7.5%, 9% and 10% in 2025, 2030 and

¹⁶ As can already be observed in estimates by Liu & Barlow (2017) presented in 3.2 Material composition.

2040 respectively. The criterium of CF use in blades over 2MW remains as blades under that capacity often do not require additional stiffness (LM, personal communication, June 8, 2020).

Natural fibres offer potential to reduce cost and improve material availability and environmental impact (Shah et al., 2013). These natural fibres include sisal, flax, hemp and jute. Bamboo is also listed as potential material. Shah et al. further demonstrate this possibility in a small-scale wind turbine blade. Full scale natural fibre blades have not been found in literature. Thermoplastic matrix material is considered an interesting alternative to thermosets as it could increase recyclability (Mishnaevsky et al., 2017; Cousins et al., 2019; Murray et al., 2017; Murray et al., 2019). However, fibre reinforced thermoplastics often have disadvantages such as high viscosity, processing temperatures and fatigue behaviour. On the other hand, unlimited shelf life and better fracture toughness provide additional advantages over conventional composites (Mishnaevsky et al., 2017).

Generator technologies

Perhaps the most interesting developments from a critical and key material perspective occur in drivetrain innovations. Historically, AG (SCIG, DFIG) are most common, after which EESG was introduced. Recently PMG direct drive and geared technologies are becoming more common. PMG are currently the most efficient technology and therefore will be used most in the offshore sector (Lacal-Arántegui, 2015). It is expected that due to cascading effects the onshore sector will follow. Generator development will likely follow the path of PMG and HTS, but could be subjected to disruptions from critical materials (Pavel et al., 2017). Weight and cost reduction of these generators is key (Lacal-Arántegui, 2015). This has secondary effects as a reduction in generator mass leads to reduction in required structural mass. For the future drivetrain scenarios, the scenarios from Carrara et al. (2020) are used. These include the low demand scenario (LDS), medium demand scenario (MDS) and high demand (HDS). The MDS is used as baseline and is shown in Figure 3-14, the other scenarios are considered concerning drivetrain materials. *Appendix D Sensitivity checks* describes these scenarios and their implications.

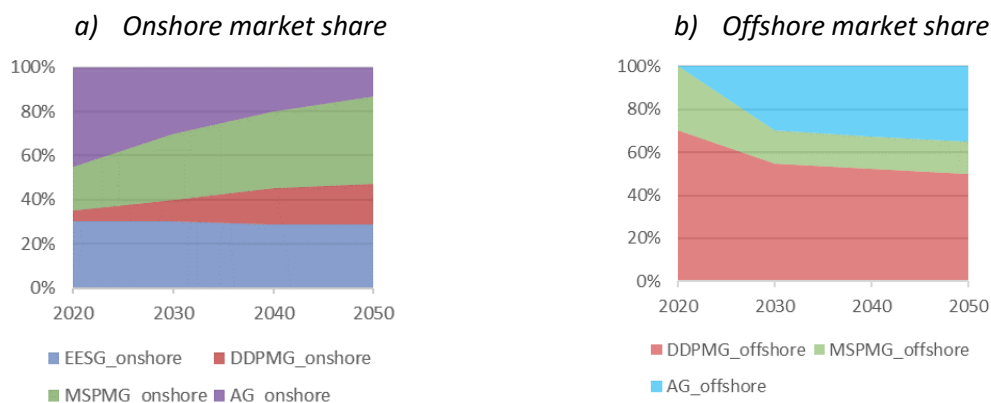


Figure 3-14: Predictions for future drivetrain market shares for the medium development scenario (MDS) based on Carrara et al. (2020). a) onshore market development, b) offshore market development. EESG: electrically excited synchronous generators, DDPMG: direct drive permanent magnet generators, MSPMG mid speed permanent magnet generators, AG: Asynchronous generators. High temperature superconductors (HTS) is only included in the low development scenario (LDS).

Viebahn et al. (2015) discuss variations in elemental compositions of permanent magnets, where reductions and changes for neodymium (Nd), dysprosium (Dy), praseodymium (Pr) and terbium (Tb) are discussed. High Temperature Superconductors (HTS) in wind turbine generators are applied in the generator rotor to create higher magnetic field strengths and thus higher power density. It can result in a generator mass reduction of up to 50% (Hill, 2010). HTS can therefore also be a very

disruptive technological development due to secondary effects on structural mass. Viebahn et al. (2015) estimate a need for Yttrium of 0.3 kg/MW in 2030 and 2050 HTSG. Song et al., (2019), Winkler et al. (2019) and Bergen et al. (2019) discuss the testing of the first HTS wind turbines, placing the technology at a technology readiness level (TRL) of 7-8, making implementation in 2030 a realistic possibility.

Composite towers

Another potentially disruptive technological development but at low TRL (proof of concept) are composite towers. The conventional towers of concrete or steel require high density materials and are therefore a dominant share of the total wind turbine weight. A composite tower could be designed differently achieving large reductions in mass. This technology is therefore analysed as well, but to limited extent due to its low maturity. The large-scale implementation of this technology could mean large reductions in steel and concrete for towers and potentially foundations (due to weight reduction), but also a major increase in composite waste at end of life. It is estimated that a 50% weight reduction can be achieved compared to conventional steel towers (TKI, 2018; Jules Dock, 2020). To analyse the effects of this potential development a separate scenario is created where composite towers are introduced, replacing conventional steel towers.

Other wind energy converters

As the temporal scope reaches 2050, other types of wind energy converters can be developed and implemented in this time period. Vertical axis wind turbines and airborne wind energy are discussed as potential technologies (Watson et al., 2019). However, for this study technological changes until 2030 are most relevant (as most outflows occur roughly 22 years later and uncertainty on material compositions for these technologies is very high. Therefore, these technologies are not analysed further, but could inspire further research.

3.3.3 Summary of future developments

In conclusion it can be said that pathways for installed capacity show a large range of possibilities but will result in a dominant offshore wind energy capacity. The three scenarios, low, prognosis and high provide a range. On technological development it can be said that hub height, rated capacity, increasing lifespan and market share for various generator types will cause incremental changes in material compositions, whereas technological developments such as HTS, composite towers and other wind energy converters might cause a more disruptive change in material flows. Single development pathways for hub height and rated capacity will be considered in the model, whereas generator scenarios are considered in more detail for its relevance to critical materials. To give a sense of impact the composite towers are analysed as well under a single scenario.

3.4 INFLOWS, STOCKS AND OUTFLOWS

This chapter discusses the intermediate model results. Historical inflow in capacity is translated to material inflows based on the results from the stock analysis and material compositions. Future developments in capacity stock are translated to capacity inflows and likewise to material inflows based on future technological developments. The joined dataset is used as input for the dynamic stock model, resulting in the stock and outflow data presented in this section.

3.4.1 Inflows

Inflows can be considered as material requirements and are interesting from a material demand and environmental impact perspective. Therefore, the future inflows of each material for the three scenarios are shown and discussed in this subsection. Figure 3-15 shows the inflows – or installation - of turbines in capacity. Peaks in inflow occur towards 2023 as currently large projects are under development (*Appendix C Future installed capacity*). It can also be observed that after 2030 a strong increase appears. This can be explained through additional inflows for stock maintenance. The prognosis shows a sharp decrease around 2030, this is caused by the sudden relative decrease in stock growth in this scenario after 2030. Figure 3-16 shows material inflows for the major material groups. The components that make up these flows are shown in *Appendix E Stacked results*. Similar developments can be observed with exceptions of permanent magnets that are strongly influenced by PMSG implementation and concrete that is only used for onshore wind turbines

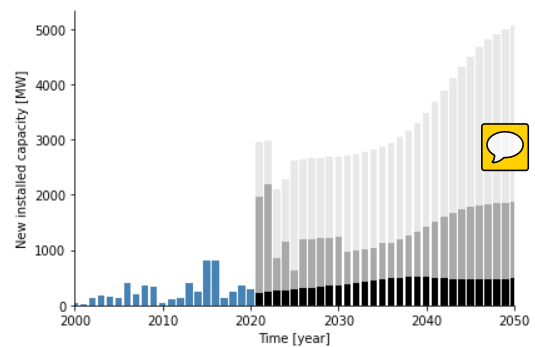


Figure 3-15: Inflows/installation of turbines in MW. Blue indicates historic inflows, black the minimum inflows, grey the inflows for the prognosis scenario and light grey the maximum.

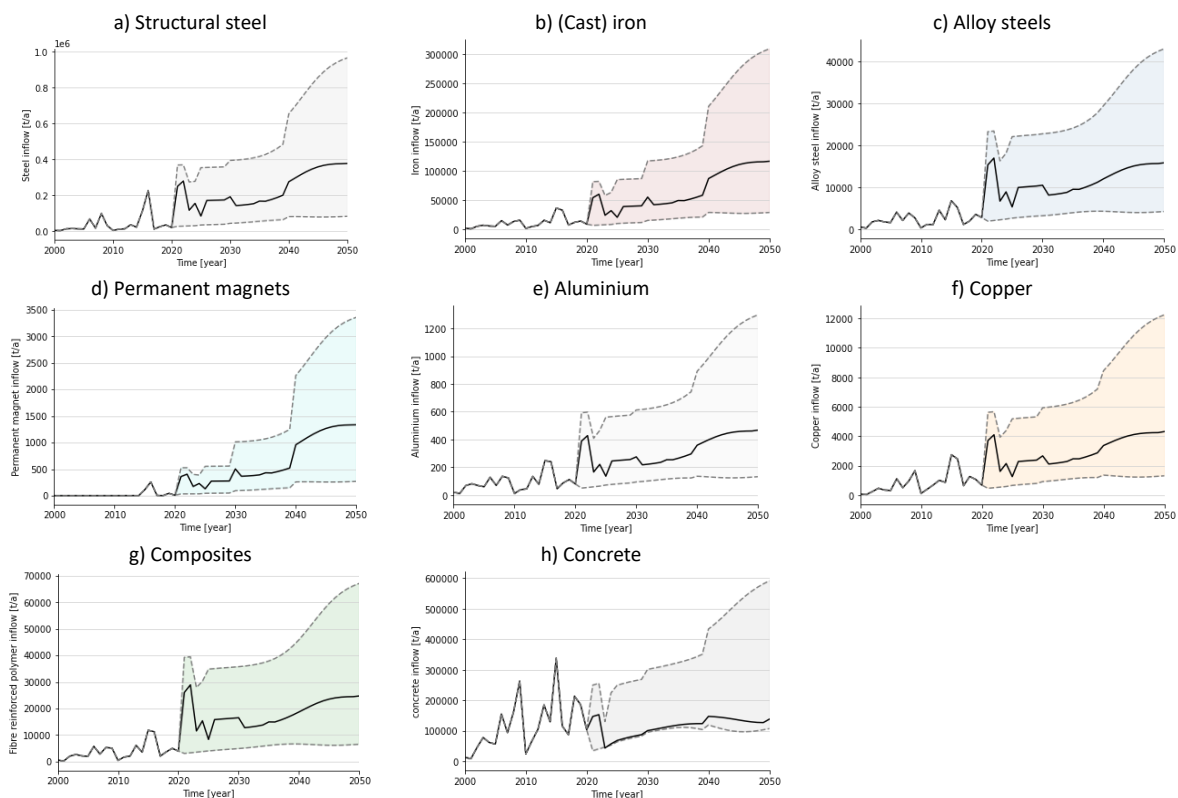


Figure 3-16: Inflows of major material groups. The black line indicates the prognosis scenario according to NEV. A range is highlighted between the minimum and maximum scenarios with different colours to differentiate the materials.

Further analysis of individual inflows is done for critical, valuable and high environmental impact materials.

Steel and Iron

First, structural steel inflows are dominated by tower and offshore support structures. Peaks in historical inflow are amplified as they represent installations of offshore wind parks which require more steel than onshore wind turbines.

An interesting environmental aspect of steel use is its high contribution to climate change through a high carbon intensity ($\sim 2 \text{ tCO}_2/\text{t-eq}$ for primary steel production¹⁷). This does not include various other activities required to manufacture and transport the components and is therefore a rough approximation. Due to these high environmental impacts, alternative steelmaking technologies and more secondary production that have lower emissions are desirable for future primary steel production (Milford et al., 2013). The lowering of emissions for future steel production is not included in the model calculations.

The demand for structural steel (s355) includes demand for silicon (Si) and Manganese (Mn) as alloying elements. The elemental composition of s355 is presented in *Appendix B Material compositions*. The shares of Si and Mn are used to determine required material inflows in Figure 3-17 a) and b). Due to the use of higher-grade structural steel (s460), a Si and Mn use could increase up to 20% in the future.

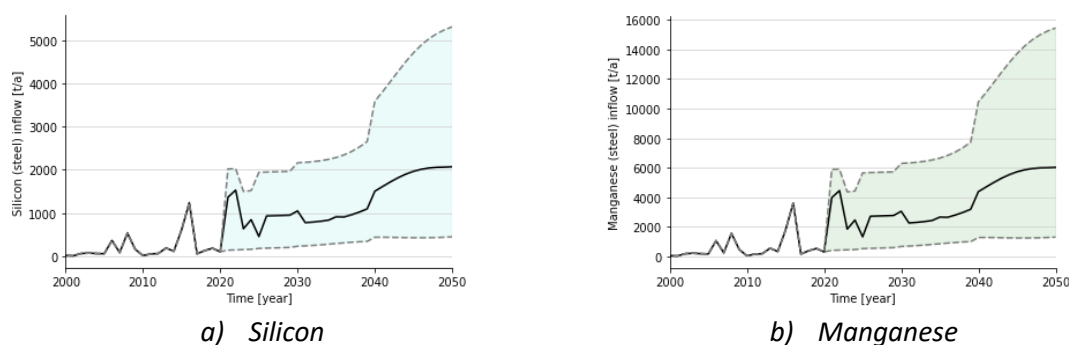


Figure 3-17: Silicon (a) and manganese (b) inflow/demand in structural steel.

Alloy steel inflows contain valuable cross-cutting and critical elements. In *Appendix B Material composition* it is determined that CrMo steels (general group), 31CrMoV9 and 17CrNiMoS6 are used in wind turbine gearboxes, shafts and bearings. Using the elemental compositions defined in *Appendix B*, the material inflows shown in Figure 3-18 a-f can be determined. Vanadium (V) is particularly interesting due to its criticality (European commission, 2017). Although the magnitude of alloy steel inflows is smaller than bulk steel, its alloying elements and additional processing steps could increase the CO₂ intensity¹⁸. The variability and uncertainty in alloy steels associated environmental impact make a clear estimation difficult, but it can be stated that this is at least equivalent to structural steel.

¹⁷ Ranging from 1.7 – 2.1 tCO₂/t-eq, including coke making, pelletizing, sintering, iron- and steel making, casting, hot- and cold rolling, and processing (galvanizing, coating) according to Hasanbeigi et al. (2016).

¹⁸ Silicon can be sourced from SiMn (~15% Si, ~66.5% Mn) or FeSi (15-90% Si) with associated emissions of 2.8 tCO₂/t-eq and 3.4 tCO₂/t-eq respectively. Manganese can be sourced from SiMn and FeMn (~80% Mn) with an associated CO₂-eq emission of 1.8 tCO₂/t-eq. Nickel is sourced from FeNi (10-30% Ni) and has a CO₂-intensity of 13.9 tCO₂/t-eq. Chromium is sourced from FeCr (~60% Cr) with 3 tCO₂/t-eq. Emissions are calculated based on cradle-to-gate LCA from raw material extraction through ferroalloy production and refining, including transport between stages. (Haque & Norgate, 2013).

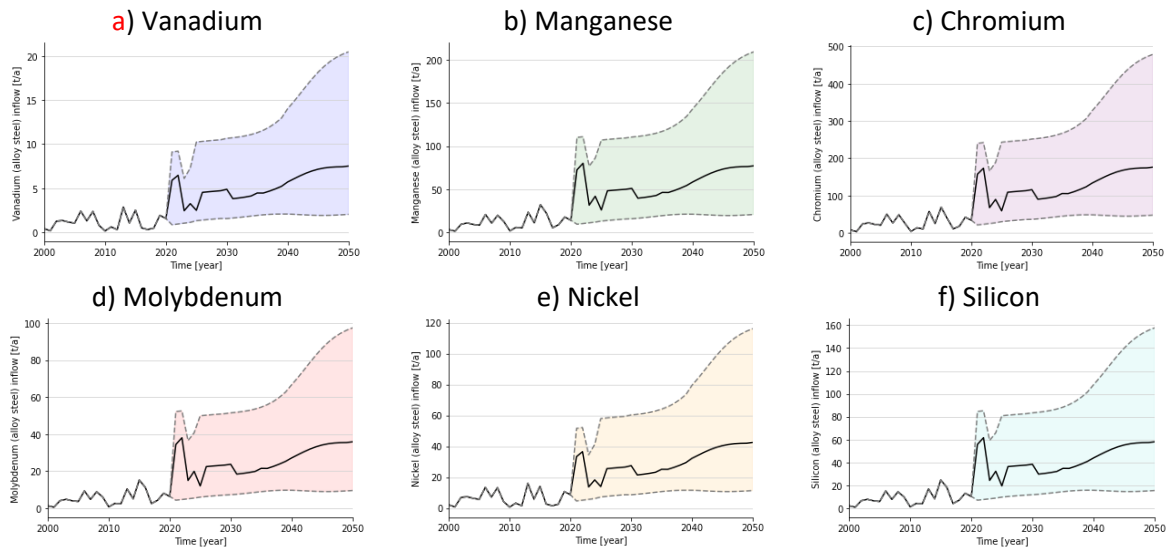


Figure 3-18: Inflow/demand for various alloying elements in alloy steels.

Iron inflows are largely from hub- and generator iron, which is spheroidal graphite cast iron. The alloying elements present in this type of iron are described in *Appendix B Material compositions*. Using these elemental compositions, a demand for these elements is determined and shown in Figure 3-19 a-e. In this case, magnesium is of most interest due to its criticality (European commission, 2017).

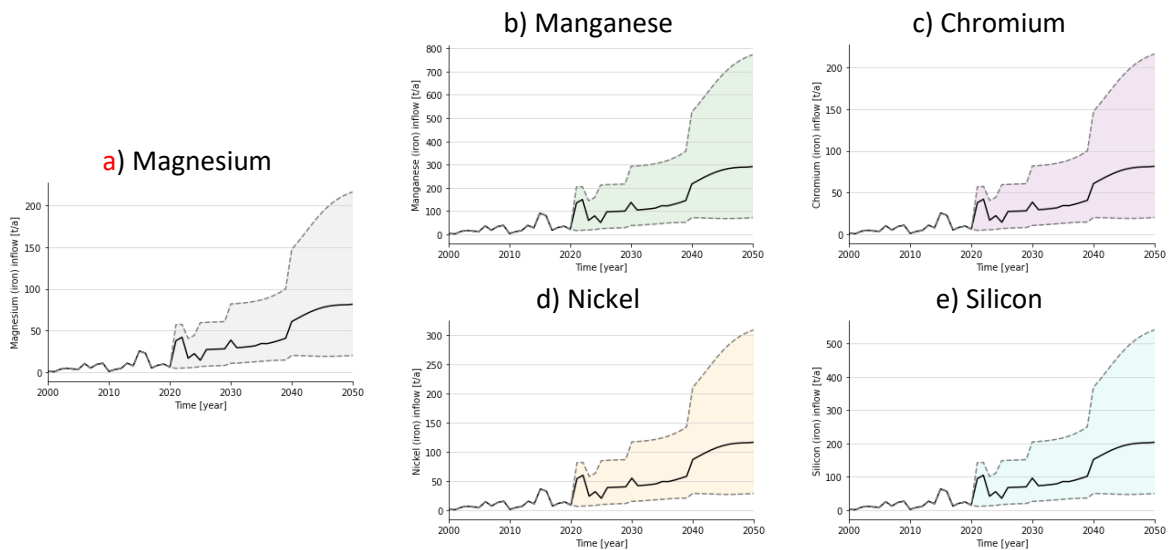


Figure 3-19: Inflow/demand for various alloying elements in cast iron.

A summary of steel and iron inflows and associated impact on climate change assuming a 2 tCO₂-eq/t CO₂-intensity is presented in Table 3-6.

Table 3-6: Summary table for steel inflows and annual CO₂ emissions.

		Low (2030-2050)	Prognosis (2030-2050)	High (2030-2050)
Structural steel (S355)	Inflows/demand [kt/a]	50-100	200-390	400-950
	Impact on climate change [kt CO ₂ -eq/a]	100-200	400-780	800 - 1900
Alloy steels	Inflows/demand [kt/a]	5-5	10-15	22-42
	Impact on climate change [kt CO ₂ -eq/a]	10-10	20-30	45-84
Cast Iron	Inflows/demand [kt/a]	10-40	50-120	120-300
	Impact on climate change [kt CO ₂ -eq/a]	20-80	100-240	240-600

Composites

Inflow of composite material is relevant for estimations on the effect of variations in blade material composition. These effects include the material demand for glass-, carbon- and natural fibres, thermoset and thermoplastic polymers and their associated environmental impacts to limited extent. Another major impacting factor could be the use of composite instead of steel for towers. The extent of the effect of this development is discussed here as well.

Blade material makes up most of the composite material inflow, with only minor additions for from other nacelle cover and nose cone. Since carbon fibre has much larger associated energy use, the environmental impact increase accordingly. The major contributor to carbon fibre environmental impacts is impact on climate change to CO₂ associated with its energy use. Liu & Barlow (2016) estimate a 60% higher CO₂ footprint¹⁹ for blades with higher CF content.

When including the possible development of composite towers, assuming from 2030 all new towers would be composite instead of steel or hybrid more than double the demand for composites (GFRP) can be expected (Results are presented in *Appendix D Sensitivity checks*).

Table 3-7: Summary table for composite inflows.

	Low (2030-2050)	Prognosis (2030-2050)	High (2030-2050)
Composite Inflows/demand [kt/a]	5-8	15 -25	35 – 65
Glass fibre Inflows/demand [kt/a]	4-4	10-16	22-42
Carbon fibre Inflows/demand [kt/a]	0.3-0.4	1 -1.5	2-4
Increased CF content fibre Inflows/demand [kt/a]	0.4-0.8	1.4-2.4	3-6.4
Composite tower Inflows/demand [kt/a]	20-25	40-100	80-250

¹⁹ The system boundary includes the blade factory, transportation and wind farm (Liu & Barlow, 2016).

Permanent magnets

Demand for permanent magnets and consequently among others Neodymium and Dysprosium is important from a critical material perspective. Besides installed capacity scenarios, the inflow of NdFeB is dependent on generator market share scenarios. Therefore, Figure 3-20 shows the LDS, MDS and HDS for generator market shares as described in subsection 3.3.2 Technological developments.

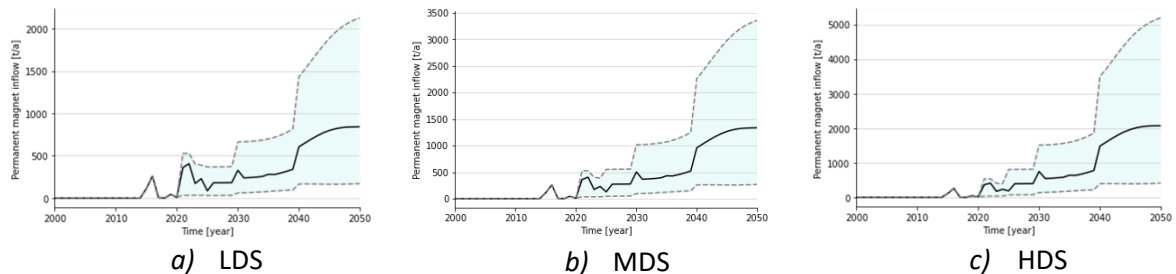


Figure 3-20: Inflow/demand for permanent magnets according to various generator market share scenarios.

Table 3-8 shows the inflows of permanent magnet (NdFeB) under the various scenarios for generator market share development in 2030 and 2050. The specific amounts for Nd and Dy in these magnets can be determined through estimates from Viebahn et al. (2015) of 31% and 2.3% of magnet mass respectively. The resulting demand for these elements is shown in Figure 3-21.

Table 3-8: Summary table permanent magnet inflows.

Inflows/demand	Low (2030-2050)	Prognosis (2030-2050)	High (2030-2050)
LDS [kt/a]	0.1-0.2	0.3-0.8	0.7-2.1
MDS [kt/a]	0.1-0.25	0.5-1.4	1-3.3
HDS [kt/a]	0.2-0.5	0.8-2	1.5-5.2

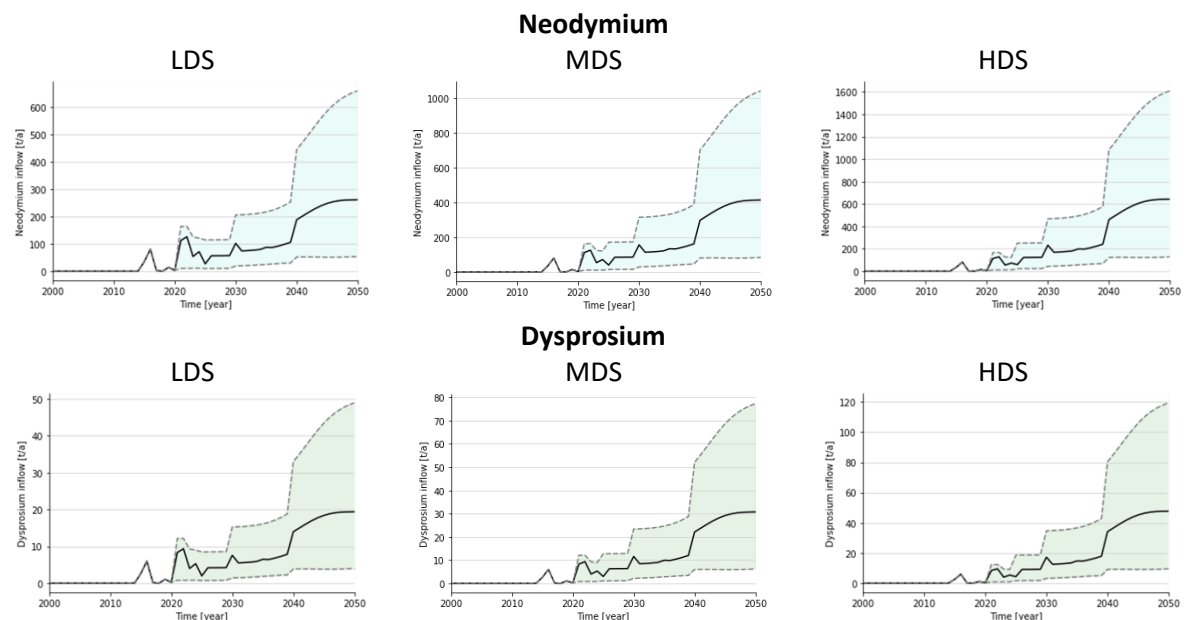


Figure 3-21: Inflow/demand for Nd and Dy following the demands for permanent magnets.

To put these results in perspective, currently the total inflows for the European Union for Neodymium in vehicles and electronic & electrical equipment are 2.9 kt/a (Huisman et al., 2016). Current (2016) world production is estimated at 7.17 kt/a according to USGS (Gambogi, 2019a).

Yttrium

Yttrium (Y) is considered in this case to be used for high temperature superconductor generators. Gadolinium (Gd) is also considered a potential material used in these generators, but for yttrium 0.3 kg/MW material requirement is provided by Viebahn et al. (2015). Yttrium is found in combination with other rare earth elements/lanthanides. This puts the material in the same supply risk as the other REEs, making it potentially critical as the economic importance becomes higher due to application in wind turbine generators or other applications. Therefore, an understanding of potential inflows is useful. Only the LDS scenario considers the use of HTS wind turbines, starting from 5% in 2030 and 10% in 2050 for offshore. Under this scenario the cumulative demand for yttrium until 2050 for this scenario amount to 0.12 - 1.43 tonne, with 5-7 kt/a world production (Gambogi, 2019b). Further stock and outflow developments are presented in *Appendix F Additional results*.

Copper and aluminium

Copper and aluminium are used mostly for electrical purposes in wind turbines. For aluminium, use in tower infrastructure (e.g. ladders, lighting) is omitted and therefore only applications in cables and transformers are included. Copper is also strongly influenced by generator copper use and therefore analysed under the various generator scenarios. Results for MDS and LDS are very similar and therefore grouped. Inflows are summarized in Table 3-9.

Table 3-9: Inflows of copper (under various generator market share scenarios) and aluminium.

	Low (2030-2050)	Prognosis (2030-2050)	High (2030-2050)
Copper MDS/LDS Inflows/demand [kt/a]	1-1.5	2-4	6-12
Copper HDS Inflows/demand [kt/a]	1-1.9	3-6	6.5-13.5
Aluminium Inflows/demand [kt/a]	0.1-0.15	0.25-0.45	0.6-1.25

Concrete

Concrete inflows for the low and prognosis are very similar, since concrete is only used onshore and low and prognosis are similar for onshore wind energy development. Variations in hybrid tower share are analysed in *Appendix D Sensitivity checks*. As foundations create most of the concrete demand, little variation can be observed for the low and prognosis scenario. The high scenario shows a decrease in inflows up to 100 kt/a in 2050 when no hybrid towers are used. Inflows are summarized in Table 3-10.

Table 3-10: Inflows of concrete

	Low (2030-2050)	Prognosis (2030-2050)	High (2030-2050)
Inflows/demand [kt/a]	100-100	100-130	300-600

3.4.2 Stock

The societal stock of materials in wind turbines is relevant to estimate its potential for secondary materials. As capacity is an important variable, Figure 3-22 a) shows the development of capacity stock or total installed capacity. In addition, Figure 3-22 b) shows the total number of turbines installed, which, due to an increase in average rated turbine capacity, is relatively decoupled from increase in installed capacity.

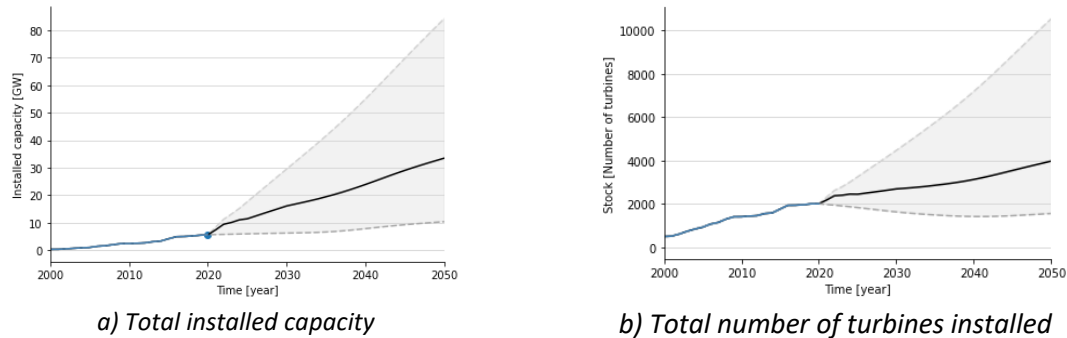


Figure 3-22 a): Installed capacity (stock) of wind turbines in MW, the currently installed capacity of 5.7 MW is indicated with a blue dot. b) Installed number of turbines.

An overview of material stocks is presented in Figure 3-23 a-h. The components that make up these flows are shown in *Appendix E Stacked results*. Similar developments can be observed with exceptions for permanent magnets that are strongly influenced by PMG implementation and concrete that is only used for onshore wind turbines.

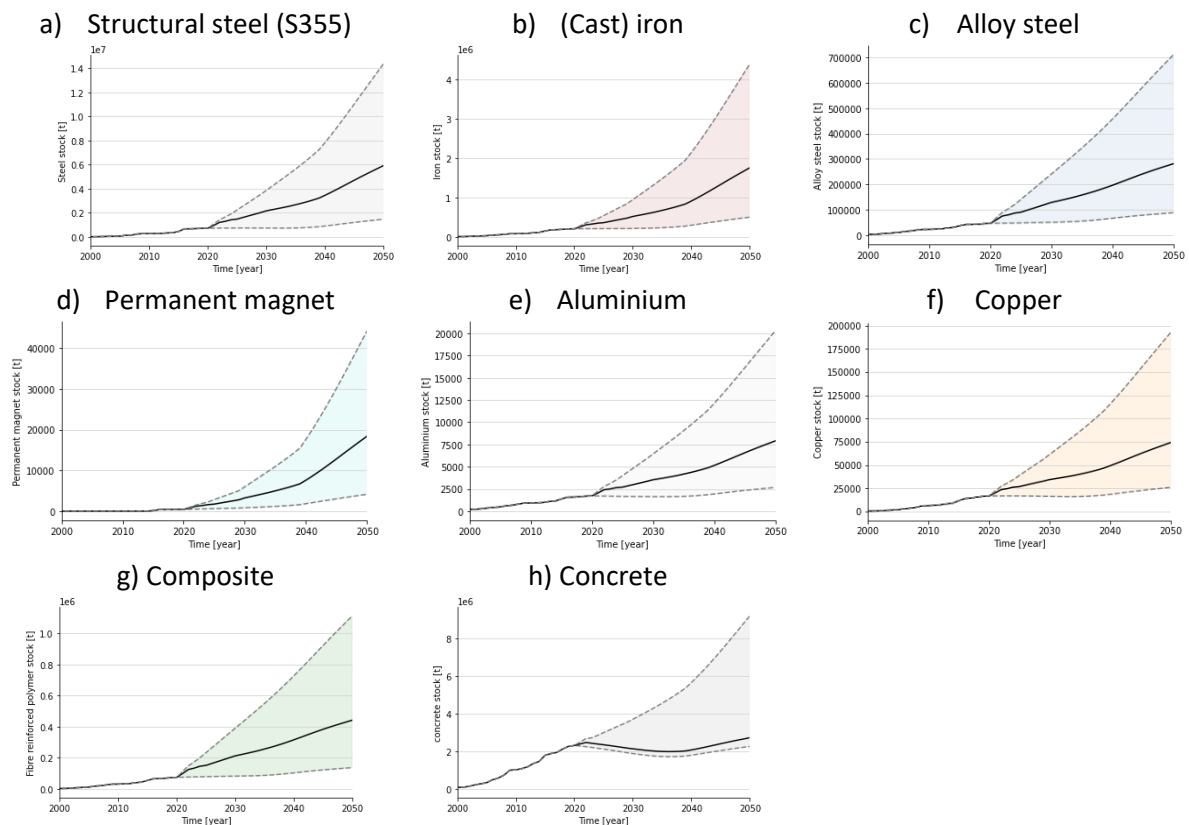


Figure 3-23: Stocks of major material groups.

Further analysis of individual inflows is done for critical, valuable and bulk materials. An overview of material stocks is presented in Table 3-11.

Steel and Iron

Where steel and iron and their alloying elements were discussed for the inflows to describe demand, the stock for these materials is analysed without going further into specific stocks for alloying elements. *Appendix F Additional results* shows the stocks for alloying elements. Increasing stock is dominated by offshore support structures, which is expected due to offshore installed capacity increase. Iron increase is mainly due to generator iron and hub iron.

Composites

As most of the composite stock is from blade material (scaling with capacity) the development in stock is similar to installed capacity. Stock of carbon fibre in blades builds up after 2010, because only blades after 2010 and above a turbine rated capacity of 2 MW contain carbon fibre. Composite use in towers could lead to a composite stock of around 1 Mt in 2050 (Table 3-11), substituting roughly double that in steel. This is under the assumption that after 2030, all steel towers would be substituted with composite towers. This scenario leads to a strong increase in composite stock after 2030.

Permanent magnets

Stock buildup for NdFeB occurs after 2015 as the first PMG's were implemented. As this is highly influenced by generator technology market shares, variations for the LDS and HDS scenario are considered. The LDS scenario shows very similar permanent magnet stock, while for the HDS scenario,

Copper and aluminium

Stocks develop as expected, with variations for copper in the HDS scenario.

Concrete

As mentioned, concrete is dominated by onshore wind turbines and therefore develops similarly in low and prognosis scenario. As the share of concrete towers is difficult to estimate, these flows are very uncertain. The decrease in concrete stock could indicate the share of concrete that is determined for the historical inflows and future inflows is not balanced.

Table 3-11: Summary table for material stocks for 2030 and 2050 under low, progenies and high scenario.

Material	Stock [kt]		
	Low (2030-2050)	Prognosis (2030-2050)	High (2030-2050)
Steel	700-1500	2000-6000	4000-14200
Alloy steel	75 - 100	120-290	250-700
Iron	250-500	500-1750	1000-4200
Composites	100-180	200-410	400-1150
GF	60-100	150-300	250-700
CF	5-9	12-25	22-65
CF (increased content)	5-15	15-40	30-100
Composite towers	0-400	0-1250	0-3500
Permanent magnets LDS	1-2.5	2.5-12	5-27
Permanent magnets MDS	1-4	3-19	6-45
Permanent magnets HDS	1-8	4-28	10-67
Copper LDS/MDS	20-25	27-75	60-190
Copper HDS	20-25	40-80	60-210
Aluminium	2-2.5	3.8-7.6	7-20
Concrete	2000-2100	2100-2200	3900-9000

3.4.3 Outflows

Modelled outflows in capacity are shown in Figure 3-24. Additionally, historic decommissioning is shown in red bars, which validates the model results until 2019. It can be observed that the shape of the outflows shows two peaks around 2030 and 2050. These peaks can be explained through an early peak in outflows from onshore wind and a larger late peak in outflows from offshore wind turbines (As demonstrated in *Appendix F Additional results*). The maturity of the current onshore stock and rapid increase for offshore wind energy are the main drivers here, but an effect from variations in dynamic lifespan can also be observed in *Appendix D Sensitivity checks*. This effect can be observed in any dynamic system that reaches a steady state as delayed response.

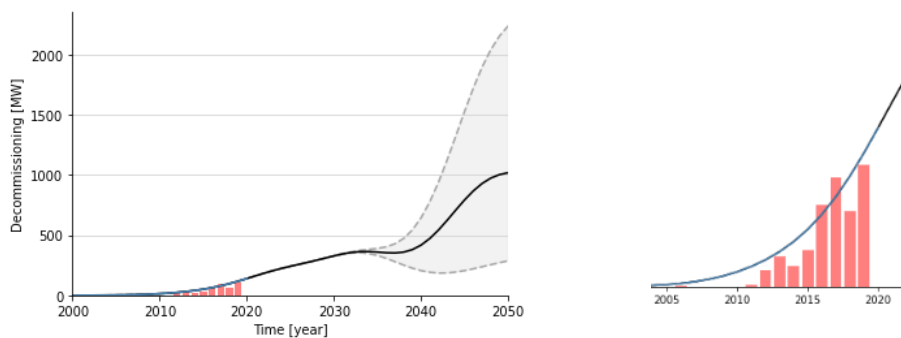


Figure 3-24: Outflows in capacity or decommissioning [MW]. The red bars indicate historic decommissioning and validate the model results up to 2019.

An overview of material outflows if presented in Figure 3-25 a - h.

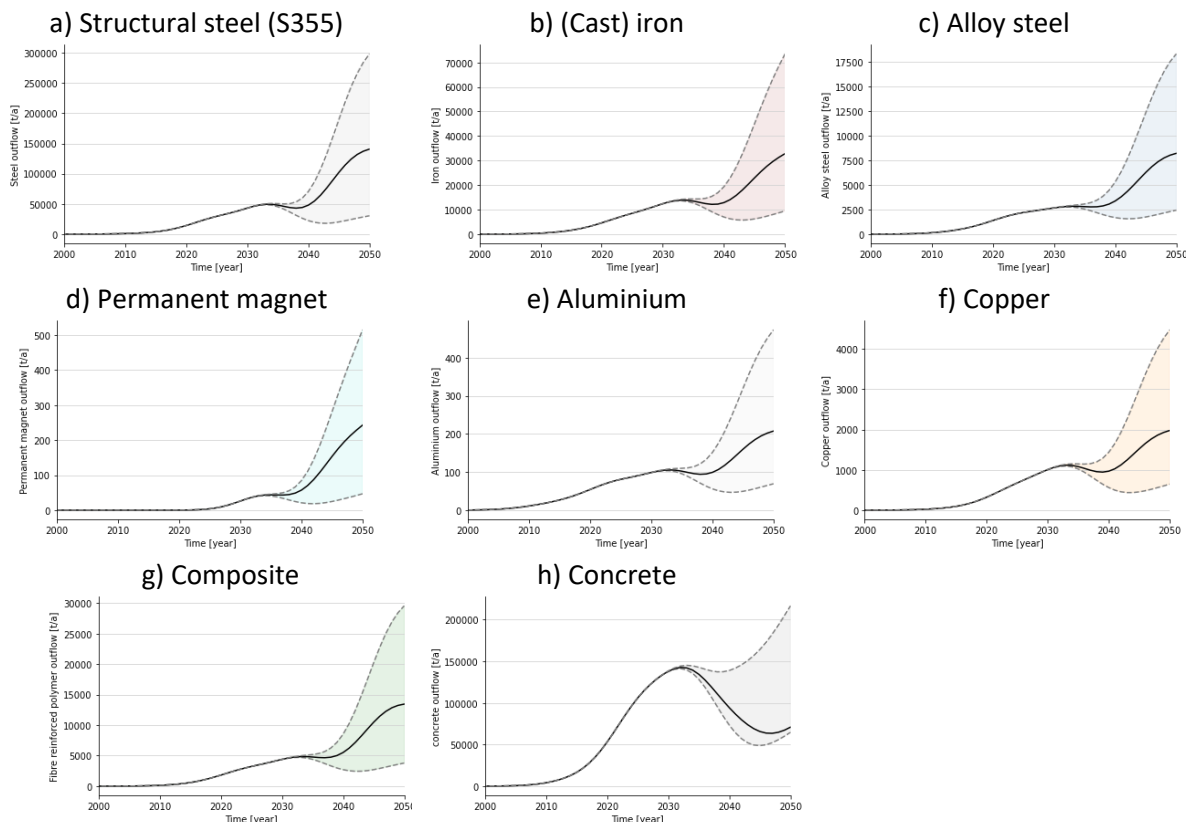


Figure 3-25: Estimated outflows of major material groups

Further analysis of individual inflows is done for critical, valuable and high environmental impact materials. Outflows are summarized in Table 3-12.

Steel and Iron

Being strongly influenced by offshore support structures, structural steel shows a stronger peak around 2050 as this is where most offshore outflows occur. Cast iron and alloy steel are less strongly associated with offshore developments and therefore show a smaller peak. Furthermore, alloy steel is influenced by the use of geared drivetrain technology that could affect its outflows. The outflows include critical alloying elements that are a valuable input for material recovery.

Composites

Composite outflows occur in a similar shape as the other flows. Carbon fibre has a stronger increase before peaking as it is used only after 2010 in the model. Under the increased CF content, a stronger effect can be observed.

Permanent magnets

Also due to later implementation and increasing PMG shares, permanent magnets show a steeper increase. Outflow of permanent magnets leads to a potential supply for critical materials and therefore a valuable input for material recovery.

Concrete

Concrete outflows are again dominated by onshore wind energy and therefore show different shapes. The low and prognosis scenario show a peak outflow of 140 kt, the high scenario shows the same, but without the decrease.

Table 3-12: Summary table of material outflows for 2030 and 2050 under low, prognosis and high scenario.

Material	Outflows [kt/a]		
	Low (2030-2050)	Prognosis (2030-2050)	High (2030-2050)
Steel	50-30	50-145	50-300
Alloy steel	2.5-2.5	2.5-8	2.5-17.6
Iron	11-10	11-32	11-72
Composites	5-4	5-14	5-30
GF	2.6-2.5	2.7-8	2.6-18.5
CF	0.23-0.25	0.23-0.8	0.23-1.75
CF*	0.25-0.25	0.25-1	0.25-2.2
Composite towers	0-3	0-5.5	0-14
Permanent magnets LDS	0.04-0.04	0.04-0.18	0.04-0.37
Permanent magnets MDS	0.04-0.05	0.04-0.24	0.04-0.5
Permanent magnets HDS	0.04-0.08	0.04-0.31	0.04-0.7
Copper MDS/LDS	1-0.6	1-1.9	1-4.2
Copper HDS	1-0.7	1-2	1-5
Aluminium	0.1-0.07	0.1-0.2	0.1-0.5
Concrete	140 -70	140 -75	140-210

Material recovery

Wind turbine blades being buried at end of life in Wyoming (USA). Landfilling is regarded as the least favourable waste management strategy (Skelton, 2017), but what are the alternatives?

Source: Bloomberg (2020)

Photographer: Benjamin Rasmussen for Bloomberg Green



3.5 MATERIAL RECOVERY

This section covers the results for material recovery. For each material group, possible (conventional and novel) recycling route(s) are discussed and secondary material flows are calculated. Additional background on material recovery (general waste management and recycling in the context of wind turbines) is provided in *Appendix H*. Aspects such as hibernating stock, required scrap material throughput for dedicated recycling infrastructure and potential markets for secondary material are discussed where relevant. Recycling, or any other form of material or product recovery is preferable over disposal because it makes resources available, but only when this makes economic sense and environmental sense. This entails the process should be economically viable and provide reductions in environmental impact compared to primary production and disposal. Therefore, steel, composites and permanent magnets are further analysed in context of economic and environmental aspects. This leads to identification of possible issues for future implementation.

3.5.1 Metals

Recycling of metals is often well-established for common metals like steel, copper and aluminium. A major part of a wind turbines total mass is metal, principally structural steel. Other steels, iron, copper and aluminium form the rest of the bulk metal share. Minor but valuable and/or critical metals are often used as alloying elements and therefore require specific recovery methods. Recycling of alloying elements occurs as part of the base metal recycling, but often entails non-functional recycling where alloying elements become diluted with virgin base metal. Selective recycling of stainless steels is a good example of functional recycling of these alloying elements without removing them from the base material. Two major refining routes can be distinguished for metals; pyrometallurgy²⁰ and hydrometallurgy²¹. These routes are used in primary and secondary refining depending on the specific metal. Combined pyro- and hydrometallurgical routes are common in both primary production and recycling as well. A third category is sometimes distinguished, namely electrometallurgy²².

Steel & Iron

Alloying elements are often a small share of steel and iron (0.01-20%), but can be interesting to focus on for recovery due to their value, environmental impact and/or criticality. Recycled steel is 90% less energy intensive than primary steel production (EIA, 2014), hence significant reduction in environmental impacts are achieved. Critical alloying elements include tungsten (W), niobium (Nb), magnesium (Mg) and vanadium (V) of which only V and Mg are identified as present in wind turbines. Another aspect of this wide variety in elemental compositions and heavily recycled material is the occurrence of tramp elements. Tramp elements can have detrimental effects on the quality of the steel or iron and are often difficult to remove (e.g. sulphur, phosphorus and copper).

Collection rates of steel in wind turbines are expected to be very high due to high concentration and legislation, with exception of monopiles. Monopiles are currently cut 1-2 m below the sea floor (Topham et al., 2019), leaving roughly 57% on site (depending largely on sea floor depth and soil conditions).

²⁰ Pyrometallurgy consists of roasting, melting and/or smelting and therefore involves high temperatures.

²¹ Hydrometallurgy operates at lower temperatures and makes use of chemical solving and leaching.

²² Electrometallurgical refining uses differences in electric potential through which metal is deposited in very pure form on the cathode. The metal can be in the anode in less pure form, dissolved or precipitated. Some processes use molten salts and hence higher temperatures, but the majority can be performed at low temperatures with water-based solutions.

Separation of steels from other materials often occurs via magnetic separation. When various steel alloys are mixed, magnetic separation can also be used to separate austenitic steels from the scrap. Ferromagnetic steels cannot be separated by a magnetically from other carbon steels. Nakajima et al. (2013) discuss material flows for nickel, chromium and molybdenum in steel as they constitute the principal alloying elements and conclude that better separation of steel alloys can lead towards more efficient resource use. It is generally not feasible to extract alloying elements from steel and iron due to reduction of metal-oxides equilibrium, but selectively recycling specific steel grades can result in functional recycling and reduce tramp elements. Therefore, this option is considered for this study. Two major steel recycling routes can be distinguished: scrap addition in primary production (25-30%, blast furnace and basic oxygen furnace (BOF)) and secondary production with electric arc furnaces (EAF). Both routes lead to a remelting yield of 94% (Pauliuk et al., 2017). Meaning that 6% of base metal and alloying elements are lost to the slag and dust. Steel making is generally a batch process where batch sizes for the BOF-route range from 50-350 tonne and for EAF 80-150. This indicates required mass for selective recycling.

First, structural steel is considered. This material generally represents most of the wind turbine mass and consists of a s355 or similar. For this it is interesting to see only total steel mass as quality requirements for this type of steel are generally not high and therefore downcycling of alloying elements is not a major issue. Figure 3-26 shows the availability of secondary steel. As steel recycling in the Netherlands only occurs in primary steel production at Tata steel IJmuiden, this route can be considered for domestic recycling, but the steel is likely traded on the international scrap market. The availability of secondary structural steel is presented in Table 3-13.

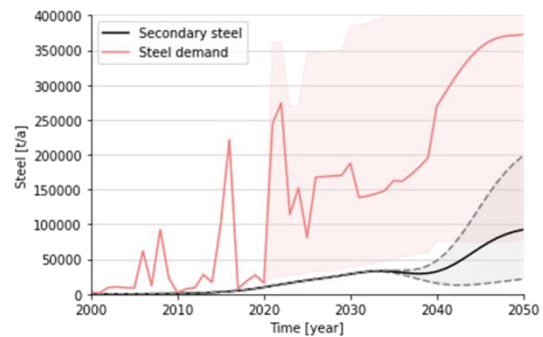


Figure 3-26: Secondary structural steel supply (grey) for a major part from towers and offshore support structures and demand from wind energy (red)

The bulk of losses occurs in hibernating stock of monopiles remaining in the sea floor. Collection of monopiles is therefore a limiting factor in steel recovery from wind turbines. Methods to remove the monopile completely are being developed (GROW, 2020) and could potentially lead to additional steel recovery of 200 kt in 2050 under the prognosis scenario (Appendix H, Figure H-2). When business as usual continues, hibernating stock could range from 150 kt – 650 kt steel by 2050 as shown in Figure 3-27. The availability of secondary structural steel with full monopile removal is presented in Table 3-13.

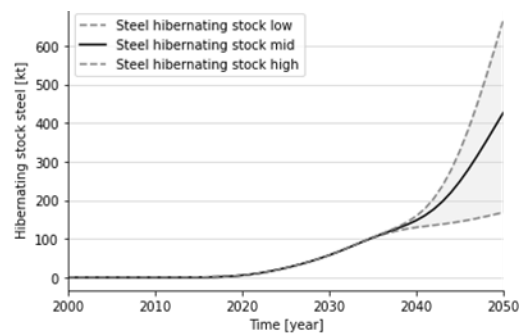


Figure 3-27: Steel hibernating stock due to partial monopile recovery.

Alloy steels can be found in gears, generator, shafts and bearings. As exact application of specific alloys is uncertain, the outflows are subject to a varying degree of certainty. Secondary alloy steels are shown in Figure 3-28. These contain various alloys, including CrMo, CrNiMoS and CrMoV. These alloys can be separately collected and recycled to enable functional recycling of all alloying elements. If these alloys were to be mixed with primary steel production, the specific function of the alloying elements would be lost. Since alloy (stainless) steels are valuable, separate collection and recycling of these steels is common practice (ALURVS, 2020). More accurate identification of specific alloys could however improve the separation and therefore efficiency of recovery. The potential for recovery of individual alloying elements is shown in *Appendix F Additional results*. Vanadium, present in CrMoV steel in gears, is considered critical. Therefore, Figure 3-29 shows the potential of meeting demand (from wind energy) with secondary supply is roughly 30% by 2050. However, share of geared and direct drive wind turbines is subject to variation. The availability of secondary alloy steel is presented in Table 3-13.

Spheroidal graphite cast iron (SG-iron) can be found in bed plate, hub, casings for generators and gearboxes. SG-iron is not particularly high in alloying elements, but contains critical Mg and could therefore warrant separate collection and recycling. However, as it is less valuable than alloy steel it might be more interesting to be mixed with structural steel scrap in primary production. Secondary iron supply is shown in Figure 3-30. The availability of secondary iron is presented in Table 3-13. If selectively recycled, up to 25% of Mg demand can be supplied through secondary material by 2050.

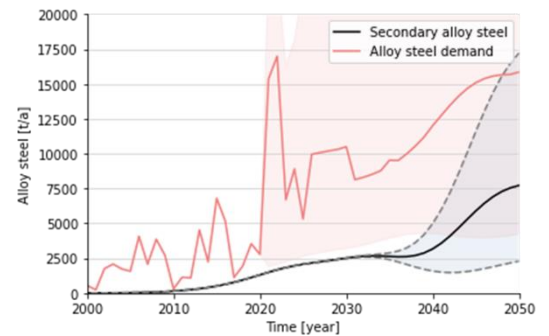


Figure 3-28: Secondary alloy steel, containing a mix of various alloy steels (grey) and demand from wind energy (red)

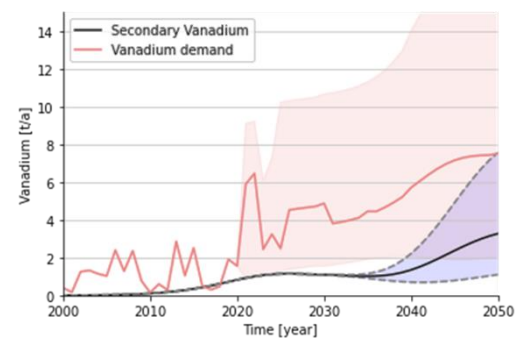


Figure 3-29: Potential for secondary Vanadium (blue) in alloy steel to meet demand from wind energy (red).

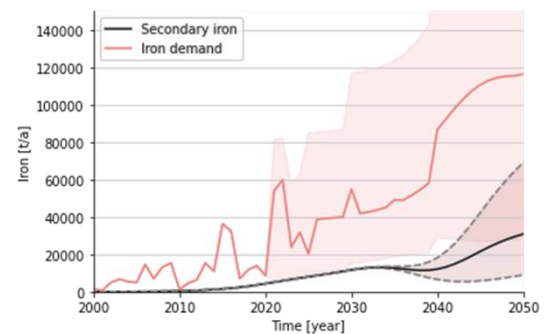


Figure 3-30: Estimated availability of secondary iron (brown) and demand for aluminium from wind energy (red)

Table 3-13: Supply of secondary steel, alloy steel and iron.

Primary material	Recycling route	Secondary material(s) [kt/a]			
		Material	Low (2030-2050)	Prognosis (2030-2050)	High (2030-2050)
Steel	Primary/EAF	Steel	30-20	30-90	30-200
	Primary/EAF, full monopile recovery	Steel	40-25	40-130	40-270
Alloy steel	EAF	Alloy steel	2.5-2.5	2.5-7.5	2.5-17.5
Iron	(EAF)	Iron	12-10	12-30	12-70

Copper

Copper is found in many components associated with the electrical systems in wind turbines. Very small amounts (e.g. for wind turbine control) are too detailed for this study. The copper recycling system is perhaps one of the most efficient and well-established recycling systems as copper is a high value metal. In a dynamic analysis of European copper flows, Soulier et al. (2018) mention 50% of copper in the EU comes from secondary sources (30% worldwide). Very pure copper can, if selectively collected, be melted directly to high quality secondary copper. For lower quality scrap or higher end-quality, electro refining is applied where impure copper on the anode is deposited on the cathode in very high purity.

The copper in wind turbines is almost exclusively for electrical purposes (99.99% purity) and therefore assumed to be of high purity. Separation of copper from other materials differs per component. Cables are composed of copper, aluminium and polymers for protective coating. Dedicated cable stripping machines (Cable recycling, 2020) are most efficient at separating these materials. The copper in transformers and generators is present in coils and represent the largest share of copper in wind turbines. Most efficient removal of the copper is likely manual disassembly, which could be economically viable due to high value and concentration. Further disassembly of the coil could involve cutting or shredding of the coils to remove the steel and polymers present in the coil. The mix of copper, steel and polymers can be separated by consecutive magnetic (steel) and eddy current (copper) separation. Copper in blades might not be economically interesting due to the low volume but concentrates in the tip and a conductor cable down the length of the blade. The tip conductor might be easy to remove but the conductor cable would be integrated in the composite material and hence not easy to remove.

Ruhrberg (2006) Assesses the recycling efficiency of copper from end-of-life products in Western Europe. End of life wind turbines are considered as industrial electrical equipment waste (IEW). According to Ruhrberg (2006) the recovery rates are therefore 98% for cables and transformers and 93% for generators. The copper in blades is very specific (and dependent on blade recycling methods) therefore its recovery rate is assumed to be similar to complex waste flows similar to municipal solid waste incineration (recovery from bottom ash), 13.5%. Using these rates on the copper outflows, the secondary supply of copper can be calculated as shown in Figure 3-31. The availability of secondary copper is presented in Table 3-14.

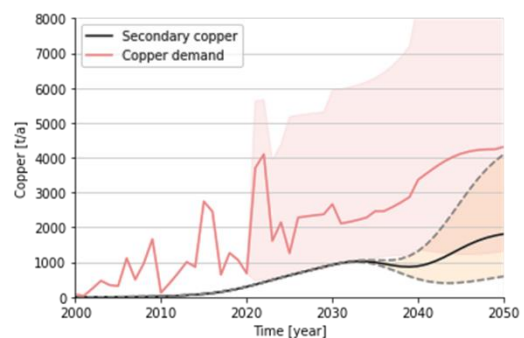


Figure 3-31: Estimated availability of secondary copper (orange) and demand for copper from wind energy (red)

Table 3-14: Supply of secondary copper.

Primary material	Recycling route	Secondary material(s) [kt/a]			
		Material	Low (2030-2050)	Prognosis (2030-2050)	High (2030-2050)
Copper	(s)melting/refining	Copper	1-0.6	1-1.8	1-4

Aluminium

The use and separation of aluminium in cables and power converters is similar to copper. Recycling aluminium is a well-established process and can be described through remelting and refining. Remelting offers potential due to the expected purity of the scrap, contamination of the melt with unwanted elements is minimal. However, if same grade aluminium is desired, refining must be considered. This leads to an estimated 85% material recovery, based on process losses in Boin & Bertram (2005). Recovered aluminium and demand is shown in Figure 3-32. As primary production is very energy intensive, recycled aluminium can reduce energy use by 74 % (EIA, 2014). The availability of secondary aluminium is presented in Table 3-15.

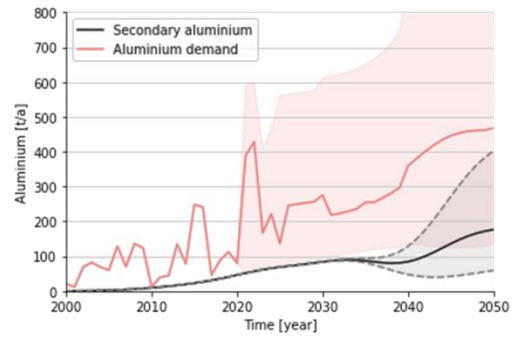


Figure 3-32: Estimated availability of secondary aluminium (grey) and demand for aluminium from wind energy (red)

Table 3-15: Supply of secondary aluminium.

Primary material	Recycling route	Secondary material(s) [kt/a]			
		Material	Low (2030-2050)	Prognosis (2030-2050)	High (2030-2050)
Aluminium	(s)melting/refining	Aluminium	0.1-0.05	0.1-0.18	0.1-0.4

Permanent magnets

Recycling can take place as magnet-to-REE or magnet-to-magnet (reprocessing). Critical REEs specifically neodymium (Nd), dysprosium (Dy), Praseodymium (Pr) and Terbium (Tb) are present in varying quantities in permanent magnets. Several strategies to limit criticality exist among which the improvement of recycling and recyclability of these materials (Offerman, 2019). Recycling processes for these critical REEs is therefore much needed, but currently only at lab scale as volumes are not yet large enough to develop recycling infrastructure and technologies are still under development.

The process of removing the magnets from the generator could be manual or automated²³ but requires demagnetizing the magnets because of their high magnetic strength (Tanaka et al. 2013). This involves heating the magnets to the point where they lose their magnetic properties. Wind turbines specifically provide a highly concentrated source of permanent magnets enabling easier recovery compared to consumer electronics (e.g. harddrives) or electric vehicles (electric motors). Furthermore, the sintered (instead of bonded) type is more commonly used indicating a single magnet type (Pavel et al. 2016). Material compositions have changed historically due to substitution and efficiency improvements (Viebahn et al. 2015) creating variations in elemental composition.

For magnet-to-REE, Schulze & Buchert (2016) estimate global REE recycling potentials from NdFeB magnet material and give an overall REE extraction efficiency of 75%²⁴. As many conceptual recycling routes for magnet-to-REE recycling are under development this number is subject to much variability (Table 3-16). Furthermore Habib & Wenzel (2014) assume a 90% recycling efficiency for wind turbines specifically and Sprecher et al. (2014) assume 99% recycling efficiency through leaching

²³ Assembly is already automated according to ExceptionalEngineering (2020), potentially making automated disassembly possible.

²⁴ Including 90% collection rate, 90% efficiency rate disassembly and 92% efficiency rate recycling

for permanent magnets in hard disk drives. With 70%-99,9% recycling rates of Nd from NdFeB magnets, high recycling efficiencies seem possible²⁵.

Table 3-16: Neodymium (Nd) yield from various recycling routes for permanent magnets (NdFeB). Based on an overview from Tanaka et al. (2013).

Method	Recycling efficiency Nd from NdFeB
Fractional crystallization	97.1%
Whole leaching process	70-98%
Oxidative roasting	95.7 – 99.99%
Selective leaching	70%
Hydrothermal method	99%

Magnet-to-magnet recycling could provide options without the need to extract REE's and consequential processing required to make new magnets. However, magnet to magnet recycling often involves quality losses with 10-20% decrease in strength (Zakotnik et al., 2006), making application in wind energy less likely. Walton et al. (2015) use hydrogen-based recycling leading to roughly 90% extraction with >90% of magnetic properties. Binnemans et al. (2013) exclude downcycling and estimate a 30%-60% collection rate and 55% recycling efficiency rate, leading to estimates for global magnet recovery of 16.5% -33%.

The availability of secondary permanent magnets is presented in Table 3-17. For fair comparison, collection and extraction efficiencies (0.81) from Schulze & Buchert (2016) are used for each recycling route. Results for magnet-to-magnet recycling are presented based on estimates from Walton et al. (2015) (0.9) leading to secondary magnets with >90% of magnetic properties and Binnemans et al. (2013) (0.55) where no downcycling is assumed. Magnet-to-REE recycling is based on Schulze & Buchert (2016).

Depending on the required volume for efficient and economic recycling, these magnets will be mixed with other magnets or not. For efficient material recovery, a closed loop for wind turbines would be ideal, but sufficient scale would be needed. Current pilot plants (SusMagPro, 2020) operate at 6-50 t/a. No estimates for required full-scale plant throughput are found in literature, but according to TU Delft recycling expert (dr. Y.Yang, personal communication, June 5, 2020) at least several thousand tonnes throughput is required. As shown in Figure 3-33 a, b, c, this is not attained in any of the scenarios for generator market share. It can also be observed, up to 15% of permanent magnet and therefore REEs can be supplied through secondary material.

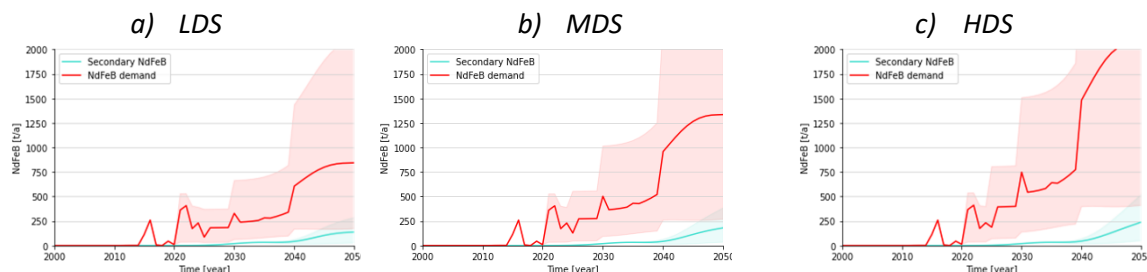


Figure 3-33: Estimated recovered NdFeB (turquoise) and NdFeB demand (red) from wind energy in the Netherlands according to three generator market share scenarios.

²⁵ Most are still at lab scale and are therefore not always representative for full-scale commercial recycling technologies.

The recycling of permanent magnets can alleviate criticality by creating a more diverse supply. Additionally, recycling can be beneficial from an environmental perspective. Environmental impact from REE and permanent magnet production is substantial as demonstrated by Schreiber et al. (2019) in a comparative LCA²⁶ between DFIG, EESG and PMSG wind turbines. Here, the major difference is the drivetrain configuration and therefore use of alloy steel, copper and permanent magnets. Although the EESG wind turbine is estimated to have the largest normalized impact, substantial impacts can be observed for permanent magnets in the PMSG wind turbine that are attributed to abiotic resource depletion (ADP)²⁷. Schreiber et al. further analyse the impact of recycling, which removes the impact of ADP and reduce the normalized impacts significantly. Furthermore, the rare earth origin can result in 50%-66% reduction of these impacts (Schreiber et al. 2019). Sprecher et al. (2014) compare the environmental impacts of primary production, recycling through shredding and recycling through hand-picking of NdFeB magnets in hard disk drives. As losses are significant (>90%) in shredding and wind turbine magnets are suitable for manual dismantling, hand-picking is considered most relevant. Here, 88% reduction in energy use and 98% lower human toxicity values are obtained for recycling versus primary production.

Table 3-17: Secondary permanent magnets through magnet-to-magnet recycling with 0.9 (Walton et al., 2015) and 0.55 (Binnemans et al., 2013) recycling rates for >90% magnetic properties (rPM) and virgin magnetic properties (PM) respectively. Magnet-to-REE recycling (Schulze & Buchert, 2016) has a 0.92 recycling rate, also yielding virgin magnetic properties. Collection and extraction rates are taken from Schulze & Buchert (2016) for fair comparison.

Primary material	Recycling route	Secondary material(s) [t/a]			
		Material	Low (2030-2050)	Prognosis (2030-2050)	High (2030-2050)
Permanent magnet	Magnet-to-magnet	rPM	19 -29	19 -175	19 -370
	Magnet-to-magnet	PM	12-18	12-107	12-225
	Magnet-to-REE	PM	20-30	20 - 180	20-380

²⁶ Cradle-to-grave LCA, system boundary includes raw material supply, manufacturing, transport & assembly, operation & maintenance, replacement, dismantling & transport, waste disposal and recycling.

²⁷ Abiotic resource depletion (ADP) is defined as "...the ratio of the annual production and the square of the ultimate (crustal content based) reserve for the resource divided by the same ratio for a reference resource (antimony (Sb))." (van Oers et al., 2019).

3.5.2 Composites

Blades, nose cone and nacelle are made of complex composite materials which results in challenges in recycling. Composites, in this case, refers for a major part to glass fibre reinforced polyester and epoxy. Other constituents can be carbon fibre reinforced polymers, balsa wood, foams and fillers. For composites, no established industrial recycling routes currently exist. Therefore, multiple options ranging from repurposing to feedstock and material recovery are discussed in this sub-section.

Options for repurposing composites range from using blades as artwork (very limited) to bridges and bike shelters (WindEurope, 2020). Similarly, parts of blades, up to 90wt% of composite (e.g. spar and shell) can be used as beam and sheet materials in construction as more common purposes (J. Joustra, personal communication March 18, 2020). This involves some processing but could still be considered repurposing. The potential for repurposing is very difficult to estimate, but considered to be very limited for full blade repurposing and more adequate for blade section repurposing. The availability of repurposed blade segments is presented in Table 3-19.

Composite recycling can be seen on separate levels; feedstock recovery, composite recycling and fibre recovery. Hagnell & Åkermo (2019) present a clear overview of the various products that can be obtained via the described recycling routes (Figure 3-34). Feedstock recovery overlaps with fibre recovery as matrix material is recoverable as chemical feedstock.

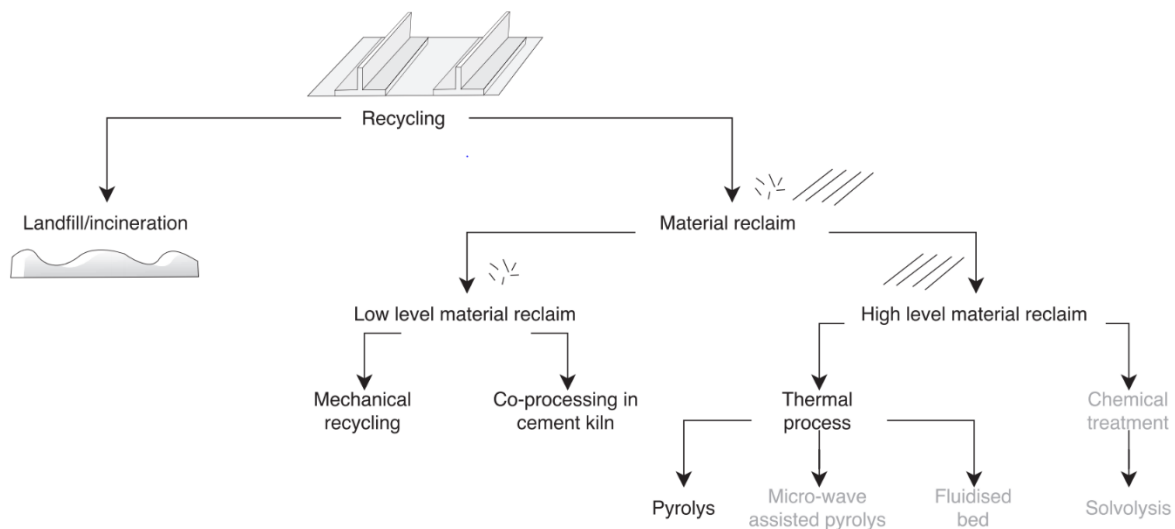


Figure 3-34: Secondary materials for various composite recycling routes. Technologies at lab or pilot scale are shown in grey. Image obtained from Hagnell & Åkermo (2019)

Currently, mechanical grinding is most discussed for glass fibre reinforced polymers and pyrolysis is most suitable for carbon fibre recovery (Rybicka et al., 2016). The economic value of the primary and secondary material plays an important role here as primary glass fibre is relatively inexpensive and secondary glass fibre has degraded material properties. Therefore, recycling becomes costly compared to primary materials. Carbon fibre degrades less and is more expensive. Therefore, it is more economically interesting for extensive recycling methods. Dong et al. (2018). Table 3-18 describes composite recycling technologies based on their technology readiness levels (TRL). Implementation of recycling routes is considered along their respective technology readiness level, meaning cement co-processing, mechanical and pyrolysis will be considered. A wide range of scenarios is imaginable towards 2050 for these and lower TRL recycling technologies. For this study, estimations are made for individual recycling routes, to obtain maximum potential yields.

Table 3-18: Technology Readiness Levels of composite waste management strategies. (Rybicka et al., 2016; Pickering et al., 2015; Pillain et al., 2019).

Waste management strategy	Technology readiness level (TRL)
Incineration and landfill	TRL 9
CFRP pyrolysis and mechanical grinding	TRL 8
GFRP pyrolysis and CFRP mechanical grinding	TRL 7-8
Fluidised bed pyrolysis and solvolysis	TRL 4-(5), lab or almost pilot scale
Microwave heating	TRL 3, further proof of concept

Economic viability of composite recycling is an important aspect that is closely associated with the quality (reinforcement potential) of the recycled material. Figure 3-35 shows a cascading effect in material quality and material cost. As no material to same material recycling exists for composites, the cascading or downcycling results in growing demands for high-end applications and a potential surplus of low-quality materials. The application of recyclates is therefore an important aspect (Liu et al., 2017).

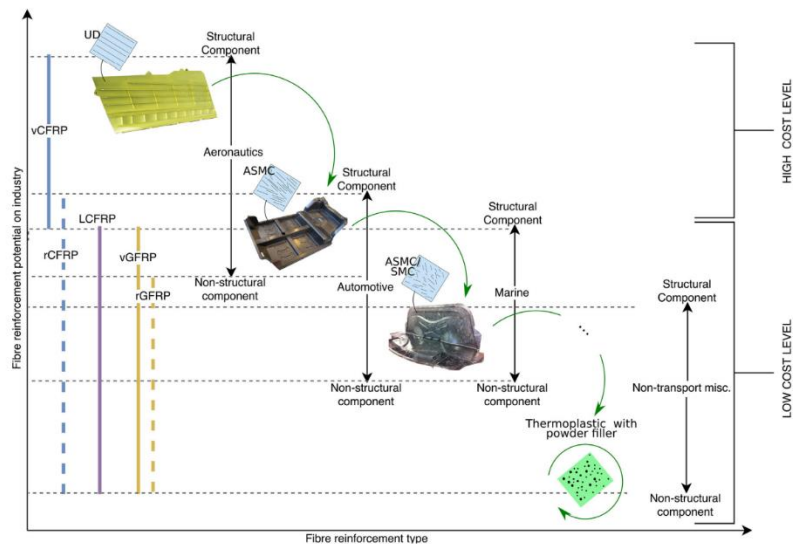


Figure 3-35: Cascading quality and cost level for composite materials. rCFRP and rGFRP indicate recycled carbon- and glass fibre reinforced polymers and v indicates virgin materials. UD stands for uni-directional fibres, which are high-quality, continuous fibres. (A)SMC is (advanced) sheet molding compound uses shorter and less aligned fibres and is therefore of lower quality. LCFRP uses a lignin-based precursor for carbon fibre, which is not relevant for this study. Image obtained from Hagnell & Åkermo (2019).

The first technology that is recognized for composite recycling in the form low level material reclaim is cement co-processing (cement kiln route). This process (Figure 3-36) converts the mineral constituents (fibres) into cement clinker that can be used in cement production, where it is ground and used as binder (Job, 2013). Additionally, energy in the form of heat is recovered. 12 MJ/kg composite waste can be provided by combustion of the organic resin (Job, 2013). It is assumed 100% of fibre material is converted to cement clinker as Jacob (2011) describes 67% material recovery (which is around the composites fibre mass fraction). A major advantage of the cement co-processing route is its existing infrastructure and potential to reduce the environmental impact of cement production. By replacing coal or natural gas used in cement production 16% of CO₂ emissions can be avoided²⁸ (WindEurope, 2020; EPRI, 2020). A major disadvantage is its low level of recovered material quality. Cement clinker recovery from composite waste is shown in Figure 3-37. Additionally, demand for cement in wind energy is shown to identify potential to use the recovered material in a new wind turbine. Assuming a concrete mix ratio of 1:3:6 (cement, aggregate, sand). As cement clinker from composite recycling requires mixing with virgin materials (EPRI, 2020), enough demand is present for the supply of this secondary material. The availability of cement clinker is presented in Table 3-17.

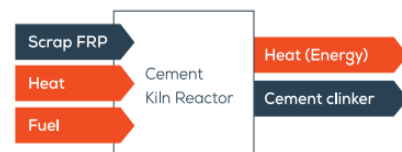


Figure 3-36: Cement co-processing. Image obtained from WindEurope (2020)

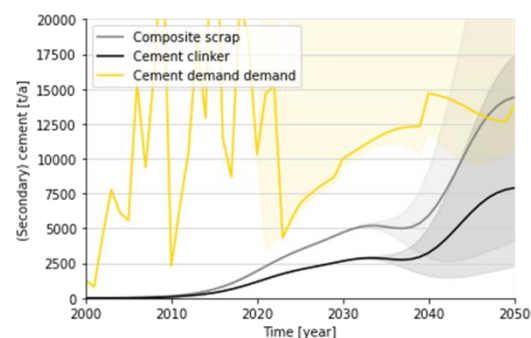


Figure 3-37: Cement clinker from scrap glass fibres compared to composite scrap and cement demand from wind energy.

Mechanical recycling involves shredding or grinding the composite and using the composite scrap as reinforcement or filler. Mechanical composite recycling can be used to form new composites (using the composite scrap as reinforcement in thermoplastic composites (Ecobulk, 2020; Mamanpush et al., 2018; WindEurope, 2020) or filler material in a wide variety of other applications. While being a low-cost option, the material properties of the initial composite material are reduced or completely removed (filler) and problems can occur with abrasive CF in blade material.

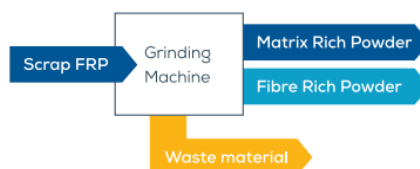


Figure 3-38: Mechanical grinding. Image obtained from WindEurope (2020)

²⁸ No specific system boundary is provided for this statement, but as the “...carbon footprint of cement manufacturing...” discussed it is assumed to cover cradle-to-gate emissions from mineral extraction to cement production including transportation between stages.

Mechanical recycling is discussed as two options, shredding of composite material and use as coarse reinforcement material equivalent (Ecobulk, 2020) and grinding (Figure 3-38). Shredding could lead to high recovery rates equivalent to composite scrap outflows, but has low material quality recovery. Mechanical grinding yields fibre and matrix rich powders, which can be used for fillers and in secondary composites. WindEurope (2020) estimates 40% waste generated in the process and report issues pertaining dust emissions and the necessity for a dedicated recycling plant. Another potential issue for both recycling routes could be the presence of abrasive carbon fibres for the machinery. Dong et al. (2018) estimate 4 kt/a would be the minimum required capacity (break-even) for a dedicated facility. The cost and share of GF/CF and rGF/rCF strongly influence this number, but this is taken as an approximation. The availability of fibre-rich powder or fibrous fraction and required throughput for a recycling plant is shown in Figure 3-39. The availability of the fibrous fraction presented in Table 3-17.

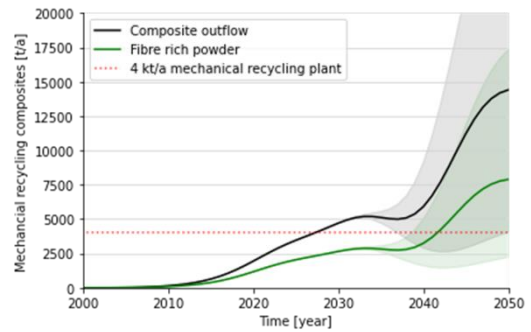


Figure 3-39: Fibre rich powder from scrap glass fibres compared to composite scrap. The dotted red line indicates the composite scrap throughput required to operate a dedicated mechanical recycling facility.

High level material reclaim provides the most valuable material. Therefore, more expensive and intensive fibre recovery methods are subject to research. Two main options currently exist; pyrolysis and solvolysis. Both methods enable fibre recovery (fibre lengths limited by pre-processing) with some degree of quality loss. Pyrolysis involves thermal degradation of the matrix material whereas solvolysis chemically dissolves the matrix. Pyrolysis therefore operates at higher temperatures, but most of the energy needed can be generated by combustion gases (WindEurope, 2020; Naqvi et al., 2018). The products that can be recovered include fibres, hydrocarbon feedstock and fillers. Other (low TRL) options for pyrolysis are microwave pyrolysis (Åkesson et al., 2012) and fluidised bed pyrolysis (WindEurope, 2020). Solvolysis enables recovery of matrix material as feedstock material for new polymers and as it operates at lower temperatures potentially higher fibre quality, but is currently only applied for CF. Finally, high voltage pulse fragmentation uses electrical current to separate fibres from matrix efficiently (WindEurope, 2020). Pyrolysis is currently the most developed fibre recovery technology and is therefore used to determine recovered fibres.

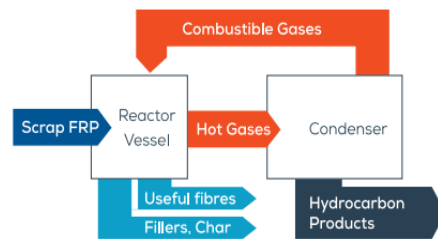


Figure 3-40: Pyrolysis. Image obtained from WindEurope (2020)

Pyrolysis involves high temperatures that lead to decomposition of organic materials, which provides the process energy. Besides fibres, hydrocarbons (fuels/chemical feedstock) can be extracted (Figure 3-40). Naqvi et al. (2018) provide the most recent overview of material recovery from pyrolyzing GFRP and CFRP. Solid, oil and gas yields are described providing multiple valuable products. Generally, up to roughly 70 wt% fibres are recovered with lowered quality, depending on the fibre recovery route used (Cunliffe et al., 2003; Oliveux et al., 2015; Pickering et al., 2006; Torres et al., 2000). Dong et al. (2018) estimate 2 kt/a would be the minimum required capacity (break-even) for a pyrolysis facility based on high value carbon fibre composites. As the value of rGF (0.25 EUR/kg) is at least 52 times lower than rCF (13-19 Eur/kg) (Dong et al., 2018), this number cannot be used for blade recycling. Pickering et al. (2000) estimate a 9 kt/a break-even throughput for glass fibre composites in a fluidized bed pyrolysis process. Although not exactly similar to conventional pyrolysis, this estimate seems most appropriate. Figure 3-41 shows estimated composite outflows, recycled fibre production and indications for required flows for Dutch domestic recycling. In addition, the required inflows of fibre in nacelle cover and nose cone is shown to illustrate potential demand for these fibres within the wind turbine. The availability of secondary fibres and pyrolysis oil is presented in Table 3-19.

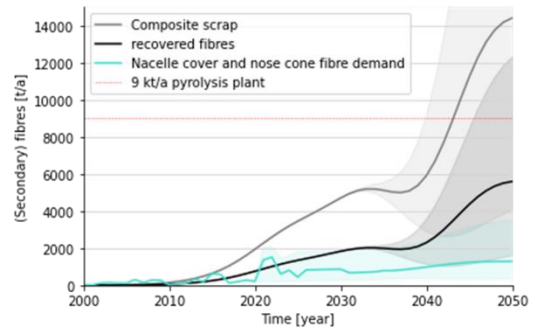


Figure 3-41: Recycled fibres (GF+CF) from scrap glass fibres compared to composite scrap and fibre demand from nacelle cover and nose cone. 9 kt/a composite scrap outflow is required throughput for a domestic pyrolysis plant.

Future trends indicate increased use of thermoplastic composites in wind turbine blades. Although it is not expected for the whole blade to be composed of thermoplastic composite (TNO, 2020), its recycling may be fundamentally different. Cousins et al. (2019) describe recycling of thermoplastic composite wind turbine blades. In addition to composite recycling routes described in this sub-section, thermoforming can be applied, where the (shredded) composite is heated to the glass transition temperature of the thermoplastic matrix. This enables reforming and thus creating a secondary composite material. The use of natural fibres could lead to more efficient incineration, as this is currently difficult due to high amounts of incombustible residue from glass fibres.

Table 3-19: Secondary materials from composite recycling, based on cement co-processing, mechanical recycling, pyrolysis and repurposing. rFiber indicates a fibre is recovered with reduced mechanical properties (quality).

Primary material	Recycling route	Material	Secondary material(s) [kt/a]		
			Low (2030-2050)	Prognosis (2030-2050)	High (2030-2050)
Composite	Cement co-processing	Cement clinker	2.5-2.5	2.5-7.5	2.5-17.5
	Mechanical grinding	Fibrous fraction	2.5-2.5	2.5-7.5	3-17.5
	Pyrolysis	rFiber	2-1.8	2-5.8	2-12
		Pyrolysis oil	1-0.8	1-2.8	1-6
	Repurposing	Sheet	4 - 3	4-11	4-24
Beam		0.5-0.4	0.5-1.5	0.5-3	

3.5.3 Concrete

The recycling of concrete involves several size reduction- and sorting-steps (Figure 3-42). While a less distinctive material for wind energy and almost negligible²⁹ compared to the built environment, concrete use in foundations and towers requires further analysis of concrete recycling. Currently, in the Netherlands 97% of concrete demolition waste is used as road base material (RBM) (Lotfi et al., 2014). However, Lotfi et al. argue a shift towards higher value recycling is needed and expected as road construction in the Netherlands has stabilized and will not create enough demand for increasing concrete waste flows. Hu et al. (2013) assess the sustainability of clean aggregate (CA) concrete recycling. For this process additional processing steps are needed to use concrete aggregate as replacement for conventional aggregates in new concrete. 4-22 mm aggregates can be used for CA, <4mm as RBM and potentially, <1mm aggregates can be used for secondary cement production. Lotfi et al. (2014) describe this technology in more detail and results indicate 15% fines (<1mm), 27% for RBM, 53% for CA (4-22 mm) and 5% larger than 32 mm (possible for CA with crushing). This leads to the secondary materials shown in Figure 3-43.

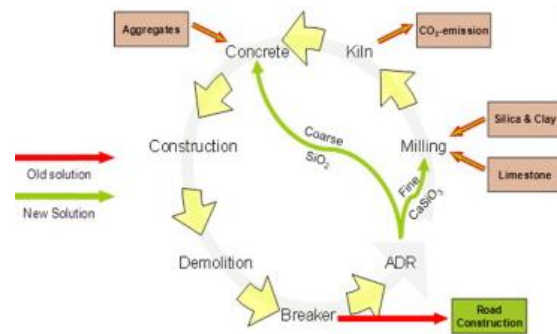


Figure 3-42: Process of mechanical concrete recycling. Image obtained from Lotfi et al. (2014).

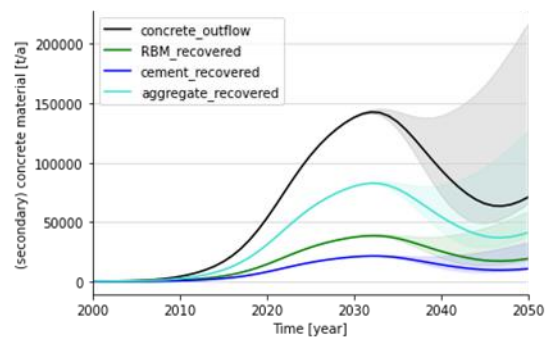


Figure 3-43: Concrete outflow and recycles through high grade clean aggregate recycling (CA).

Table 3-20: Secondary materials from composite recycling

Primary material	Recycling route	Secondary material(s) [kt/a]			
		Material	Low (2030-2050)	Prognosis (2030-2050)	High (2030-2050)
Concrete	Clean aggregate	Cement	20-10	20-10	20-30
		Aggregate	80-25	80-40	80-120
		RBM	40-15	40-20	40-55

²⁹ Flows of roughly 10 Mt/a in the Dutch building sector occur according to Müller et al. (2006)

4 DISCUSSION

This chapter reflects on the method and results to generate insights in underlying limitations, challenges and opportunities. These insights put this study in a broader context and identify areas for improvement and further research. First, method related aspects are discussed, followed by results and finally the research is put in a broader context.

4.1 REFLECTION ON METHODOLOGY

Dynamic material flow analysis is used to describe the inflows, stock and outflows of materials. This method proves very applicable for this type of study. The large number of material flows, scenarios and variables are difficult to handle in conventional dMFA software. Therefore, the Python- based Dynamic Stock Model module is used, that can easily be expanded on. The resulting model is available (*Appendix G Python model*) for further improvement or simple adjustments for various other scenarios, using the Input Excel file (*Input_data.xlsx*). This ensures results of this study can be updated if needed and allows for transparency.

The scenarios chosen for installed capacity represent the maximum ambitions, reasonable prognosis under current policy and minimum relying on market mechanisms only. The current global pandemic demonstrates that extreme events can occur that potentially strongly affect the global- and national economy and consequently expected developments in wind energy. Although not all imaginable events can be included, extremes within the realm of reasonable expectation are useful for considering these future scenarios. Prospective studies face inherent uncertainty of future developments. This study therefore aims to describe material flows in correct orders of magnitude, highlight possible variations in development and provide a basic understanding of scale and timing of (secondary) material flows.

4.1.1 Data uncertainty

Due to the large data requirements on various aspects, such as installed capacity, lifespan, technological developments and material compositions, data uncertainty plays an important role. Several sensitivity checks have been performed that show no extreme variations in results occur.

The lifespan of wind turbines has been discussed in detail (subsection 3.1.4). As there have been only few generations of wind turbines that have reached their end of life, the actual distribution of wind turbine life span remains uncertain. By running the model with a static mean lifespan instead of dynamic, changes can be observed in outflows. These changes are within a reasonable range below 10% of outflows in MW (*Appendix D Sensitivity checks*).

Technological developments are subject to many factors. Among which supply of critical materials. Depending on developments in material cost, technology improvement rates and expectations, a wide variety of possibilities exist. This has been taken into account by including three scenarios for generator market shares and varying material compositions for blades and towers. Further technological developments, including various other wind energy converter designs such as vertical axis and airborne wind energy converters may be commercially interesting after 2030. Due to a vastly different and still conceptual design, these technologies have not been considered, but could strongly influence material use in wind energy.

Material compositions have been derived empirically and based on literature, leading to a variety of estimates that have been validated to some extent using available data and expert opinion. In combination with indicators for specific technologies, there is a strong reliance on the underlying

assumptions. Although most of these assumptions are supported by literature or strong correlations, some components could be improved upon as discussed in *Appendix B Material composition*.

For all uncertainty related aspects, the open-source and adaptable structure of the model is useful for future updates when new insights on development, lifespan or other variables are gained.

4.2 REFLECTION ON RESULTS

The results in this report and appendices are presented within the context of material recovery from Dutch wind energy. Besides recovered material, aspects such as demand for key (critical-, cross-cutting- and bulk-) materials, material stocks, outflows and environmental and economic aspects have been discussed to varying extent.

4.2.1 Scope

The geographical scope of the Netherlands has been considered as this enables a more detailed analysis and identifies specific aspects for the Dutch circular economy. This entails that in reality, inflows occur mostly as wind turbines (with exception of domestically produced components) and individual material inflows should be considered as material requirement that is embodied in the product.

While most accurate for describing materials in Dutch society, this scope leads to limitations as in practice scrap material outflows quickly find their way to international scrap markets. The minimum required throughput for dedicated recycling facilities is not sufficient for recycling Dutch wind turbines alone. Therefore, like in established recycling routes, combination with other sectors (e.g. aviation for composites and electric vehicles for magnets) could address this issue. Furthermore, domestic recycling for every material might not be desirable due to economies of scale that can be obtained by international collaboration. Likewise, criticality is an EU issue that does not require solving on a national scale, but on an EU scale. The scope of the Netherlands and wind turbines is therefore exceeded here.

Another aspect of the limited scope is the second-hand market. High level reuse is preferable according to the waste management framework and discussed in this study to limited extent. No data is found on how much wind turbines are reused domestically or exported annually. This could lead to unaccounted outflows in this study that could influence the results.

4.2.2 Economic and environmental aspects

As recycling should only take place in the absence of preferential waste management strategies and be economically and environmentally interesting, these aspects are discussed for novel recycling routes. Established recycling routes for copper, steel and aluminium are economically interesting and provide environmental benefits through reduced energy use and resource extraction. The economic and environmental aspects for materials like composites and permanent magnets require a more in-depth analysis.

Composite recycling is difficult due to material complexity and inherent downcycling. The economic value and quality of recycled products are low while primary materials are cheap and high quality. Economic incentive is therefore limited. Environmental gains of composite recycling are also less than for the established (metal) recycling routes due to the absence of closed loop recycling where primary material production is substituted. Secondary use of composites is discussed to limited extent as blade material repurposing, which adds functional lifetime to the material. However, doing this also distributes the material over space (compared to high concentration in wind turbines) and time making final recycling more difficult. For composite waste management, there is an interesting trade-

off between material quality, economic viability and environmental impacts for composite recycling that is not yet solved. Depending on scale, potential secondary markets and priorities, different recycling routes can be optimal.

Permanent magnet recycling revolves mostly around its critical constituents Nd and Dy. Therefore, economic aspects also include economic importance. The supply risk and economic importance cause its criticality from the perspective of the EU. The economic incentive, based purely on primary and secondary material value and production cost, is currently unknown but could be supplemented with EU subsidies due to the critical status of the material. Environmental benefits from recycling can be substantial as resource extraction and human toxicity in the primary production process are absent.

4.3 BROADER CONTEXT

The use of dynamic material flow analysis for estimating future stocks and flows is essential for the implementation of a circular economy. Therefore, this combination of methods - data analysis, material flow analysis and recycling technologies - can be used in broader context.

Findings in this study indicate that the product centric approach leads to new insights in (partial) closed-loop recycling (e.g. recycled fibres in nacelle cover or cement clinker) within a product. On the other hand, potentials to combine same or similar material flows can be overlooked when focussing on a single product. Composites and permanent magnet recycling could both benefit from an increase in scale for minimum required recycling plant capacity, which could be found in EV and aviation respectively. It is therefore argued that product centric and material centric perspectives are both required to find optimal solutions.

The framework used in this study could be applicable to many other topics, but is limited by the availability of data on historic and projected inflows, material compositions and recycling routes. The inflow data for wind energy is documented with high accuracy as are some material compositions and recycling routes. Detailed material compositions are often not available due to confidentiality. Novel recycling routes exist only on small scale or conceptual level and provide issues as well in data collection. However, for new technologies, more complex and/or smaller components and novel recycling routes data is very limited. Similar issues might be more difficult to solve for other topics.

5 CONCLUSIONS & RECOMMENDATIONS

The potential for material recovery from Dutch wind energy is determined through analysis of wind turbines in the Netherlands, their development in capacity and technology and various routes for material recovery. The use of a dynamic stock model allows for further variations in input parameters, optimization and customization for different scopes. Through this model, results are obtained that lead to conclusions on material requirements (inflows), societal stock, waste flows (outflows) and secondary materials. First, the research sub-questions are covered individually to conclude with potential material recovery from Dutch wind energy towards 2050, answering the main research question. Additionally, key findings and implications are covered that lead to the recommendations, which are discussed in a section 5.1.

The **analysis of the currently installed stock** of wind turbines in the Netherlands answers the first sub-question. The current (early 2020) stock of wind turbines in the Netherlands, is composed of a wide variety in wind turbines due to rapid technological developments in wind energy. The age, rated capacity and manufacturer are used as indicators for identification of wind turbine characteristics such as drive train technology and blade material compositions. The decommissioning of wind turbines has started since 2010. Using this data, the lifespan of Dutch wind turbines is determined. This analysis provides the following key findings:

- The onshore installed capacity is roughly 6 GW, whereas offshore 1 GW is installed.
- A few large manufacturers (Enercon, Vestas and Siemens Gamesa) provide most of the wind turbines, which can be observed on the Dutch and European scale.
- The lifespan of wind turbines in the Netherlands is estimated at an average 18-year lifespan for currently installed wind turbines that increase towards a 24 and 25-year average lifespan for onshore and offshore respectively in 2050.

An extensive analysis of the **material composition** of current and future wind turbines results in estimations on component weight and material shares for most common wind turbine components, answering the second sub-question. This includes linear and non-linear relationships with rated capacity and hub height based on literature, manufacturer data and online databases. Improvements on estimates for generator materials are made by using generator scaling studies instead of linear estimations commonly used in literature. Future **technological developments** are analysed and included to create additional insight in the material compositions of wind turbines under development. Future technological development occurs for:

- Trends for increasing rated capacity, hub height and lifespan
- Drivetrain configurations including direct drive, geared, permanent magnet, induction and superconducting technologies.
- Changes in material compositions for structural steel alloys, carbon fibre content in blades and blade weight.
- Disruptive changes in material compositions such as composite towers, natural fibres in blades and thermoplastics in blades.

Scenarios for **future installed capacity** are analysed and compiled to create plausible and relevant scenarios as input for this study, concluding on the third sub-question. The scenarios used for this research are based on a variety of studies where the minimum is based on minimal policy intervention, the prognosis is based on current policy and the maximum on additional stimulation for wind energy. These scenarios are used in combination with the current stock of wind turbines, material

compositions and technological development to create material inflows for wind turbines towards 2050.

- The onshore wind capacity is likely stabilizing, where offshore wind energy is at the beginning of a period of strong growth.
- Offshore, there will be more potential for further growth in rated capacity and hub height of individual wind turbines.
- Due to increasing rated capacity per turbine, the number of onshore turbines is relatively decoupled from increasing installed capacity.

The material **inflows** that follow from the installed capacity and material compositions are used as input in the dynamic stock model to calculate **stock** and **outflow** for these materials under the three main scenarios. These results have been discussed in detail in section 3.4 Inflows, stocks and outflows. A summary of results for inflow, stock and outflow under the prognosis scenario is shown in Table 5-1, covering the fourth research sub-question.

Table 5-1: Material inflow, stock and outflow [kt/a] for Dutch wind energy in 2030,2040 and 2050 for the prognosis scenario.

	Inflow [kt/a]			Stock [kt]			Outflow [kt/a]		
	2030	2040	2050	2030	2040	2050	2030	2040	2050
Structural steel	200	300	400	2000	3000	6000	50	50	140
Alloy steels	10	12	15	120	200	290	2.5	3	8
Iron	50	80	120	500	1000	1800	14	13	32
Permanent magnets	0.5	1	1.4	3	7	18	0.02	0.05	0.25
Aluminium	0.2	0.3	0.5	3.5	5	7.5	0.1	0.1	0.2
Copper	2	3	4	30	50	75	1	1	2
Composites	15	20	25	200	300	420	5	5	14
Concrete	100	150	150	2000	2000	2250	140	80	70

- Inflows show a sharp increase in the near future (>2023) due to large offshore projects and additional inflows needed for stock maintenance after 2040.
- Stock of materials in wind turbines develop similarly with exceptions of concrete as this is only used for onshore wind turbines and (relatively) new materials such as permanent magnets.
- Outflows occur as two distinct ‘peaks’ where the first (2030) is caused by mostly onshore wind turbines and the second (2050) mostly by offshore wind turbines.

For the fifth sub-question recycling methods are analysed and described. The **recycling methods** discussed in this study include conventional recycling routes for steel, copper and aluminium. Selective recycling for alloy steel and potentially iron is discussed for functional recycling of valuable, cross-cutting critical alloying elements. Additionally, blade repurposing is discussed. Several novel recycling technologies are considered:

- Composites recycling: mechanical recycling, cement co-processing and pyrolysis
- Permanent magnet recycling: magnet-to-magnet and magnet-to-REE
- Concrete recycling: clean aggregate

As most composite and permanent magnet recycling technologies are in an early stage of development, estimates on material yield and quality vary.

Material outflows and recovery rates are used to calculate secondary material flows. The total of potential **secondary materials** from decommissioned wind turbines in the Netherlands is shown in Table 5-2, which answers the sixth and main research question.

Table 5-2: Potentially recovered materials [kt/a] from Dutch wind energy for 2030 and 2050 under low, prognosis and high installed capacity scenarios. Additionally, recycling routes and resulting secondary materials are presented. The prefix *r*- indicates a material is recovered with degraded material properties (quality).

Primary material	Recycling route	Material	Secondary material(s)		
			Low (2030-2050)	Prognosis (2030-2050)	High (2030-2050)
Steel	Primary/EDF	Steel	30-20	30-90	30-200
	Primary/EDF, full monopile recovery	Steel	40-25	40-130	40-270
Alloy steel	EDF	Alloy steel	2.5-2.5	2.5-7.5	2.5-17.5
Iron	(EDF)	Iron	12-10	12-30	12-70
Copper	(s)melting/refining	Copper	1-0.6	1-1.8	1-4
Aluminium	(s)melting/refining	Aluminium	0.1-0.05	0.2- 0.18	0.1-0.4
Permanent magnet	Magnet-to-magnet	rPM	19 -29	19 -175	19 -370
	Magnet-to-magnet	PM	12-18	12-107	12-225
	Magnet-to-REE	PM	20-30	20 - 180	20-380
Composite	Cement co-processing	Cement clinker	2.5-2.5	2.5-7.5	2.5-17.5
	Mechanical grinding	Fibrous fraction	2.5-2.5	2.5-7.5	3-17.5
	Pyrolysis	rFiber	2-1.8	2-5.8	2-12
		Pyrolysis oil	1-0.8	1-2.8	1-6
	Repurposing	Sheet	4 - 3	4-11	4-24
Beam		0.5-0.4	0.5-1.5	0.5-3	
Concrete	Clean aggregate	Cement	20-10	20-10	20-30
		Aggregate	80-25	80-40	80-120
		RBM	40-15	40-20	40-55

For established recycling routes for steel, iron, copper and aluminium, no limitations are observed for material recovery from wind energy. Collection rates are high, except for monopile foundations that are partly left on-site. Key findings and implications include.

- Not all materials can be competitively recycled domestically due to scale advantages of the regional and global recycling infrastructure.
- Secondary steel, iron, copper and aluminium can for a large part be considered for closed-loop recycling. Losses occur for steel in collection of monopiles, and for a minor part in recycling processes.
- Stock hibernation of up to ~0.5 Mt structural steel occur for monopiles under conventional removal procedures and sacrificial materials. Full monopile removal is identified as a solution to avoid hibernating steel stock.
- Concrete recycling provides aggregates, cement and roadbed material that can be widely applied in the construction sector.

Composite recycling provides many alternatives on varying levels of product and material recovery. A degradation in functionality or material properties seems inevitable for these materials.

- It is estimated that between 2020 and 2025 all recovered fibres could be applied within the wind turbine industry as nacelle cover and nose cone reinforcement. After 2030, additional demand is required.
- If fibre recovery is to be implemented before 2040, additional supply of composite scrap from outside the Netherlands is likely required for a dedicated recycling facility.
- Composites can be recycled without significant losses, yet always involve a downcycling/cascade effect in quality.

Critical materials. Secondary supply of critical materials can alleviate its criticality and therefore is interesting from an EU supply security perspective.

- The implementation along the prognosis requires Nd, Dy, Pr, Tb, V and Mg as critical materials in permanent magnets, alloy steel and cast iron.
- It is estimated that with maximum recycling efforts, secondary supply of critical materials can meet up to ~15% of REE, ~30 of V and ~25% of Mg demand by 2050.
- Vanadium and magnesium can be functionally recovered through selective recycling in electric arc furnaces.
- Magnet-to-magnet recycling could involve high recovery rates with some degree of quality loss. This means secondary use in wind turbines may be unlikely due to this quality loss, but as demand from electric vehicles increases, ample demand is expected.
- For alloy steels, selective collection is required to functionally recycle its valuable and critical alloying elements.
- The maximum estimated outflow of permanent magnets seems insufficient to run a dedicated recycling facility with a minimum of several kiloton input. Therefore, there is a need for regional (European) collaboration efforts.

As the need for a renewable energy system has and will continue to drive wind energy development, it will also cause a higher strain on resources and waste management. Material recovery from wind energy is an essential part of a circular approach to this development. The results from this study can be used to inform decision makers on what can be expected for the future of wind energy in the Netherlands.

5.1 RECOMMENDATIONS

Based on the discussion and conclusions, recommendations for circular economy policy are given. Additionally, recommendations for further research are made that can improve- or supplement the findings in this study. In general, similar works on material intensive sectors in society are important to realise a more circular economy. This study is only a small aspect of an inventory of societal stocks and flows that enable systemic improvement of resource use and sustainability.

5.1.1 Recommendations for circular economy policy

Cross-border collaboration: For materials without established recycling routes, a national scope provides insufficient scrap throughput dedicated recycling facilities. A wider scope could lead to opportunities for more efficient and cost-effective recycling.

- On the short term, domestic composite recycling facilities will require additional throughput. International collaboration can be realized with several neighbouring countries. Denmark has the oldest stock of wind turbines and Germany the largest, providing interesting sources or destinations for composite scrap material.

- For the longer term, The North Sea Region will become an increasingly important source of scrap composite material in the future due to UK, Dutch, Belgian, German and Danish offshore developments.³⁰
- Critical material recycling involves low-volume materials and will not be feasible on a national scale before 2050. International collaboration is most advisable on a European Union scale as REE criticality requires increased supply from within the EU to mitigate its criticality through secondary supply.

Cross-sector collaboration: Alternatively or additionally to cross-border collaboration, other sectors provide or are expected to provide large scrap flows that could supplement scrap from wind energy to enable domestic recycling facilities. However, this will cause less homogenous scrap and hence likely lower quality secondary materials.

- The automotive sector (EV) could increase scrap material availability for permanent magnets.
- For composite material, the aviation sector could increase scrap material availability.

Secondary material demand

- Additional markets for various recovered materials from composites (e.g. sheet material, fibrous dust, recovered fibres) need to be determined as full closed-loop or recycling within wind turbines is currently not feasible.

Stimulation

- Selective recycling of iron and steel alloys allows functional recovery of valuable and critical alloying elements that would lose their function through dilution in conventional mixed recycling. Separate collection should be stimulated where economic incentive based on market value lacks if these materials are to be recovered.
- Full monopile removal is under development, but challenged by cost-effectiveness. Additional material can be recovered, but would require regulatory or economic incentive.

5.1.2 Recommendations for further research

Master theses for studies similar to industrial ecology and/or materials science and engineering or bachelor projects could provide interesting insights through exploring the wider scope, but also more in-depth aspects. Furthermore, research at TNO continuing on the topic of key materials in wind energy and blade recycling and CML on material stocks in the electricity system are very relevant for the topic of this study. Further research can be inspired by the following policy- and technology related areas of inquiry.

Policy-related areas of inquiry

- Full monopile removal is under development, but challenged by cost-effectiveness. Economic and environmental assessment of this aspect can reveal if and how regulation and economic incentive could stimulate full monopile removal and avoid large hibernating stocks.
- The limited scope of the Netherlands presents limitations for recycling infrastructure. A wider geographical scope is needed to identify necessary scale of collaboration for sufficient scrap volumes in recycling permanent magnets and composites. Therefore, a similar study on these specific materials for a larger geographical scope can be useful.

³⁰ Currently under investigation by TNO

Technology-related areas of inquiry

Wind turbine technological development

- As the scope of this research considers wind energy development until 2050, currently expected developments might change due to breakthrough technologies. Further analysis of potentially disruptive technologies, i.e. vertical axis- and airborne wind energy converters could lead to more variations in material demand towards 2050 and outflows after that.

Environmental and economic aspects

- Due to the wide scope of this study, economic and environmental aspects for recycling are discussed to limited extent. Detailed environmental and economic assessment for composite recycling routes (specifically for blades) is needed to gain insight in relevant trade-offs and identify the best options from both perspectives.
- As a side-track, material inflows and relevant environmental impacts are discussed in this study. Comparative LCAs on various scenarios for wind energy development, using the material inflow data from this study, could reveal how various pathways influence the environmental impact of the transition to more wind energy in the Netherlands. As discussed, the prospective aspect of this study would also require estimations on environmental impacts of future material production (e.g. steel production).

Spatial aspects

- Detailed information on location (Province, Municipality and Project) is available in the WindStats and could be used to determine spatially where stocks of wind turbines reside. As this study focuses on quantifying material flows and the spatial aspect is therefore out of scope. However, considering the logistics for recycling infrastructure, it can be valuable to know where the stock resides. Therefore, using the spatial data in WindStats in combination with Geographic Information System (GIS) mapping this aspect can be researched.

Recycling technology

- Recycling rates and minimum throughput for novel recycling technologies
- Effect on quality of combined recycling of permanent magnets from EV and wind turbines
- Combined recycling of wind turbine blades and composites in aviation

Improvement

- Finally, the results in this study can be further detailed, improved and analysed for specific material and component flows. The Excel based input file (*Input_data.xlsx*) allow users (without knowledge of Python) to easily change important variables. The model allows for further adjustment (for experienced Python users) within the script.

REFERENCES

- Åkesson, D., Foltynowicz, Z., Christeen, J., & Skrifvars, M. (2012). Microwave pyrolysis as a method of recycling glass fibre from used blades of wind turbines. *Journal of Reinforced Plastics and Composites*, 31(17), 1136-1142.
- Alfman & Rooijers (2018) Net voor de toekomst. CE Delft & Netbeheer NL
- Bang, D. J., Polinder, H., Shrestha, G., & Abraham Ferreira, J. (2008a). Promising direct-drive generator system for large wind turbines. *EPE Journal*, 18(3), 7-13.
- Bang, D., Polinder, H., Shrestha, G., & Ferreira, J. A. (2008b). Review of generator systems for direct-drive wind turbines. In *European wind energy conference & exhibition, Belgium* (Vol. 31).
- Bang, D., Polinder, H., Shrestha, G., & Ferreira, J. A. (2009). Possible solutions to overcome drawbacks of direct-drive generator for large wind turbines. *EWEC 2009: Europe's Premier Wind Energy Event, Marseille, France, 16-19 March 2009*.
- Bergen, A., Andersen, R., Bauer, M., Boy, H., Ter Brake, M., Brutsaert, P., ... & Kellers, J. (2019). Design and in-field testing of the world's first ReBCO rotor for a 3.6 MW wind generator. *Superconductor science and technology*, 32(12), 125006.
- Binnemans, K., Jones, P. T., Blanpain, B., Van Gerven, T., Yang, Y., Walton, A., & Buchert, M. (2013). Recycling of rare earths: a critical review. *Journal of cleaner production*, 51, 1-22.
- Blagoeva, D. T., Aves Dias, P., Marmier, A., & Pavel, C. (2016). Assessment of potential bottlenecks along the materials supply chain for the future deployment of low-carbon energy and transport technologies in the EU. *JRC Science for Policy Report (European Union, Luxembourg)*.
- Bloomberg. (2020). Wind turbine blades can't be recycled so they're piling up in landfills. Obtained on July 13th 2020 from <https://www.bloomberg.com/news/features/2020-02-05/wind-turbine-blades-can-t-be-recycled-so-they-re-piling-up-in-landfills>
- BloombergNEF. (2020). *Vestas Still Rules Turbine Market, But Challengers Are Closing In*. February 18th, 2020. <https://about.bnef.com/blog/vestas-still-rules-turbine-market-but-challengers-are-closing-in/>
- Boin, U. M. J., & Bertram, M. (2005). Melting standardized aluminum scrap: A mass balance model for Europe. *JOM*, 57(8), 26-33.
- Busby, R. L. (2012). *Wind Power: The Industry Grows Up*. PennWell Books.
- Cable recycling (2020). *Cable recycling equipment*. Accessed on July 14th on: <https://www.cable-recycling.com/>
- Cao, Z., O'Sullivan, C., Tan, J., Kalvig, P., Ciacci, L., Chen, W., ... & Liu, G. (2019). Resourcing the Fairytale Country with wind power: a dynamic material flow analysis. *Environmental science & technology*, 53(19), 11313-11322.
- Carrara S., Alves Dias P., Plazzotta B. and Pavel C. (2020). Raw materials demand for wind and solar PV technologies in the transition towards a decarbonised energy system, EUR 30095 EN, Publication Office of the European Union, Luxembourg, 2020, ISBN 978-92-76-16225-4, doi:10.2760/160859, JRC119941

Cousins, D. S., Suzuki, Y., Murray, R. E., Samaniuk, J. R., & Stebner, A. P. (2019). Recycling glass fiber thermoplastic composites from wind turbine blades. *Journal of cleaner production*, 209, 1252-1263.

Cunliffe, A. M., Jones, N., & Williams, P. T. (2003). Recycling of fibre-reinforced polymeric waste by pyrolysis: thermo-gravimetric and bench-scale investigations. *Journal of analytical and applied pyrolysis*, 70(2), 315-338.

Deetman, S., Pauliuk, S., Van Vuuren, D. P., Van Der Voet, E., & Tukker, A. (2018). Scenarios for demand growth of metals in electricity generation technologies, cars, and electronic appliances. *Environmental science & technology*, 52(8), 4950-4959.

Den Ouden, Lintmeijer, Bianchi & Warnaars (2018) Richting 2050: systeemkeuzes en afhankelijkheden in de energietransitie. Berenschot

Desmond, C., Murphy, J., Blonk, L., & Haans, W. (2016). Description of an 8 MW reference wind turbine. In *Journal of Physics: Conference Series* (Vol. 753, No. 9, p. 092013). IOP Publishing.

Dong, P. A. V., Azzaro-Pantel, C., & Cadene, A. L. (2018). Economic and environmental assessment of recovery and disposal pathways for CFRP waste management. *Resources, Conservation and Recycling*, 133, 63-75.

Ecobulk. (2020) *Ecobulk webpage*. Accessed on July 14th 2020 at: <https://www.ecobulk.eu/>

EIA. (2014). Recycling is the primary energy efficiency technology for aluminum and steel manufacturing. Accessed on July 14th 2020 at: https://www.eia.gov/todayinenergy/detail.php?id=16211#tabs_SpotPriceSlider-2

EPRI. (2020) Wind Turbine Blade Recycling: Preliminary Assessment. Electric Power Research Institute, Palo Alto, CA

European commission (2017) Study on the review of the list of Critical Raw Materials - Critical Raw Materials Factsheets. doi:10.2873/398823

ExceptionalEngineering. (2020). *The Making of a Wind Turbine | Exceptional Engineering | Free Documentary*. Viewed on March 15th 2020 at <https://www.youtube.com/watch?v=8NXLKRW1IEU>

Gaertner, E., Rinker, J., Sethuraman, L., Zahle, F., Anderson, B., Barter, G. E., ... & Scott, G. N. (2020). *IEA Wind TCP Task 37: Definition of the IEA 15-Megawatt Offshore Reference Wind Turbine* (No. NREL/TP-5000-75698). National Renewable Energy Lab.(NREL), Golden, CO (United States).

Gambogi. (2019a). 2016 Minerals Yearbook U.S. Department of the Interior U.S. Geological Survey RARE EARTHS [ADVANCE RELEASE]. Retrieved on July 14th from: <https://prd-wret.s3-us-west-2.amazonaws.com/assets/palladium/production/atoms/files/myb1-2016-raree.pdf>

Gambogi. (2019b). 2016 Minerals Yearbook U.S. Department of the Interior U.S. Geological Survey RARE EARTHS [ADVANCE RELEASE] Retrieved on July 14th from: <https://prd-wret.s3-us-west-2.amazonaws.com/assets/palladium/production/atoms/files/mcs-2019-yttri.pdf>

Graedel. (2019). Material flow analysis from origin to evolution. *Environmental Science & Technology*, 53(21), 12188-12196.

Grow. (2020). *Monopile removal*. Accessed on July 14th on: <https://grow-offshorewind.nl/project/hype-st>

Habib, K., & Wenzel, H. (2014). Exploring rare earths supply constraints for the emerging clean energy technologies and the role of recycling. *Journal of Cleaner Production*, 84, 348-359.

Hagnell, M. K., & Åkermo, M. (2019). The economic and mechanical potential of closed loop material usage and recycling of fibre-reinforced composite materials. *Journal of cleaner production*, 223, 957-968.

Haque, N., & Norgate, T. (2013). Estimation of greenhouse gas emissions from ferroalloy production using life cycle assessment with particular reference to Australia. *Journal of cleaner production*, 39, 220-230.

Hasanbeigi, A., Arens, M., Cardenas, J. C. R., Price, L., & Triolo, R. (2016). Comparison of carbon dioxide emissions intensity of steel production in China, Germany, Mexico, and the United States. *Resources, Conservation and Recycling*, 113, 127-139.

Hertwich, E. G., Gibon, T., Bouman, E. A., Arvesen, A., Suh, S., Heath, G. A., ... & Shi, L. (2015). Integrated life-cycle assessment of electricity-supply scenarios confirms global environmental benefit of low-carbon technologies. *Proceedings of the National Academy of Sciences*, 112(20), 6277-6282.

Hu, M., Kleijn, R., Bozhilova-Kisheva, K. P., & Di Maio, F. (2013). An approach to LCSA: the case of concrete recycling. *The International Journal of Life Cycle Assessment*, 18(9), 1793-1803.

Huisman, J., Habib, H., Brechu, M. G., Downes, S., Herreras, L., Løvik, A. N., ... & Rotter, S. (2016). ProSUM: Prospecting Secondary raw materials in the Urban mine and Mining wastes. In 2016 Electronics Goes Green 2016+(EGG) (pp. 1-8). IEEE.

Jacob, A. (2011). Composites can be recycled. *Reinforced Plastics*, 55(3), 45-46.

Job, S. (2013). Recycling glass fibre reinforced composites—history and progress. *Reinforced Plastics*, 57(5), 19-23.

Jonkman, J., Butterfield, S., Musial, W., & Scott, G. (2009). *Definition of a 5-MW reference wind turbine for offshore system development* (No. NREL/TP-500-38060). National Renewable Energy Lab.(NREL), Golden, CO (United States).

Jules dock (2020). *Composite wind turbine towers*. Accessed on July 14th 2020 at: <https://julesdock.nl/towers-nl/>

Kleijn, R., Van der Voet, E., Kramer, G. J., Van Oers, L., & Van der Giesen, C. (2011). Metal requirements of low-carbon power generation. *Energy*, 36(9), 5640-5648.

Klimaatakkoord. (2019a). Dutch climate accord 2019

Lacal-Arántegui, R. (2015). Materials use in electricity generators in wind turbines—state-of-the-art and future specifications. *Journal of Cleaner Production*, 87, 275-283.

Lefevre, A., Garnier, S., Jacquemin, L., Pillain, B., & Sonnemann, G. (2019). Anticipating in-use stocks of carbon fibre reinforced polymers and related waste generated by the wind power sector until 2050. *Resources, Conservation and Recycling*, 141, 30-39.

Lindeboom, H. J., Kouwenhoven, H. J., Bergman, M. J. N., Bouma, S., Brasseur, S., Daan, R., Fijn, R.C., de Haan, D., Dirksen, S., van Hal, R., Hille Ris Lambers, R., ter Hofstede, R., Krijgsveld, K. L., Leopold, M., Scheidat, M. (2011) Short-term ecological effects of an offshore wind farm in the Dutch coastal zone; a compilation

Liu, P., & Barlow, C. Y. (2016). The environmental impact of wind turbine blades. In *IOP Conference Series: Materials Science and Engineering* (Vol. 139, No. 1, p. 012032). IOP Publishing.

Liu, P., & Barlow, C. Y. (2017). Wind turbine blade waste in 2050. *Waste Management*, 62, 229-240.

Liu, Y., Farnsworth, M., & Tiwari, A. (2017). A review of optimisation techniques used in the composite recycling area: State-of-the-art and steps towards a research agenda. *Journal of Cleaner Production*, 140, 1775-1781.

Lotfi, S., Deja, J., Rem, P., Mróz, R., van Roekel, E., & van der Stelt, H. (2014). Mechanical recycling of EOL concrete into high-grade aggregates. *Resources, conservation and Recycling*, 87, 117-125.

MacArthur, E. (2013). Towards the circular economy. *Journal of Industrial Ecology*, 2, 23-44.

Macrosammon. (2020). Negative and positive skewness. Image retrieved on August 14th, 2020 from: <https://marcosammon.com/2016/08/09/skewness.html>

Mamanpush, S. H., Li, H., Englund, K., & Tabatabaei, A. T. (2018). Recycled wind turbine blades as a feedstock for second generation composites. *Waste management*, 76, 708-714.

Månberger, A., & Stenqvist, B. (2018). Global metal flows in the renewable energy transition: Exploring the effects of substitutes, technological mix and development. *Energy Policy*, 119, 226-241.

Milford, R. L., Pauliuk, S., Allwood, J. M., & Müller, D. B. (2013). The roles of energy and material efficiency in meeting steel industry CO₂ targets. *Environmental science & technology*, 47(7), 3455-3462.

Mishnaevsky, L., Branner, K., Petersen, H. N., Beauson, J., McGugan, M., & Sørensen, B. F. (2017). Materials for wind turbine blades: an overview. *Materials*, 10(11), 1285.

Müller, D. B. (2006). Stock dynamics for forecasting material flows—Case study for housing in The Netherlands. *Ecological economics*, 59(1), 142-156.

Murray, R. E., Jenne, S., Snowberg, D., Berry, D., & Cousins, D. (2019). Techno-economic analysis of a megawatt-scale thermoplastic resin wind turbine blade. *Renewable Energy*, 131, 111-119.

Murray, R., Snowberg, D. R., Berry, D. S., Beach, R., Rooney, S. A., & Swan, D. (2017). *Manufacturing a 9-meter thermoplastic composite wind turbine blade* (No. NREL/CP-5000-68615). National Renewable Energy Lab.(NREL), Golden, CO (United States). Blaabjerg, F., Liserre, M., & Ma, K. (2011). Power electronics converters for wind turbine systems. *IEEE Transactions on industry applications*, 48(2), 708-719.

Nakajima, K., Ohno, H., Kondo, Y., Matsubae, K., Takeda, O., Miki, T., ... & Nagasaka, T. (2013). Simultaneous material flow analysis of nickel, chromium, and molybdenum used in alloy steel by means of input–output analysis. *Environmental science & technology*, 47(9), 4653-4660.

Naqvi, S. R., Prabhakara, H. M., Bramer, E. A., Dierkes, W., Akkerman, R., & Brem, G. (2018). A critical review on recycling of end-of-life carbon fibre/glass fibre reinforced composites waste using pyrolysis towards a circular economy. *Resources, conservation and recycling*, 136, 118-129.

Offerman (2019). General introduction to critical materials in *Critical Materials: Underlying Causes and Sustainable Mitigation Strategies* (Vol. 5). World Scientific.

Oliveux, G., Dandy, L. O., & Leeke, G. A. (2015). Current status of recycling of fibre reinforced polymers: Review of technologies, reuse and resulting properties. *Progress in Materials Science*, 72, 61-99.

OneEnergy. (2020). Wind turbine information. Obtained on July 13th 2020 from: <https://oneenergy.com/wind-knowledge/wind-turbine-information/>

Ørsted. (2020). *Borssele 1 & 2 offshore wind parks*. Accessed on July 14th at: <https://orsted.nl/onze-windparken/borssele-1-and-2>

Pauliuk, S., Kondo, Y., Nakamura, S., & Nakajima, K. (2017). Regional distribution and losses of end-of-life steel throughout multiple product life cycles—insights from the global multiregional MaTrace model. *Resources, Conservation and Recycling*, 116, 84-93.

Pauliuk. (2014) Python Dynamic Stock Model module. Documentation available at: <https://github.com/stefanpauliuk/pyDSM>

Pavel, C. C., Lacal-Arántegui, R., Marmier, A., Schüller, D., Tzimas, E., Buchert, M., ... & Blagoeva, D. (2017). Substitution strategies for reducing the use of rare earths in wind turbines. *Resources Policy*, 52, 349-357.

Pavel, C. C., Marmier, A., Alves Dias, P., Blagoeva, D., Tzimas, E., Schüller, D., ... & Buchert, M. (2016). Substitution of critical raw materials in low-carbon technologies: lighting, wind turbines and electric vehicles. *JRC Science for Policy Report, JRC103284, EUR, 28152*.

PBL. (2019) *Circulaire economie in kaart*.

Peck, P., Richter, J. L., Dalhammar, C., Peck, D., Orlov, D., Machacek, E., ... & Modis, K. (2019). *Circular Economy-Sustainable Materials Management: A compendium by the International Institute for Industrial Environmental Economics (IIIEE) at Lund University*.

Pickering, S. J., Turner, T. A., Meng, F., Morris, C. N., Heil, J. P., Wong, K. H., & Melendi-Espina, S. (2015). Developments in the fluidised bed process for fibre recovery from thermoset composites. In *2nd Annual Composites and Advanced Materials Expo, CAMX 2015; Dallas Convention Center Dallas; United States* (pp. 2384-2394)

Pillain, B., Loubet, P., Pestalozzi, F., Woidasky, J., Erriguible, A., Aymonier, C., & Sonnemann, G. (2019). Positioning supercritical solvolysis among innovative recycling and current waste management scenarios for carbon fiber reinforced plastics thanks to comparative life cycle assessment. *The Journal of Supercritical Fluids*, 154, 104607.

Polinder, H., Van der Pijl, F. F., De Vilder, G. J., & Tavner, P. J. (2006). Comparison of direct-drive and geared generator concepts for wind turbines. *IEEE Transactions on energy conversion*, 21(3), 725-733.

Port of Rotterdam. (2020). *Prototype most powerful wind turbine in the world*. Accessed on July 14th on: <https://www.portofrotterdam.com/nl/nieuws-en-persberichten/prototype-krachtigste-windturbine-ter-wereld-haliade-x-12-mw-deze-zomer>

Rademaker, J. H., Kleijn, R., & Yang, Y. (2013). Recycling as a strategy against rare earth element criticality: a systemic evaluation of the potential yield of NdFeB magnet recycling. *Environmental science & technology*, 47(18), 10129-10136.

Reuter, M. A., van Schaik, A., Gutzmer, J., Bartie, N., & Abadías-Llamas, A. (2019). Challenges of the Circular Economy: A Material, Metallurgical, and Product Design Perspective. *Annual Review of Materials Research*, 49, 253-274.

Rijksoverheid. (2016) Nederland circulair in 2050 - Rijksbreed programma circulaire economie.

Ruhrberg, M. (2006). Assessing the recycling efficiency of copper from end-of-life products in Western Europe. *Resources, Conservation and Recycling*, 48(2), 141-165.

RVO. (2020a). Wind op Zee - Data obtained from “windparken in bedrijf”, “windparken in aanbouw” and “Windparken in voorbereiding”, Accessed on July 14th on: <https://www.rvo.nl/onderwerpen/duurzaam-ondernemen/duurzame-energie-opwekken/woz>

RVO. (2020b). *Wind op Land*. Accessed on July 14th at: <https://www.rvo.nl/onderwerpen/duurzaam-ondernemen/duurzame-energie-opwekken/windenergie-op-land>

RVO. (2020c). Windkaart. Obtained on July 13th 2020 from: <https://www.rvo.nl/sites/default/files/2019/07/Windkaart%20NL.jpg>

Rybicka, J., Tiwari, A., & Leeke, G. A. (2016). Technology readiness level assessment of composites recycling technologies. *Journal of Cleaner Production*, 112, 1001-1012.

Sacchi, R., Besseau, R., Perez-Lopez, P., & Blanc, I. (2019). Exploring technologically, temporally and geographically-sensitive life cycle inventories for wind turbines: A parameterized model for Denmark. *Renewable Energy*, 132, 1238-1250.

Schreiber, A., Marx, J., & Zapp, P. (2019). Comparative life cycle assessment of electricity generation by different wind turbine types. *Journal of cleaner production*, 233, 561-572.

Schubel, P. J., & Crossley, R. J. (2012). Wind turbine blade design. *Energies*, 5(9), 3425-3449.

Schulze, R., & Buchert, M. (2016). Estimates of global REE recycling potentials from NdFeB magnet material. *Resources, Conservation and Recycling*, 113, 12-27.

Shah, D. U., Schubel, P. J., & Clifford, M. J. (2013). Can flax replace E-glass in structural composites? A small wind turbine blade case study. *Composites Part B: Engineering*, 52, 172-181.

Shammugam, S., Gervais, E., Rathgeber, A., & Schlegl, T. (2017). Effects of increasing wind energy share in the German electricity sector on the European steel market. In *Heading Towards Sustainable Energy Systems: Evolution or Revolution?*, 15th IAEE European Conference, Sept 3-6, 2017. International Association for Energy Economics.

Sheldon, C. (2020) The new kids on the block: redefining critical minerals essential for a clean energy future. May 11th, 2020.

Siemens Gamesa. (2018) Annual report 2018. Accessed on July 14th at: <https://www.siemensgamesa.com/-/media/siemensgamesa/downloads/en/investors-and-shareholders/annual-reports/2018/siemens-gamesa-renewable-energy-annual-report-2018-en.pdf>

Skelton, K. (2017). Discussion paper on managing composite blade waste. WindEurope

Slavik, K., Lemmen, C., Zhang, W., Kerimoglu, O., Klingbeil, K., & Wirtz, K. W. (2019). The large-scale impact of offshore wind farm structures on pelagic primary productivity in the southern North Sea. *Hydrobiologia*, 845(1), 35-53.

Smith, K. (2001). WindPACT turbine design scaling studies technical area 2: Turbine, rotor and blade logistics (No. NREL/SR-500-29439). National Renewable Energy Lab., Golden, CO (US).

Song, X., Bühner, C., Brutsaert, P., Ammar, A., Krause, J., Bergen, A., ... & Wessel, S. (2019). Ground Testing of the World's First MW-Class Direct Drive Superconducting Wind Turbine Generator. *IEEE Transactions on Energy Conversion*.

Soulier, M., Glöser-Chahoud, S., Goldmann, D., & Espinoza, L. A. T. (2018). Dynamic analysis of European copper flows. *Resources, Conservation and Recycling*, 129, 143-152.

Sprecher, B., Xiao, Y., Walton, A., Speight, J., Harris, R., Kleijn, R., ... & Kramer, G. J. (2014). Life cycle inventory of the production of rare earths and the subsequent production of NdFeB rare earth permanent magnets. *Environmental science & technology*, 48(7), 3951-3958.

SusMagPro. (2020) *NdFeB recycling and reprocessing pilot plants*. Accessed on July 14th 2020 at: <https://www.susmagpro.eu/where-find-us/susmagpro-plants>

Sustainability-soapbox. (2020) Evolution of wind turbine size. Retrieved on January 30th 2020 from: <http://sustainability-soapbox.com/wp-content/uploads/2018/09/soapbox-turbine-image-2.jpg>

Tanaka, M., Oki, T., Koyama, K., Narita, H., & Oishi, T. (2013). Recycling of rare earths from scrap. In *Handbook on the physics and chemistry of rare earths* (Vol. 43, pp. 159-211). Elsevier.

Teske, S. (2019). *Achieving the Paris climate agreement goals*. Springer International.

TKI (2018) Jules Dock: Lichtgewicht en onderhoudsarme windturbinetoren. Nieuwsbericht TKI Wind op Zee. February 22nd 2018. Accessed on July 14th at: <https://www.topsectorenergie.nl/nieuws/baanbrekend-mkb-julesdock>

Topham, E., & McMillan, D. (2017). Sustainable decommissioning of an offshore wind farm. *Renewable energy*, 102, 470-480.

Topham, E., McMillan, D., Bradley, S., & Hart, E. (2019). Recycling offshore wind farms at decommissioning stage. *Energy policy*, 129, 698-709.

Torres, A., De Marco, I., Caballero, B. M., Laresgoiti, M. F., Legarreta, J. A., Cabrero, M. A., ... & Gondra, K. (2000). Recycling by pyrolysis of thermoset composites: characteristics of the liquid and gaseous fuels obtained. *Fuel*, 79(8), 897-902.

van Oers, L., Guinee, J. B., & Heijungs, R. (2019). Abiotic resource depletion potentials (ADPs) for elements revisited-updating ultimate reserve estimates and introducing time series for production data. *International Journal of Life Cycle Assessment*, 25(2), 294-308. <https://doi.org/10.1007/s11367-019-01683-x>

Van Oorschot, J., Van der Zaag, J. Van der Voet, E. Van Straalen, V., Delahaye, R. (2020). Voorraden in de maatschappij: de grondstoffenbasis voor een circulaire economie. *CML & CBS*.

Van Wingerde. (2015). *Use of steel for towers of wind turbines and support structures*. Fraunhofer IWES.

VanOord. (2020). Offshore installation vessel Aeolus. Obtained on July 13th 2020 from: https://www.vanoord.com/sites/default/files/offshore_installation_vessel_aeolus_0.jpg

Vattenfall. (2020). *Hollandse kust zuid wind park construction started*. Accessed on July 14th at <https://group.vattenfall.com/press-and-media/news--press-releases/newsroom/2020/vattenfall-gives-green-light-to-worlds-largest-offshore-wind-project>

Viebahn, P., Soukup, O., Samadi, S., Teubler, J., Wiesen, K., & Ritthoff, M. (2015). Assessing the need for critical minerals to shift the German energy system towards a high proportion of renewables. *Renewable and Sustainable Energy Reviews*, 49, 655-671.

Walton, A., Yi, H., Rowson, N. A., Speight, J. D., Mann, V. S. J., Sheridan, R. S., ... & Williams, A. J. (2015). The use of hydrogen to separate and recycle neodymium–iron–boron-type magnets from electronic waste. *Journal of Cleaner Production*, 104, 236-241.

Watson, S., Moro, A., Reis, V., Baniotopoulos, C., Barth, S., Bartoli, G., ... & Croce, A. (2019). Future emerging technologies in the wind power sector: A European perspective. *Renewable and Sustainable Energy Reviews*, 113, 109270.

WindEurope (2020a) Accelerating Wind Turbine Blade Circularity

WindEurope (2020b) End of life issues and strategies webinar. May 27th 2020.

WindparkNoordoostpolder. (2020) Windpark Noordoostpolder. Obtained on July 13th 2020 from: https://www.windparknoordoostpolder.nl/wp-content/uploads/2016/01/Windpark-Noordoostpolder_AIR2381.jpg

WindStats (2020) Wind energy statistics on the Netherlands. Access provided by TNO. Accessed on July 7th 2020 at: <https://windstats.nl/>

Wind-turbine-models. (2020). *Wind turbine models – manufacturers*. Accessed on July 14th on: <https://en.wind-turbine-models.com/manufacturers>

Winkler, T., & EcoSwing Consortium. (2019). The EcoSwing Project. In *IOP Conference Series: Materials Science and Engineering* (Vol. 502, No. 1, p. 012004). IOP Publishing.

Wiser, R. H., & Bolinger, M. (2019). 2018 Wind Technologies Market Report.

World Bank Group. (2017). *The growing role of minerals and metals for a low carbon future*. World Bank.

Zakotnik, M., Devlin, E., Harris, I. R., & Williams, A. J. (2006). Hydrogen decrepitation and recycling of NdFeB-type sintered magnets. *Journal of iron and steel research, international*, 13, 289-295.

Zimmermann, T., Rehberger, M., & Gößling-Reisemann, S. (2013). Material flows resulting from large scale deployment of wind energy in Germany. *Resources*, 2(3), 303-334.

APPENDICES



A. STOCK ANALYSIS

Additional results for section 3.1 Stock analysis is presented here, including Manufacturer information, characterizing technology and historic inflow and stock in number of turbines.

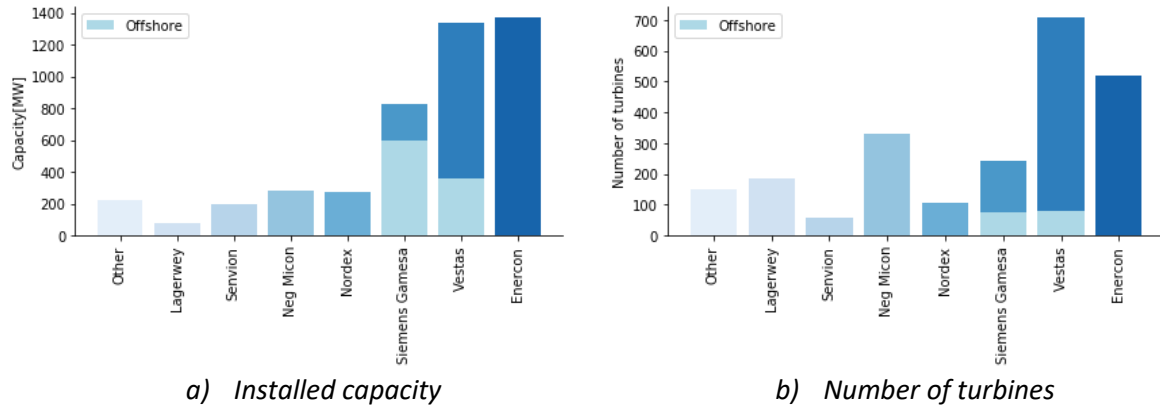


Figure A-1: Installed capacity (a) and number of turbines (b) per manufacturer. Light blue for Siemens Gamesa and Vestas indicates offshore wind turbines.

The 'Other' group consists of thirteen manufacturers, of which Bouma, Tacke, Bonus, NedWind are not in business anymore or have been taken over (Wind-turbine-models, 2020). Micon merged with Nordtank, becoming Neg Micon in 1997, which has been taken over by Vestas again in 2004 (Vestas, 2020a) and Siemens merged with the Spanish manufacturer Gamesa in 2017 to become Siemens Gamesa (Siemens Gamesa, 2020). Neg Micon is still shown separately as a large share of wind turbines are still around from the time this was a separate company. Data for Nordtank and Micon are added to this. 2-B Energy, Alstom, EWT, Nordex and GE wind are still in business. Globally, GE wind is even a very large player and perhaps will gain in the Dutch offshore sector as it recently deployed the 12 MW GE Haliade X as test turbine (Port of Rotterdam, 2020). Senvion is, like GE wind a large manufacturer globally but has been acquired by SG in 2020 (Senvion, 2020). Lagerwey is a Dutch wind turbine manufacturer with many small wind turbines in the Netherlands, but is also still active as a manufacturer of modern wind turbines.

Share of manufacturers onshore versus offshore

Detailed information on location (Province, Municipality and Project) is available in the WindStats and could be used to determine spatially where stocks of wind turbines reside. However, this study focuses on quantifying material flows and the spatial aspect is therefore largely out of scope. One distinction is relevant however, as onshore wind turbines are considerably different from offshore turbines. Therefore, this distinction is applied to analyse the share of manufacturers. For onshore wind turbines, dominant manufacturers remain Enercon and Vestas, but Siemens Gamesa is currently less relevant onshore. This is shown in Figure A-2. Compared to the total, the shares for onshore wind energy per manufacturer have changed to Enercon being the largest with 41%, Vestas following with 29% and the remaining larger manufacturers around 7%. Current total installed offshore capacity is 957 MW, with Vestas' total capacity at 357 MW and Siemens Gamesa at 600 MW.

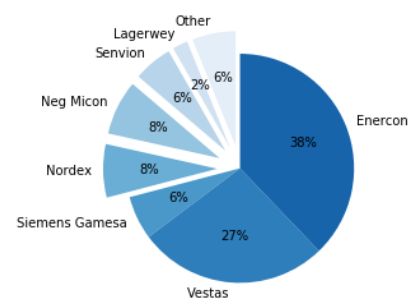


Figure A-2: Shares of manufacturer for onshore wind turbines.

Characterizing technology

Characterizing technologies for each manufacturer can be used in determining material compositions of installed capacity.

Therefore, the six largest manufacturers are analysed further to determine key characteristics of each brand. Specifics of these characterizing technologies are discussed in section 3.2 Material composition.

Being the main wind turbine supplier for the Netherlands and globally in the top 5 (BloombergNEF, 2020), **Enercon** is a well-established manufacturer. The German manufacturer has been active since 1984 and in 1993 already focused on gearless drivetrain (direct drive) technology. This leads to the assumption that all currently installed Enercon wind turbines have gearless synchronous generators. These generators are electrically excited synchronous generators (EESG). Another key technology that impacts material composition significantly is the use of modular hybrid (concrete and steel) towers. The lower sections of concrete towers are made up of concrete rings, joined together by tension cables and extended by steel tubular sections on top (Enercon, 2020). Besides concrete towers, Enercon uses regular steel tubular towers as well, depending on rated capacity and hub height. Since November 2019, Lagerwey LP4 turbines are sold by Enercon under EP5, meaning Enercon turbines of this type are direct drive permanent magnet generators (DDPMG) (Lagerweywind, 2020a).

Globally, the Danish **Vestas** is the largest manufacturer (BloombergNEF, 2020). The company built its first wind turbine in 1979 (Vestas, 2020a). Vestas partnered with Mitsubishi Heavy Industries to form MHI Vestas for offshore turbines in 2014, creating a separate offshore dedicated brand (MHI Vestas, 2020). Meanwhile, Vestas also remains with a focus on onshore wind turbines. The data previously shown does not make a distinction between the two names as the data does not contain this information. Contrary to Enercon, Vestas uses geared drivetrain technology. The gearbox and generator type vary per model but include multiple stage gearboxes, asynchronous generators (AG) and permanent magnet synchronous generators (PMG). (Vestas, 2020b)

Siemens Gamesa is formed from a merger between Gamesa, Bonus and Siemens. Siemens acquired Bonus in 2004 and in 2017 merged with Gamesa to form Siemens Gamesa. (Siemens Gamesa, 2020b) The acquisition of Bonus by Siemens is not shown in the data as a distinction between old and newer model turbines is useful for further analysis. Siemens Gamesa applies a mix of technologies, with a focus on geared drivetrain technologies onshore and gearless offshore (Siemens Gamesa, 2018).

Neg Micon Before being acquired by Vestas in 2004 (Vestas 2020a). Neg Micon produced wind turbines in the range of 600 - 4200 kW, using geared asynchronous generator drive train technology.

After being owned by Suzlon between 2007 and 2015, **Senvion** has been acquired by Siemens Gamesa in 2019 (Senvion, 2020a). The originally German company produces wind turbines with geared doubly fed induction generator (asynchronous) technology (Senvion, 2020b).

The Dutch company **Lagerwey** started manufacturing wind turbines in 1979 using geared technology. After 1995 the company started using direct drive technology and still does today (Lagerweywind 2020a). The company report on as strategic partnership with Enercon since 2018 and since November 2019 sells its LP4 turbine as Enercon EP5 (Lagerweywind (2020a).

The complete wind turbine is assembled and designed by the listed wind turbine manufacturers. However, a large number of components are made and designed by independent **component manufacturers**. This means various wind turbine manufacturers share the same supplier of components. For blades LM wind is a large player as they provide 20% of all blades manufactured (LM, 2018). This number is possibly much higher in Europe as Vestas uses LM blades and is the largest

manufacturer. GE acquired LM in 2017, while LM continues supply of blades to other manufactures (GE, 2020). SG reports on own blade manufacturing facilities. Electrical equipment such as generators and power converters are commonly manufactured by ABB, GE or Mitsubishi (Blaabjerg et al., 2012).

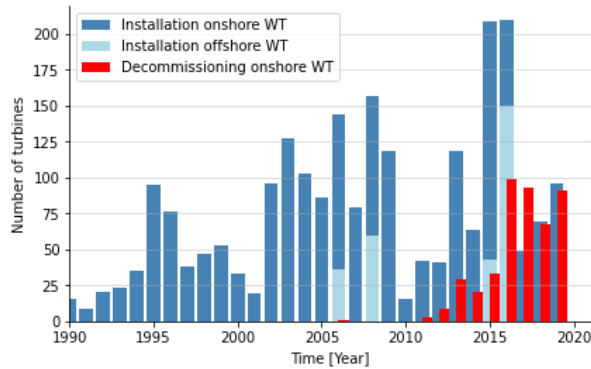


Figure A-3: In- and outflows of wind turbines in number of turbines. Colour indications are as described in capacity in- and outflows. WindStats data discrepancy is not compensated.

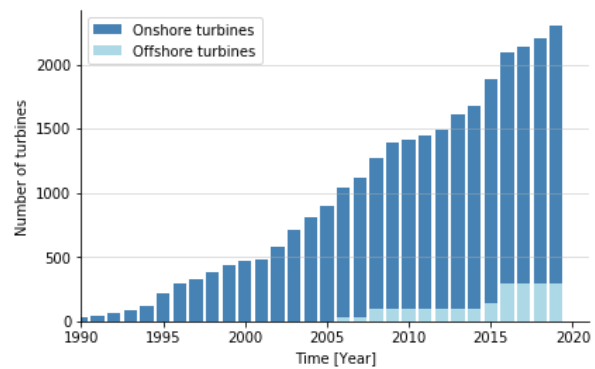


Figure A-4: Stock in number of turbines in the Netherlands. Colour indications are as described in capacity in- and outflows. WindStats data discrepancy is not compensated

Sources specific to this appendix

Blaabjerg, F., Ma, K., & Zhou, D. (2012, May). Power electronics and reliability in renewable energy systems. In *2012 IEEE International Symposium on Industrial Electronics* (pp. 19-30). IEEE.

Enercon. (2020). *Enercon components – Tower*. Accessed on July 14th at: <https://www.enercon.de/en/technology/wec-components/>

Lagerweywind (2020a) *Lagerwey LP4 now Enercon EP 5*. Accessed on July 14th on: https://twitter.com/LagerweyWind/status/1198917993071288321?ref_src=twsrc%5Etfw%7Ctwcamp%5Eembeddettimeline%7Ctwtterm%5Eprofile%3ALagerweyWind%7Ctwcon%5Etimelinedchrome&ref_url=https%3A%2F%2Fwww.lagerweywind.nl%2Ftechnologie%2Ftoeren%2F

Senvion (2020b) *Products-services: Windturbines*. Accessed on July 14th at: <https://www.senvion.com/global/en/products-services/wind-turbines/6xm/>

Senvion. (2020a). *Siemens Gamesa Acquisition*. Accessed on July 14th at: <https://www.senvion.com/global/en/newsroom/press-releases/detail/siemens-gamesa-successfully-completes-acquisition-of-european-service-assets-and-ip-from-senvion/>

Siemens Gamesa. (2018) *Annual report 2018*. Accessed on July 14th at: <https://www.siemensgamesa.com/-/media/siemensgamesa/downloads/en/investors-and-shareholders/annual-reports/2018/siemens-gamesa-renewable-energy-annual-report-2018-en.pdf>

Siemens Gamesa. (2020b). *Company history*. Accessed on July 7th 2020 at: <https://www.siemensgamesa.com/en-int/about-us/company-history>

Vestas. (2020a). *History of Vestas: 1999-2004*. Accessed on July 14th on: <https://www.vestas.com/en/about/profile!from-1999-2004>

Vestas. (2020b). *Vestas – Turbines & technologies*. Accessed on July 14th on: <https://www.vestas.com/en/products>

B. MATERIAL COMPOSITION

This appendix elaborates on the material compositions presented in section 3.2 Material composition. For each component the mass intensity, material composition, material share and accuracy indication are given in overview Table B-1. Quality of the underlying data determines the accuracy of the estimation and is visualised with green, yellow and red. Green indicates multiple corroborated sources or good direct correlation ($R^2 > 0.9$), yellow indicates limited sources or assumptions used, red indicates one or more rough approximations were used. Further description of material compositions is given in the following sections.

Table B-1: Material composition overview. Colours indicate estimated data accuracy.

Component	Mass intensity [t/MW]	Base material(s)	Accuracy
Blades	12.022 ¹	Composite	$R^2=0.9702$, further specified
Hub	11.522	Spheroidal graphite cast iron	$R^2=0.967$, 34
Nose cone	0.649	Steel/aluminium structure + GFRP cover	Based on rotor: $R^2=0.09645$, 79
Power converter/transformer	4.85		
Shaft geared	3.13	Alloy steel Ni NiCr CrV	Based on nacelle: $R^2=0.9134$, 91
Shaft DD	1.05	Alloy steel	
Bed plate	5	Steel/cast iron	Based on Martinez et al. (2008) and Gaertner (2020)
Cover	2.424	GFRP + structure	Based on nacelle: $R^2=0.9134$, 91
Pitch mechanism	2.979	Alloy steel gears/bearings + cast iron casing + copper windings	Based on rotor: $R^2=0.09645$, 79
Yaw mechanism	4	Alloy steel gears/bearings + cast iron casing + copper windings	Based on nacelle: $R^2=0.9134$
Generator	Polynomials - h	Iron, copper, (magnet)	
Tower steel	Polynomial -h	Steel	$R^2=0.9214$, 61
Tower hybrid	Linear - h	Concrete +iron	
Tower internals	Linear - h	Copper, aluminium	
Onshore foundation	Average/turbine	Concrete, iron	
Offshore foundation	Average/turbine	steel	

1,2: varies as described in section 3.2.

B.1 Rotor assembly

The rotor assembly for Horizontal Axis Wind Turbines (HAWT) as they are currently being used are similar. With exception of early (<2000) two-bladed wind turbines, current (2000>) turbines have three blades, mounted to a hub, which is covered by a nose cone. Pitch mechanisms allow rotation of the blades to enable stalling and furling. Rotor assembly weights in Figure B-1 show a strong

correlation between rated power and rotor weight. However, as the rotor consists of various complex components, further partitioning is needed to accurately determine material composition.

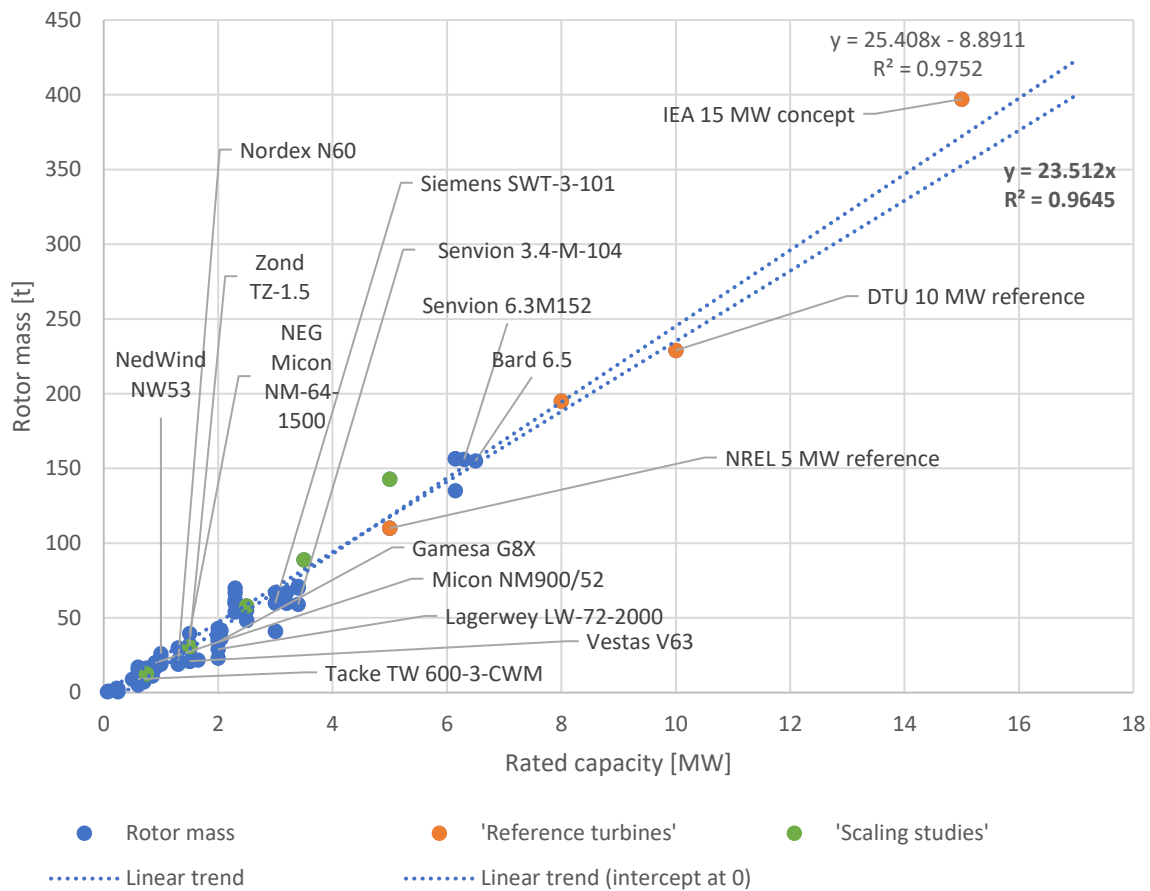


Figure B-1: Rotor mass [t] and rated capacity [MW]. Data for 79 turbines from various sources including Wind-turbine-models (2020) and concept designs.

Two trendlines are shown, the upper trend line is a linear trendline with the general formula of $y = ax + b$. For smaller x (capacity) values, y (mass) values become unrealistic (negative). Therefore, a trend line that intercepts at $0,0$ ($y = ax$) is assumed to be more accurate for smaller turbines. This does deviate more from expected masses for the 10 and 15 MW reference turbines, but as these are conceptual and there are few datapoints for turbines above 7 MW this deviation is within the expected margin of error.

Hub and blades are the main components of the hub in mass and therefore most commonly reported on. Nose cone and pitch mechanisms are not described as frequently. NREL scaling studies

(Smith, 2001) mention the estimates on hub mass include the pitch bearings and pitch mechanism. Cables for actuating the pitch mechanisms, various small fasteners and other miscellaneous components are excluded from this analysis.

B.1.1. Hub

The hub connects the blades to the drive train and is generally made of cast iron due to its complex geometry. The wind turbines component design chapter in the wind energy handbook (Burton et al., 2011) specifically mentions spheroidal graphite (SG) iron being the material of choice. Two typical designs are described, being tri-cylindrical and spherical. (Burton et al., 2011)

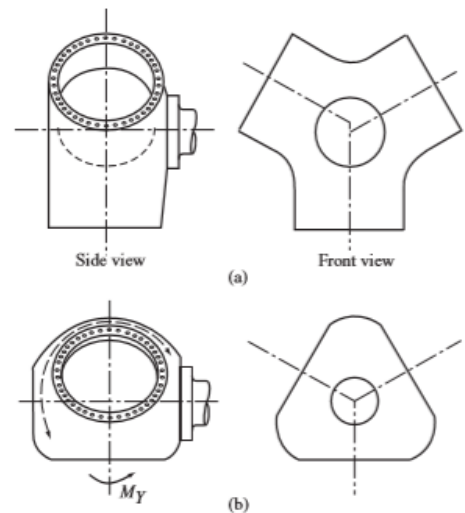


Figure B-2: Variations in hub design, a) tri-cylindrical and b) spherical. Adapted from Burton et al. 2011).

Hub weights in show a strong correlation between rated power and hub mass. The trendline agrees with NREL scaling studies ($m = 0.24D^{2.58}$) and seems a good indication for future designs as well.

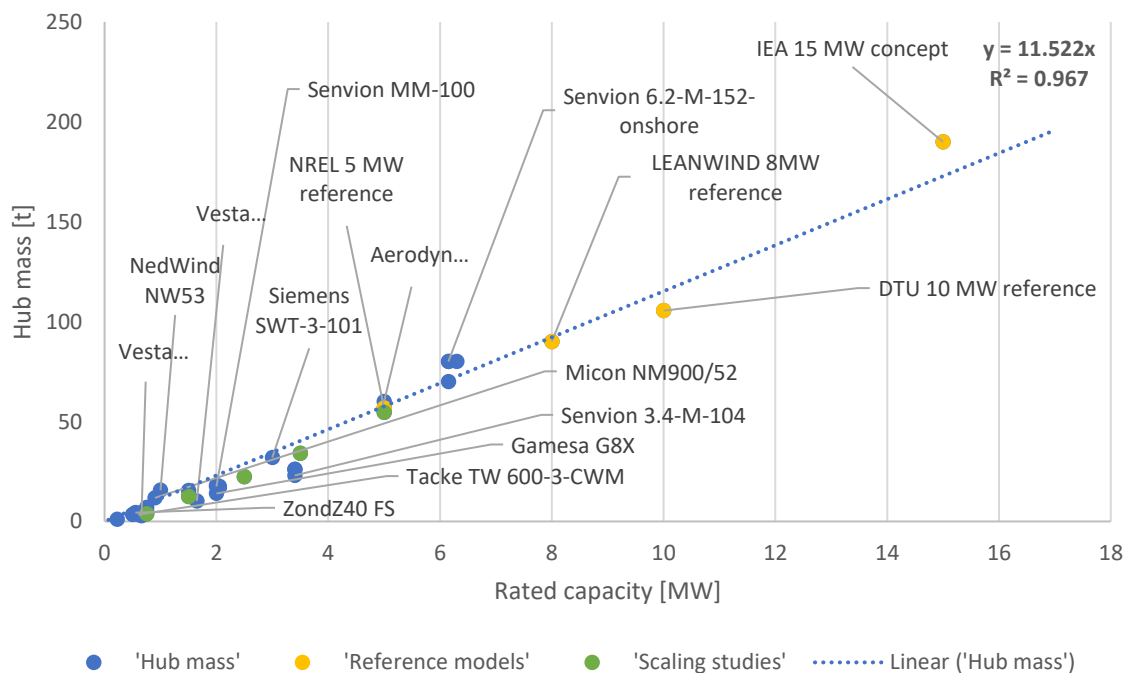


Figure B-3: Hub mass [t] and rated capacity [MW]. Data for 34 turbines from various sources including Wind-turbine-models (2020) and concept designs.

The empirically established relationship is $m[t] = 11.522 * \text{rated capacity [MW]}$. To determine the weight of various elements in the hub, the elemental composition of spheroidal graphite iron is needed. The conventional elemental composition of spheroidal graphite iron is iron (Fe), 3.0-3.7% carbon (C), 1.2-2.3% silicon (Si), 1.0% nickel (Ni), 0.25% manganese (Mn), 0.07% magnesium (Mg), 0.07% chromium (Cr), 0.03% phosphorus (P) and 0.1% copper (Cu). As the hub mass is completely cast iron, for SG cast iron becomes: $M_{hub, SG\ iron} = 11.522 * P_{rated}$. Elemental mass flows can be derived from the elemental composition and take the form of $M_{hub,i} = c_i * (11.522 * P_{rated})$, where i is the element of interest and c_i its percentage in the material.

B.1.2. Nose cone

The nose cone protects the hub and pitch mechanisms from the elements and has aerodynamic benefits. This component consists primarily of GFRP, depending on its design it also includes some metal supports and fasteners.

Based on an overview of generalized mass percentages of wind turbine components (Busby, 2012), it can be estimated that the nose cone accounts for 2.76% of rotor mass, leading to $m_{nose\ cone}[t] = 0.0276 * 23.512 * rated\ capacity\ [MW]$. Therefore, the mass intensity of the nose cone is approximately 0.65 t/MW. This estimation includes the GFRP cover, but also fasteners that could be a considerable portion of the total mass.

The IEA 15 MW concept turbine design (Gaertner et al, 2020) includes an 11.394 tonne nose cone, which can be translated to 0.76 t/MW. This is in the same order of magnitude and therefore validates the derived mass intensity of 0.65. For a 2 MW wind turbine 0.155 tonne of GFRP is needed for the nose cone (Martinez et al., 2008). This would mean roughly 25% of the nose cone weight is the GFRP cover and 75% would likely be fasteners and internal structure. As the GFRP is likely not a structural component in this case, this seems a reasonable assumption. This indicates, assuming a fibre volume fraction of 0.5 (fibre mass fraction 0.6) that 0.12 tonne of epoxy or polyester resin and 0.19 tonne of glass fibre is required. Normalizing this yields 0.16 t/MW GFRP, consisting of 0.06 t/MW resin and 0.09 t/MW glass fibre. Fasteners and internal structure are likely steel and/or aluminium and accounts for 0.49 t/MW.



Figure B-4: Rotor assembly. Obtained from IFM (2020)

Being derived from rotor mass, the nose cone mass and its material composition has medium accuracy.

B.1.3. Pitch system

Pitch systems are present in most modern wind turbines, consisting of slew drives (hydraulic/electric) and pitch gear and bearings. Slew drives (Figure B-5) are an assembly of a motor (hydraulic or electric), gearbox and pinion gear, used for pitch- and yaw mechanisms. Older wind turbines (<2000) use passive stall control (Burton et al., 2011).

From Busby (2012) it can be derived that the pitch mechanisms (all three, including bearings) account for 12.67% of rotor weight. This means $m_{pitch\ mechanisms}[t] = 0.1267 * 23.512 * rated\ capacity\ [MW]$ or ~3 t/MW. The material composition of the pitch mechanism depends largely on it being a hydraulically or electrically actuated system. It can however be assumed that the mass is mostly composed of steel/iron in both cases and a small share of copper for the electrically actuated system. As bearing- and gear steel is often high-alloy steel a large share will be this type. Linkages and electric/hydraulic motor housing will likely be cast iron. As this component relies heavily on few sources using rough and assumed data, the uncertainty is relatively large. According to a producer (Bonifiglioli, 2020) of slew drives, turbines up to 1 MW use three drives of 60-120 kg. Their largest slew drives are for 9-12 MW turbines. Assuming a 10 MW turbine 3-6 slew drives are used of 500 kg. This yields values of



Figure B-5: Pitch system slew drive. Bonifiglioli, (2020)

respectively 0.18 – 0.36 t/MW and 1.5 – 3 t/MW for both categories. The average is 1.26 t/MW for slew drives, meaning the remaining 1.74 t/MW is accounted for by the gears and bearings. For the slew drives, the material composition is part alloy steel (gears/bearings), cast iron and copper (windings). The pitch gears and bearings are mostly alloy steel.

Polinder et al. (2006) describe generator material compositions, for which 23 Wt% copper is used. As generators are very similar to electric motors, this material composition is used to determine slew drive copper content. It is assumed 25% of the slew drive is accounted for by the electric motor, leading to $m_{pitch,copper} = 0.0575 * 1.26 * P$.

Accuracy of pitch mechanisms is low due to it being derived from rotor mass and multiple crude underlying assumptions.

B.1.4. Blades

Lefeuvre et al. (2019) assume 10 kg of rotor blade material per 1 kW of installed capacity. Liu & Barlow (2017) have performed a study on wind turbine blade waste globally in 2050. Their estimations are based on data for 56 wind turbine blades with rated capacities of 0.5 - 8 MW and validated with Albers (2009) estimate of 10 t tonne/MW.

Table B-2: Mass intensity estimates for blades by Liu & Barlow (2017)

< 1 MW	1-1.5 MW	1.5 – 2.5MW	2.5 – 5 MW	>5 MW
8.43	12.37	13.34	13.41	12.58

Using data gathered for 58 turbines (including scaling and reference turbines) the mass intensity is determined, showing results ($3 * 4.0073 \approx 12$) similar to Liu & Barlow (2017) of ~ 12 t/MW in Figure B-6.

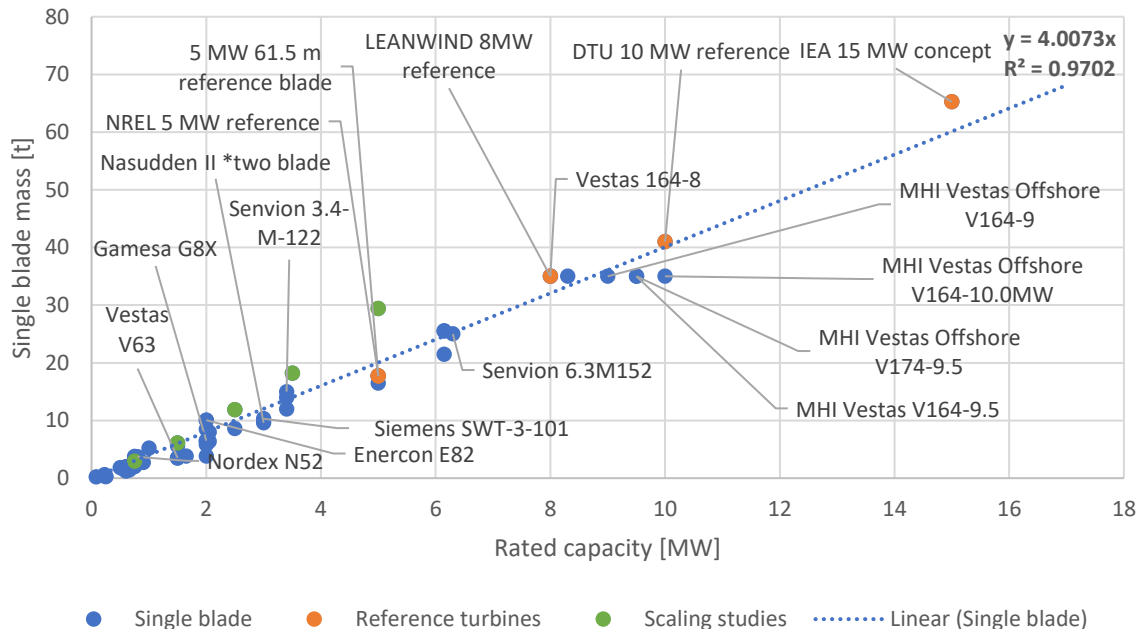


Figure B-6: Single blade mass [t] and rated capacity [MW]. Data for 58 turbines from various sources including Wind-turbine-models (2020) and concept designs.

The NREL WindPACT scaling study (Smith, 2001) uses a scaling factor of $m = 0.1D^{2.63}$. Figure B-6 shows this scaling factor over-estimates blade mass as indicated by the trendline. As the scaling is from 2001, these estimates are likely less relevant for modern wind turbines. To check if

categorisation (as in Liu & Barlow (2017)) is necessary, Figure B-7 shows the single blade mass for wind turbines with a rated capacity below 1 MW. This reveals a lower intensity is indeed justified as for three-bladed turbines 10.54 t/MW and for two-bladed turbines (more common <1MW) 7.03 t/MW would be more accurate than ~12 t/MW. Therefore, the values obtained by Liu & Barlow (2017) are used for the model.

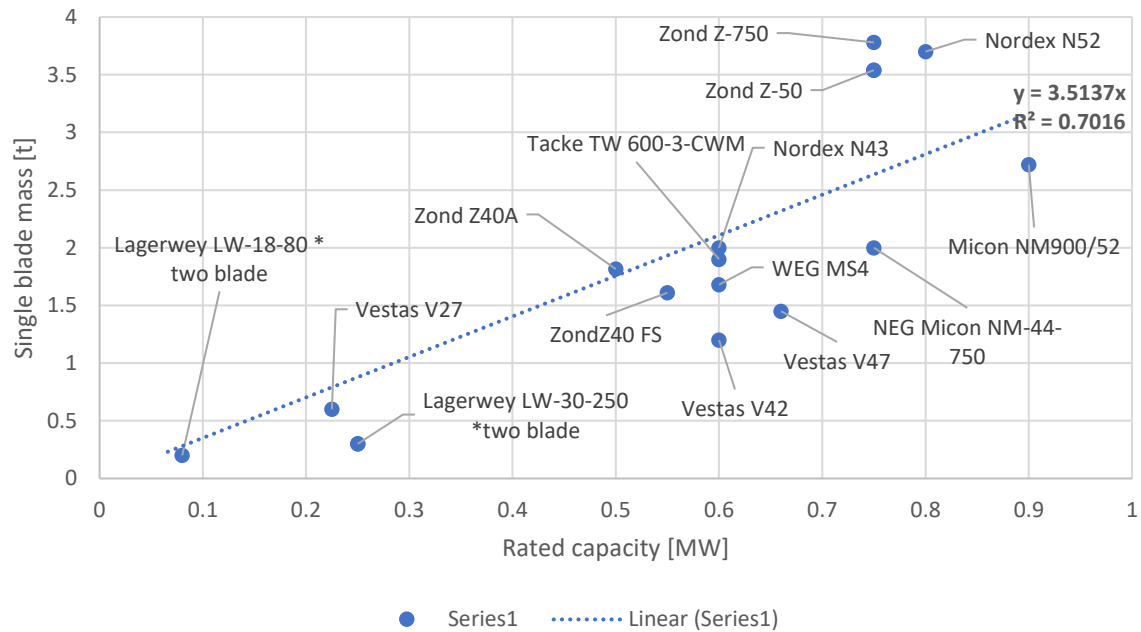


Figure B-7: Single blade mass for turbines with a rated capacity below 1 MW.

Due to their demanding application, wind turbine blades have developed into complex components, containing a variety of materials, combined and joined to optimize the difficult trade-offs in strength, deflection, fatigue, energy yield, fatigue, weight and cost (Burton et al., 2011). As blade design technology progressed, different material combinations have been applied.

Glass fibre, epoxy/polyester, PVC foam, (balsa)wood and in some cases carbon fibre are common in blades (Burton et al., 2011). These materials have been joined together to form composite materials.

Innovations in manufacturing, such as vacuum assisted resin transfer molding (VARTM) have enabled improved properties for fibre reinforced polymers by increasing fibre volume contents to 50-60% compared to traditional hand lay-up with fibre volume fractions between 30% and 40%. Similarly, 'prepregs' which consist of fibre pre-impregnated with partially cured epoxy have increased these properties.

The blade root is where the blade connects to the hub. As one of the most critical areas in blade design, high strength steel bolts are required (Burton et al., 2011). These bolts can be fitted in various ways, most commonly using steel inserts in the composite root section. Connectors are also high strength steel or spheroidal graphite iron (Burton et al., 2011).

The waste considered by Liu & Barlow is over the full life cycle of a blade and therefore includes manufacturing, discard and testing waste. It is estimated 12% - 30% of blade materials is manufacturing waste. Although significant, this lies outside the scope of this study and therefore inflow of material is considered to be the finished blade. Materials added and lost in operation and maintenance should be included in the analysis later. The ratios for manufacturing, operational and maintenance waste from Liu & Barlow can be used for this.

Materials used in wind turbine blades vary from manufacturer as well as Siemens uses integrated blade design, allowing a unibody blade without structural glue and obtaining reduction in use of other materials. LM is a large blade manufacturer, which uses polyester resin instead of the more commonly used epoxy resin. In an environmental impact study from Liu & Barlow (2016), it is estimated that the generalised material composition of a blade is as presented in Table B-3.

Table B-3: Blade material composition. Based on Liu & Barlow (2016).

Material	Material by weight %
GF/CF fabric	60.4%
Resin and adhesives	32.3%
Steel	1.1%
Copper	0.3%
Aluminium	0.0%
Balsa	2.3%
PVC	1.7%
Paint	0.9%
Putty	0.7%
Spray adhesives	0.0%

Glass fibre is composed of various mineral oxides, with shares depending on the type of GF. E-glass is commonly composed of ~54% SiO₂ ~14% Al₂O₃, (5-10% B₂O₃), 20% CaO and other, less relevant oxides. Higher quality fibres are composed of higher SiO₂ and AlO₃ shares and less trace elements. (Compositesworld, 2020)

Zimmerman (2013) describes the material composition of Enercon E-82 E2 rotor blades, where a rougher indication of materials is described. GFRP shows a similar share, steel is a factor 3 larger, which could depend on specific blade type and 0.3% copper instead of aluminium. This indicates that lightning strike protection can be either copper or aluminium. Griffin (2002) determined in a conceptual blade design study for 35m blade intended for a 1.5 MW turbine, 4.463 tonne blade material is needed and 0.253 tonne steel for the root connection. Of the 4.463 tonne blade material, 2.186 tonne is the spar section. In the study, GFRP wet layup is considered as manufacturing method, but alternative materials and manufacturing methods are discussed in a trade-off table. Resor (2013) describes a 5 MW Blade Reference Model weighing 17.7t, of which 13.8%+15.9% is glass fibre, 17.4% CF prepreg, 31% resin, 0.2% gelcoat and 21.8% foam. The CF prepreg is assumed to have a fibre mass fraction of 70% leading to 12.18% CF. These percentages correspond with Liu & Barlow (2016)

Material compositions for each blade differ due multiple variables (among which manufacturer, rated capacity and age-cohort). This means categorisation is needed to simplify the material compositions. As estimated by Lefeuvre et al (2019) blades after 2010 and above a rated capacity of 2 MW contain on average 6wt% carbon fibre. Fibres used in wind turbines include mainly variations (weave and uni-directional) of E-glass fibre with up to 75 Wt% glass fibre (Mishnaevsky et al., 2017). Fibres with superior material properties are available and include S-glass, R-glass, carbon-, basalt- and aramid fibres. Of these alternatives only carbon fibres are commonly used, although sparingly in structural spar caps of large blades. The reason for this is largely due to relatively high cost of these alternatives. Manufacturers that use carbon fibre include Siemens Gamesa and Vestas early on (Grande, 2008), but is believed to include most blades above 2 MW, in line with Liu & Barlow (2019). Matrix materials typically include thermoset polymers such as epoxies, polyesters and vinyl-esters. Epoxy is the most commonly used matrix material, used by Vestas and Siemens Gamesa. The trend

towards larger blades has increased the use of epoxy as matrix material. However, LM uses polyester and vinyl-ester resins. (Mishnaevsky et al., 2017)

A 0.6 fibre volume fraction seems a reasonable estimation based on technologies used and data from literature (Liu & Barlow, 2016; Zimmerman, 2013;), which means that a GFRP consists of 68wt% GF and 32wt% resin and a CFRP consists of 75wt% CF and 25wt% resin. The resin used is mostly epoxy, but LM uses only polyester resins. For the categorized mass intensity I_c in Table B-2, the equation for glass fibre becomes

$$m_{blades,GF} = 0.604 \cdot I_c \cdot P_{rated}$$

Or for glass- and carbon fibre for turbines above 2 MW and after 2010,

$$m_{blades,GF} = 0.544 \cdot I_c \cdot P_{rated} \text{ and } m_{blades,CF} = 0.06 \cdot I_c \cdot P_{rated}.$$

B.2 Nacelle

The nacelle houses several essential systems for the operation of the wind turbine and is hence complex in material composition. Further breakdown into several sub-components is therefore required. These include the bedplate and cover that together create the nacelle structure, drive train, mechanical brake, yaw drive and various other small components used among others for controlling the wind turbine. Due to its complexity and diversity, the drive train is discussed in a separate subsection.

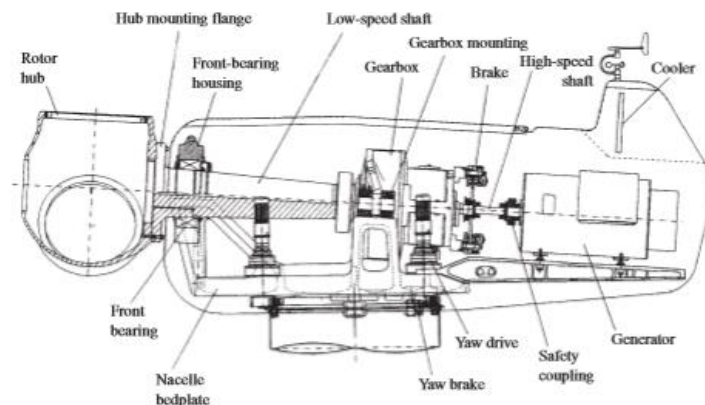


Figure B-8: Nacelle of a geared drivetrain wind turbine. Adapted from Burton et al. (2011)

Although simple mass compositions for various materials are not applicable here due to complexity, the nacelle mass can be described approximately using the equation $M_{nacelle} = 45.054 P_{rated}$ as shown in Figure B-9. The NREL scaling study (Smith, 2001) gives a similar estimation using $m = 7.4D^{2.11}$. Given the variations in drive train concepts, other components, such as bedplate, yaw mechanism and cover must be a large share in total nacelle mass.

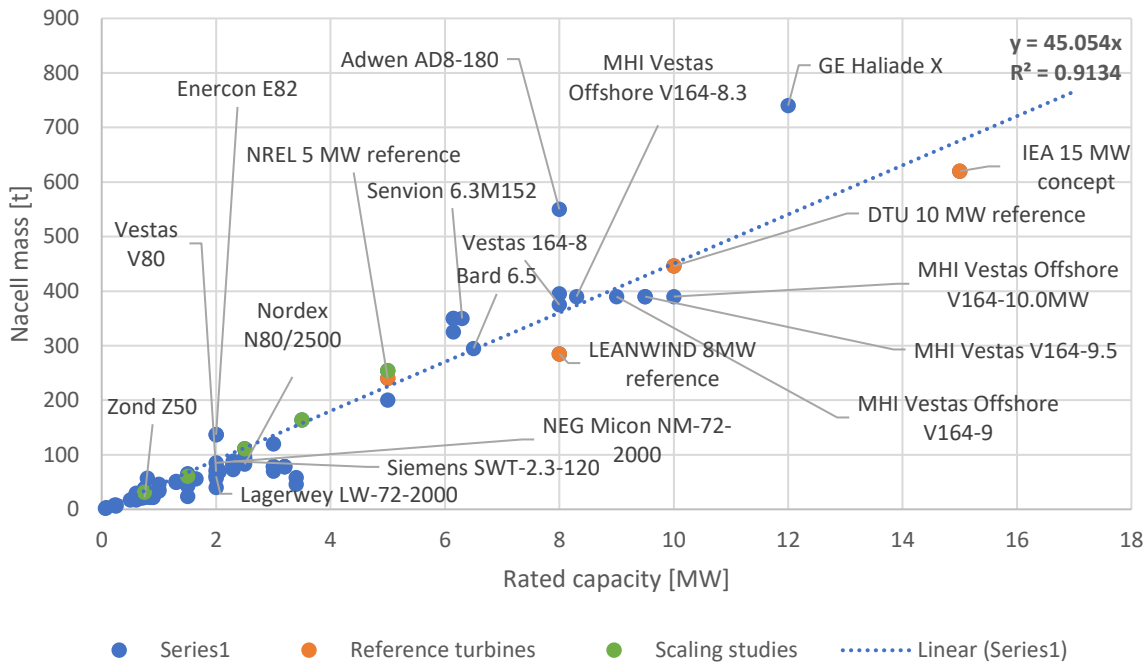


Figure B-9: Nacelle (including drivetrain) mass [t] and rated capacity [MW]. Data for 91 turbines from various sources including Wind-turbine-models (2020), scaling studies and concept designs.

B.2.1 Bedplate

The bedplate or frame is the main structural component that provides mounting for nacelle components. In some cases, the bedplate is integrated (e.g. as gearbox casing), but for simplification it is considered to be a separate component. The structure is either constructed by welding beams together or cast for more complex designs (Burton et al., 2011). This means that in some cases construction steel is used (S235, S355) and in other, more complex designs spheroidal cast iron is used as described in the hub material composition section. Figure B-8 shows a nacelle and bedplate for a geared wind turbine, whereas Figure B-10 shows the nacelle and bedplate for a direct drive turbine. It is assumed that due to its more complex shape, the direct drive bedplate is cast iron and older, simpler designs for geared wind turbines use construction steel beams. Martinez et al. (2008) estimate 10.5 tonne iron is needed for a 2 MW Gamesa G8X bedplate. Normalizing this yields 5.25 t/MW. The 15 MW IEA concept bedplate mass is 70.329 t or 4.6886 t/MW. Although the designs for these bedplates and turbines is very different, both agree on a material intensity of ~5t/MW cast iron or steel.

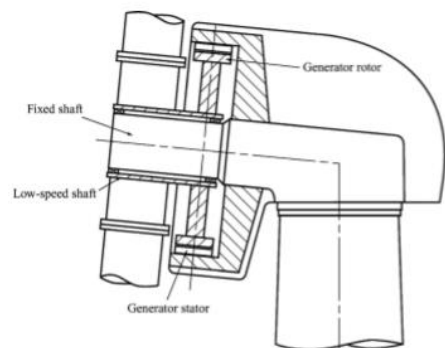


Figure B-10: Nacelle for a direct drive wind turbine. Adapted from Burton et al (2011)

Being derived from nacelle weight and not including variations in design, the accuracy of the bedplate mass estimation is limited.

B.2.2 Cover

The cover of the nacelle protects its sub-components from the elements. Having limited structural requirements, weight reduction is leading in its design. Therefore, current wind turbines use GFRP for these covers, joined to each other and the bedplate with bolts. From Busby (2012) it is determined that 5.38% of nacelle mass is account for by the cover. Applying this to the established relationship for nacelle mass results in $m = 0.0538 * 45.054 P$ or 2.42 t/MW. Martinez et al. (2008) mention 2 tonne cover material is needed for a 2 MW Gamesa G8X turbine. Assuming a fibre volume fraction of 0.5 (0.6 mass fraction) yields 1.2 tonne of fibre glass and 0.8 tonne resin. Normalizing this yields 1/MW GFRP and 0.6 t/MW fibre glass and 0.4 t/MW resin. The remainder of 0.42 t/MW could be a discrepancy or (in part) account for fasteners, but this is not specifically mentioned by Busby (2012).

The accuracy of this estimated is limited as it is derived from nacelle mass under a single source.

B.2.3 Mechanical brake

In case of aerodynamic brake failure or maintenance, a mechanical brake is required to halt the rotation of the blades. the mechanical brake consists of callipers, brake pads and a braking disc mounted to the shaft. The discs are made from spheroidal graphite cast iron or steel. Brake pads are made from sintered metal or resin-based material. Burton et al. (2011) further assume the brake weight to scale proportional to the rated power of the wind turbine. It is further assumed that direct drive turbines do not require brakes due to sufficient stopping power in the generator. Due to lack of data availability this component is not included in the model.

B.2.4 Yaw system

The mechanisms that allows the nacelle to rotate is the yaw drive. It consists of one or multiple electrical or hydraulic motors, which drive the slewing ring on the tower through a reducing gearbox (Burton et al., 2011).

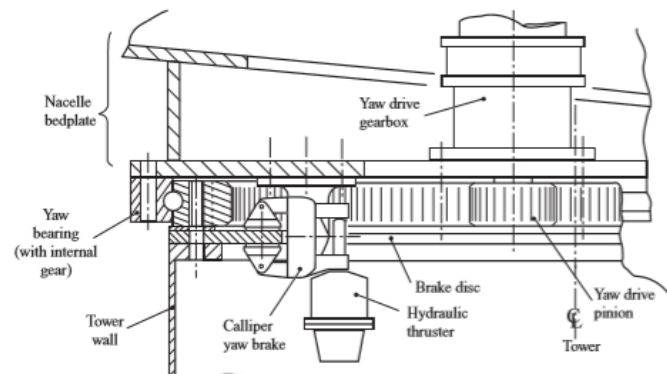


Figure B-11: Yaw system. Adapted from Burton et al (2011)

The weight of the yaw system is estimated to be 4.29% of total nacelle mass (Busby, 2012). This means the combined mass of electric motors, gearbox, yaw brake, yaw gear and bearing is $m_{yaw} = 0.043 * 45.05 * P_{rated}$ or 1.93 t/MW. For the IEA 15 MW concept, a 100-tonne mass is reported for the yaw system. This indicates a much larger mass intensity of 6.67 t/MW compared to the estimate based on Busby and nacelle mass. This could be due to non-linear effects of structural requirements for higher loads in large wind turbines. As literature and documentation often omit the yaw drive, a crude assumption of 4 t/MW is used for the yaw system mass intensity. Siemens 7 MW offshore turbine uses 16 slew drives in its yaw system (ExceptionalEngineering, 2020). These slew drives are similar to those in the pitch systems, but have more power and are larger.

Individual yaw drive weights range from 120 kg to 2100 kg for >1 MW to 9-12 MW turbines, using respectively 2-4 and 8-16 drives for one yaw system (Bonifogli). This means the drive mass intensity is 0.24-0.48 t/MW for >1 MW turbines and 1.4 – 2.68 t/MW for 9-12 MW turbines. On average it can therefore be assumed roughly 1 t/MW for the yaw drive. Subtracting this from the estimated 4 t/MW for the complete yaw system leads to the estimate of 3 t/MW for the yaw ring (bearing and gear). Like the pitch system it is estimated that the bulk of this is alloy steel and cast iron. Copper content is estimated roughly at $m_{slew,copper} = 0.0575 * 1 * P_{rated}$.

Accuracy of yaw mechanism mass is low due to it being derived from nacelle mass and multiple crude underlying assumptions.

B.2.5 Power converter and transformer

Limited data for transformer material use is available. Most onshore turbines have their transformer in the nacelle, but for larger and offshore a tower-based transformer is common. Estimates from Ghenai (2012) for a generalized 2MW turbine are 6t cast iron, 2t copper, 1.7t aluminium. Assuming this scales linearly with rated capacity yields 3t/MW cast iron, 1t/MW copper and 0.85 t/MW aluminium.

There is a converter and transformer in the turbine for grid compliance. For wind parks this is connected to a central transformer station, for HV transport. This is later converted to grid compatible current. The considered converter components are present within the turbine as defined by the technological scope. This means the converter cabinets or low-medium voltage converters are further analysed. ABB converter masses indicate a 0.65 t/MW relation can be used.

B.2.6 Other nacelle components

Various other components can be present in the nacelle, but due to variations in design and limited data availability do not enable further analysis. These components include among others cooling-, hydraulic, measurement- and control systems.

B.3 Drivetrain

The drivetrain realises the conversion from rotational energy to electrical energy. Generators function basically as inverted electric motors, by a rotating magnetic field (rotor) that induces an electric current in the stationary windings (stator). This magnetic field can be created using either electromagnets or permanent magnets. Depending on its configuration, the drive train includes a gearbox, shaft and generator (geared) or only a generator (direct drive). The drive train is designed around the generator leading to various configurations. Geared drivetrain concepts (Figure B-12) are used to match rotor and generator speeds most efficiently as low speed rotation from the rotor blades [1] turns the low speed shaft [2], which drives the gearbox [3] that converts the low speed rotation into high speed rotation on the high-speed shaft [4] which drives the generator [5]. Large bearings [6] are used to support the rotating shafts. Losses that occur due to these mechanical conversions and more importantly the high cost of maintenance and failure due to wear in bearings and gears has resulted in direct drive (DD) configurations where no gearbox is needed (Polinder, 2011; Bang et al. 2009). DD concepts require a low speed generator, which is generally much larger and therefore heavier than a conventional generator. Although a weight reduction is achieved by removing the gearbox, overall direct drive wind turbines have a higher top-weight depending on the type of generator used.

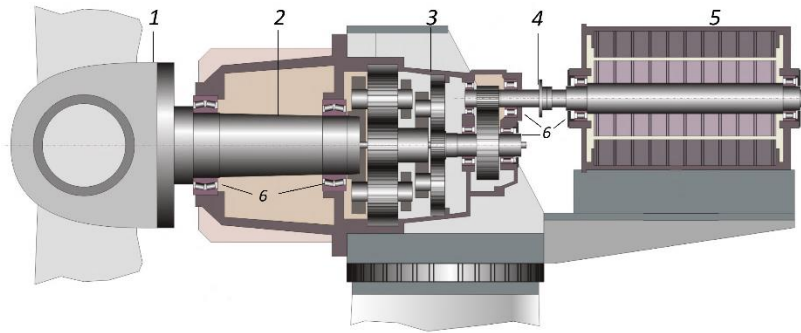


Figure B-12: Geared drive train configuration. 1. rotor, 2. low-speed shaft, 3. three-stage gearbox, 4. high speed shaft, 5. generator, 6. bearings. Figure adapted from Teng et al. (2017)

Common drivetrain designs include geared asynchronous generators (AG) (e.g. squirrel cage Induction Generator (SCIG) and doubly fed induction generator (DFIG)), direct drive - electrically excited synchronous generators (EESG), geared medium- and high speed permanent magnet generators (MS/HSPMG) and direct drive - permanent magnet synchronous generators (PMSG) (Adaramola, 2014; Polinder et al., 2006; Månberger and Stenqvist, 2018). Additionally, high temperature superconductor generators (e.g. Ecoswing) are being developed (Winkler, 2019) that are promising for further upscaling of wind turbine capacity. Figure B-13 summarizes the various configurations.

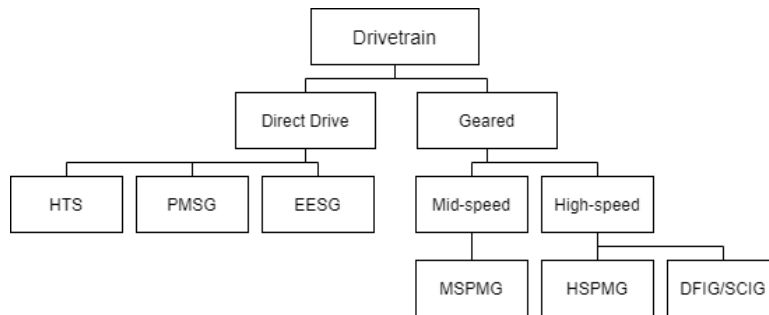


Figure B-13: Drivetrain configurations. Adapted from Manberger and stenqvist (2018)

Fixed speed induction generators were dominant from 1985 to 1995 up to a rated capacity of 1.5 MW. Around 2000, doubly fed induction generators and full power converters were introduced. Full power converters consisted of geared and directly driven wound and permanent magnet generator (Sethuraman & Dykes, 2017); Burton et al., 2011). Polinder et al. (2006) describe a similar development with fixed speed SCIG up to 1.5 MW until the late 1990s. Since then, variable speed is introduced for over 1.5 MW, using multi-staged gearboxes. Since 1991, gearless generators have been introduced. Polinder (2011) describes the drive train configurations typical for various manufacturers in 2009. For older turbines, Polinder et al. (2003) provide a similar overview. For newer turbines, data obtained from Lagerwey (website and personal communication) and wind-turbine-models.com provides additional information.

Table B-4: Drivetrain configurations per manufacturer. Based on data from Polinder et al. (2011) [1], Polinder et al. (2003) [2], wind-turbine-models.com and manufacturer data [3].

Manufacturer	Configuration	Rotor diameter [m]	Rated capacity [MW]
(MHI) Vestas	AG ¹	52-90	0.85-3
	MSPMG ¹	112	3
General Electric (GE)	AG ¹	70.5-82.5	1.5
	MSPMG ¹	100	2.5

	DDPMG ¹	110	4
Enercon	EESG ¹	33-126	0.3-7.5
Siemens (Gamesa)	AG ¹	82-107	2.3 -3.6
	DDPMG ¹	101	3
Bonus	AG fixed speed ²	-	0.6-2.3
Lagerwey	AG ²	-	0.25
	EESG ²	-	0.75-2
	DDPMG ³	-	
NEG Micon	AG fixed speed ²	-	0.6-2
	AG ²	-	2.75
Nordex	AG fixed speed ²	-	0.6-1.3
	AG ²	-	1.5-2.5

With this information and the installed turbine data from WindStats, market shares for various generator configurations are determined. The results are presented in Figure B-14.

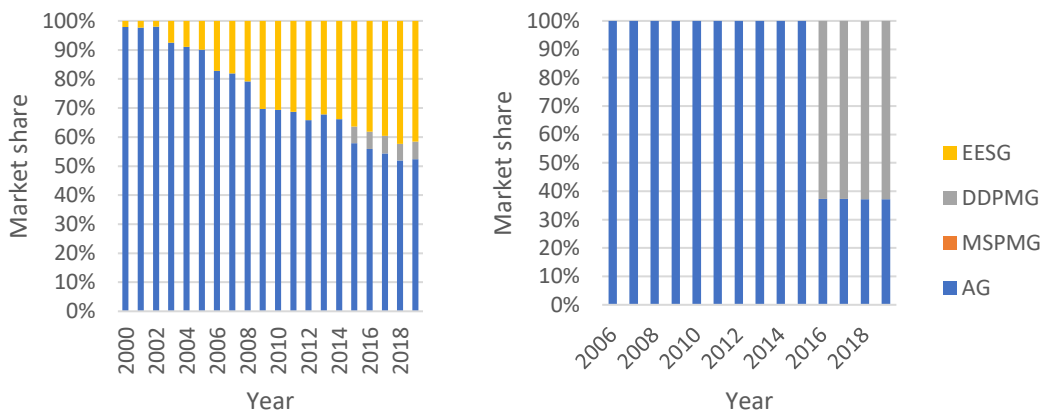


Figure B-14: Market shares for onshore (left) and offshore (right) drivetrain configurations. Based on data presented in Table B-4.

B.3.1 Low speed shaft

Being subjected to the full dynamic torque of the wind turbine, the low speed shaft needs to be strong. Hence, the weight of the low speed shaft accounts for 6.94% of nacelle weight (derived from Busby, 2012) for geared wind turbines. Using the derived nacelle weight, the mass intensity is approximately 3.13 t/MW. Direct drive configurations are estimated to have a lower mass intensity, due to a shorter shaft, based on the IEA 15 MW reference turbine, the mass intensity is 1.05 t/MW. For high strength steel shafts, alloy steel is commonly used, such as nickel, nickel-chromium or chromium-vanadium steel. Elsam (2004) report on CrMo-steel being used for the shaft. Furthermore, in their lifecycle assessment, 'high power' steel in gears has been estimated by stainless steel.

B.3.2 Gearbox material composition

Various configurations require a gearbox, which size depends on the required conversion ratio and specific configuration. For fixed speed wind turbines (generally older turbines), a fixed conversion ratio is used for rotor to generator. For variable speed wind turbines, this ratio can be adjusted to match optimal wind-, rotor- and generator speed. The conversion ratio required to go from low speed rotation to high speed is larger than from low to medium speed. Therefore, more stages are needed

and the gearbox is heavier. Gearbox mass is not often presented in literature or manufacturer data, therefore scaling is used.

For a Gamesa G8X, which has a geared DFIG configuration, Martinez et al (2008) mention the gearbox has a mass of 16 tonnes, consisting of 8 tonne steel and 8 tonne iron. It is assumed here that alloy steel is used for the gears and cast-iron for the casing and shafts in the gearbox. Normalizing these masses yields 8 t/MW total gearbox weight, of which 4 t/MW is carbon steel and 4 t/MW cast iron. Burton et al. (2011) assume the gearbox and generator weight to scale proportional to the rated power of the wind turbine. According to Busby (2012) the generator generally accounts for 23.52% of nacelle weight, meaning that $0.2352 * 45.054 = 10.59$ t/MW is the mass intensity for the gearbox. This falls in the same magnitude as derived from Martinez et al. (2008). This means 5.3 t/MW steel and 5.3 t/MW cast iron are present in the gearbox.

Elsam (2004) describes the use of 7CrNiMoS6, 31CrMoV9 and bearing steels as alloy steels in gearboxes. Together the alloy steels are estimated to account for 50% of gearbox weight. The shares of each alloy steel is not mentioned. According to SteelNumber (2020) the elemental composition of 31CrMoV9 is 0.27-0.34 % C, >0.4% Si, 0.4-0.7% Mn, >0.025 P, >0.035% S, 2.3 – 2.7% Cr, 0.15 -0.25% Mo, 0.1-0.2% V and that of 17CrNiMoS6 is 0.15 ~ 0.21% C, ≤ 0.40% Si, 0.50 ~ 0.90, ≤ 0.025% P, ≤ 0.015% S, 1.50 ~ 1.80% Cr, 0.25 ~ 0.35% Mo, 1.40 ~ 1.70% Ni

B.3.3 Generator material composition

Generator mass is a key aspect of wind turbine design and subject to much debate and improvement as illustrated by the various generator designs in wind turbines today. Generator mass is not often reported however. Therefore, generator scaling laws are used to determine the mass intensity of each generator type (Sethuraman and Dykes, 2017). This leads to estimates for SCIG, DFIG, DDPMG and EESG, shown in Figure B-15.

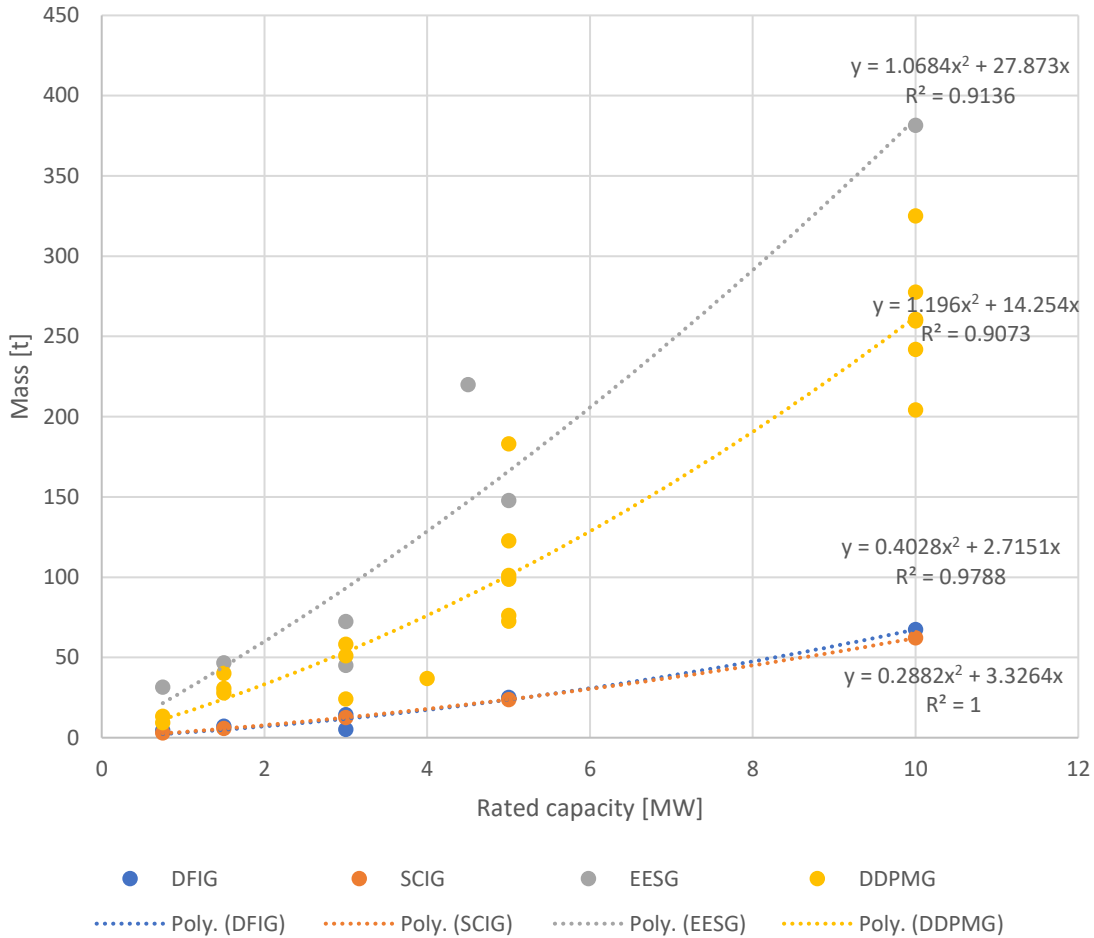


Figure B-15: Mass intensity for DFIG, SCIG, EESG and DDPMG according to NREL scaling studies (Sethuraman & Dykes, 2017)

B.3.4 Asynchronous generators

Asynchronous generators (AG) are electrically excited (electromagnet) generators. Typical asynchronous generators include the Squirrel Cage Induction Generator (SCIG) and Doubly Fed Induction Generator (DFIG). SCIGs are typically single fed and therefore fixed speed generators, typically used with a 3-stage gearbox in Vestas, Bonus, NEG Micon, Nordex, Senvion and Siemens wind turbines (Shammugam et al., 2017). The SCIG has been slowly replaced with DFIG, due to better cost-effectiveness and grid compatibility (Lacal-Arántegui, 2015). DFIGs lend their name to the fact that both rotor and stator are connected. These generators are typically wound rotor generators and therefore differ in material composition from the SCIG. DFIG generators are typically paired with a 3-stage gearbox and partial scale converter (Shammugam et al., 2017). Examples of manufacturers include Nordex, GE, Vestas, Senvion and Gamesa.

Using scaling laws for SCIG and DFIG generates very similar results for both asynchronous generators (Figure B-15, Figure B-16). Therefore, no further distinction will be made. Total generator mass can be estimated with $m_{AG} = 0.3P^2 + 3.65P$. For iron, $m_{AG,iron} = 0.29P^2 + 3.19P$ and for copper, $m_{AG,copper} = 0.1834P$.

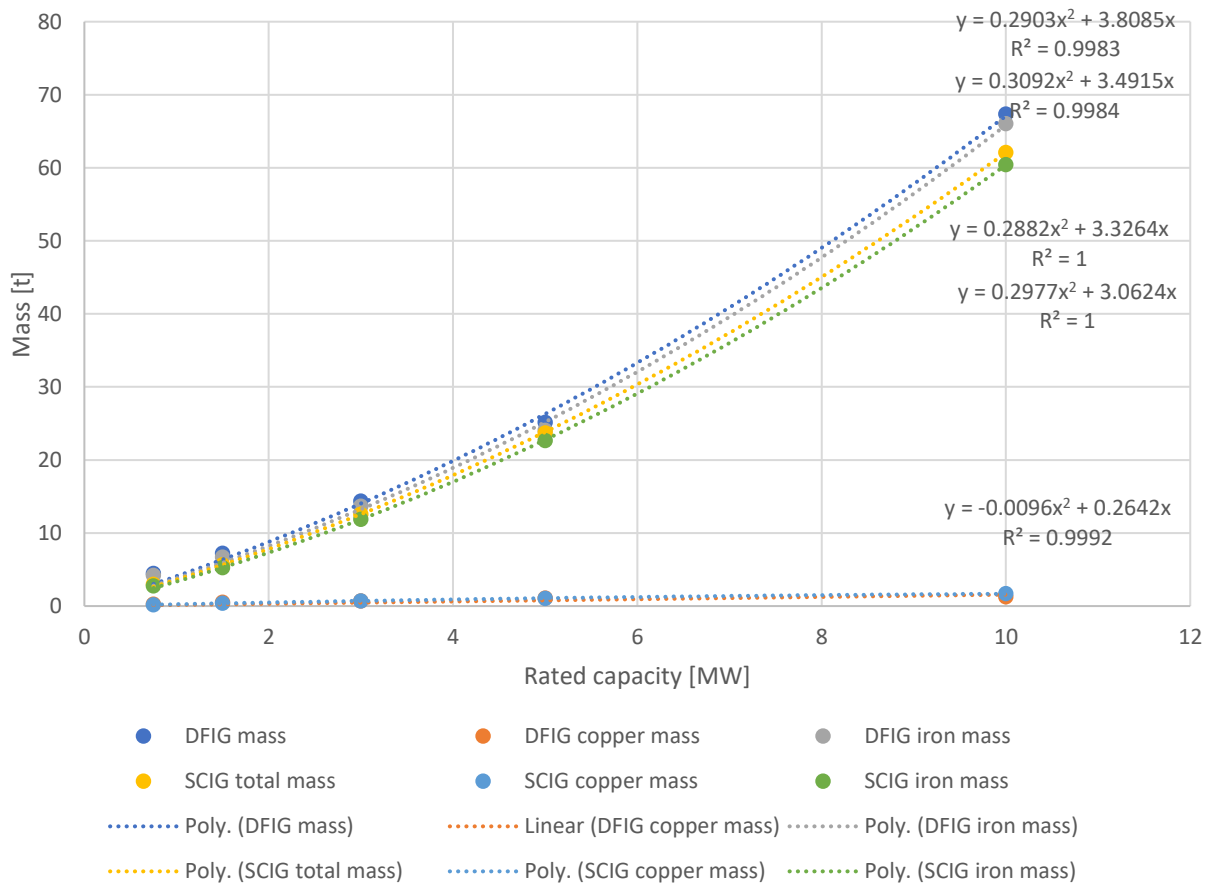


Figure B-16: Material intensities for asynchronous generators based on NREL scaling studies (Sethuraman & Dykes, 2017)

The generator in the Gamesa G8X 2 MW turbine analysed by Martinez et al. (2008) is a DFIG type generator. The total weight of this generator is 6.5 tonne, which includes 4.29 tonne steel, 2 tonne copper and 0.2 tonne silica. Normalizing this yields a total weight of 3.25 t/MW, including 2.15t/MW steel, 1 t/MW copper and 0.1 t/MW silica.

Polinder et al. (2006) describe two 3MW DFIGs for a 3-stage and 1-stage gearbox configuration, where the 3-stage generator is 5.24 t and the 1-stage generator is 11.37 t with similar material compositions. This indicates medium speed generators are roughly twice the mass of high-speed generators.

B.3.5 Permanent Magnet Generators

PMGs are found in multiple distinctive configurations according to Shammugam et al. (2017). High speed configurations use three-stage gearboxes and are common in Vestas turbines. Middle speed configurations use a 1-stage gearbox and are common in Areva, Vestas MHI, WinWind and Adwen turbines. Direct drive PMSG configurations are common in Siemens and Vensys turbines (Shammugam et al., 2017). NREL scaling studies do not include geared PMG, but do give indications for two types of DDPMG. Figure B-17 shows the material equations derived from NREL scaling studies.

For HSPMG and MSPMG, further analysis is needed. Polinder et al. (2006) describe a 3MW 1-stage gearbox PMG (medium speed) of 6.11t to be composed of 4.37t iron, 1.33t copper and 0.41t permanent magnet. This is used to derive material intensities of iron 1.46 t/MW, copper 0.433 t/MW and permanent magnet 0.137 t/MW.

Estimates for magnet mass in the three PMG types are 0.16 t/MW for medium speed (1-2 stage) and 0.08 t/MW for high speed and 0.65 t/MW for low speed/DD magnet weight (Viebahn et al., 2015; Laca Arántegui, 2015). As functioning principles are similar, it can be derived that MSPMG is 0.25 DDPMG and HSPMG is a factor 0,5 MSPMG. Given that this study derived these estimates from multiple sources and is more recent than Polinder (2006), these values are considered more accurate. Important elements here are the critical rare earths neodymium and dysprosium.

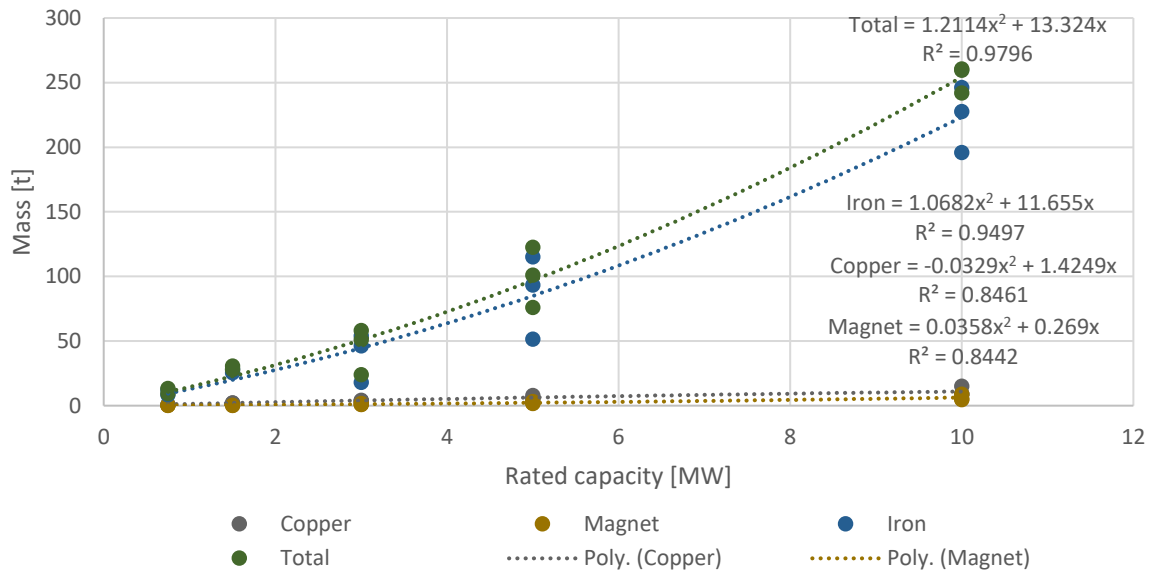


Figure B-17: DDPMG material equations based on NREL scaling studies (Sethuraman & Dykes, 2017)

$$m_{DDPMG,total} = 1.2114P^2 + 13.324P$$

$$m_{DDPMG,iron} = 1.0682P^2 + 11.655P$$

$$m_{DDPMG,copper} = -0.0329P^2 + 1.4249P$$

$$m_{DDPMG,magnet} = 0.0358P^2 + 0.269P$$

Polinder (2006) describes a 3MW DDPMG containing 18.1 t iron, 4.3 t copper and 1.7 t magnet. Applying the equations derived in Figure B-17 yields 44.58 t iron, 3.3 t copper and 1.1292 t magnet. This means compared to Polinder (2006) iron is overestimated by a factor 2.5, copper underestimated by a factor 0.77 and magnet underestimated by a factor 0.66. Although the numbers seem correct in order of magnitude, the low quantity of critical materials in the magnet require more accuracy. According to Laca Arántegui (2015) low speed (i.e. direct drive) PMG magnet content is 0.85 t/MW. This would mean a 3 MW turbine would contain 2.55 tonne magnet material, further deviating from the estimates based on Polinder and NREL. Figure B-18 breaks down the various estimates in two types described by Sethuraman & Dykes (2017), one type described by Polinder (2006) and the 0.85 t/MW material intensity from Laca Arántegui (2015)/Viebahn (2015).

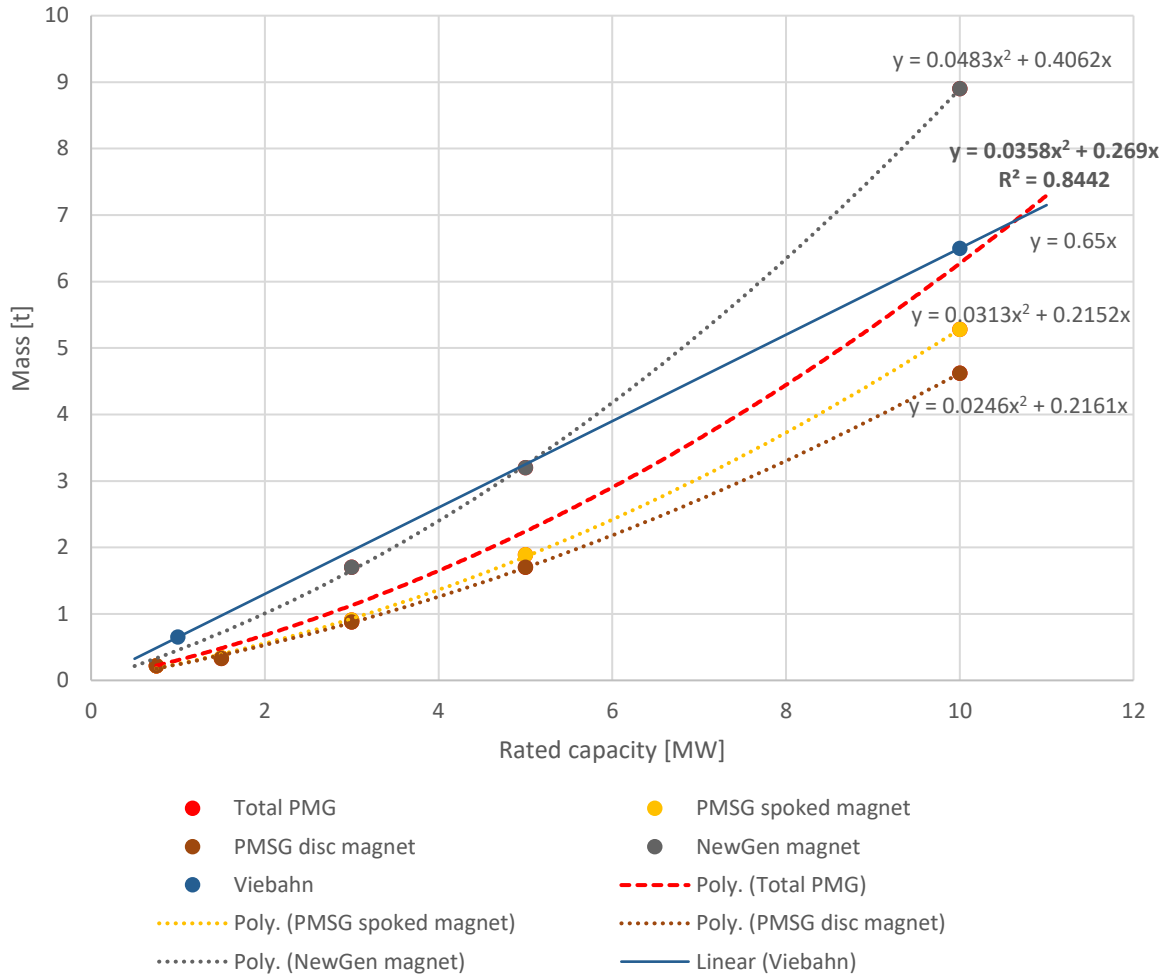


Figure B-18: Magnet content for DDPMG based on Polinder, NREL and Lacal-Arántegui (2015)/Viebahn (2015).

It can be concluded from Figure B-18 that based on generator scaling studies, a non-linear correlation is more accurate. Therefore $m_{DDPMG,magnet} = 0.0358P^2 + 0.269P$ is used. It seems the estimate of 0.85 t/MW is a good indication can create a 33% overestimation around 6 MW and could further deviate above 10 MW in the 15 MW range. Viebahn et al. (2015) give a 470 – 1000 t/MW range in which the magnet content based on their literature review, the established equation stays within this range, except for smaller (~2MW) generators. The equations based on Figure B-17 are therefore assumed to be a correct indication for DDPMG. For MSPMG and HSPMG the same equation is used combined with factors of 0.25 and 0.125 respectively.

The magnets are sintered neodymium-iron-boron (NdFeB) magnets, with small amounts of Dysprosium (Dy). The share of these elements in magnets is estimated to be 31% Nd and 2.3 % Dy (Viebahn et al. 2015). Also, Terbium (Tb) is used to retain magnetic properties at high temperatures and Praseodymium (Pr) can be used to replace Nd up to 25 % (Lacal-Arántegui, 2015).

B.3.6 Electrically Excited Synchronous Generator

EESGs are distinctive for Enercon wind turbines (Shammugam et al., 2017 ; Polinder et al., 2006) Figure B-19 shows the derived mass equations based on NREL scaling studies for total-, iron-, and copper mass.

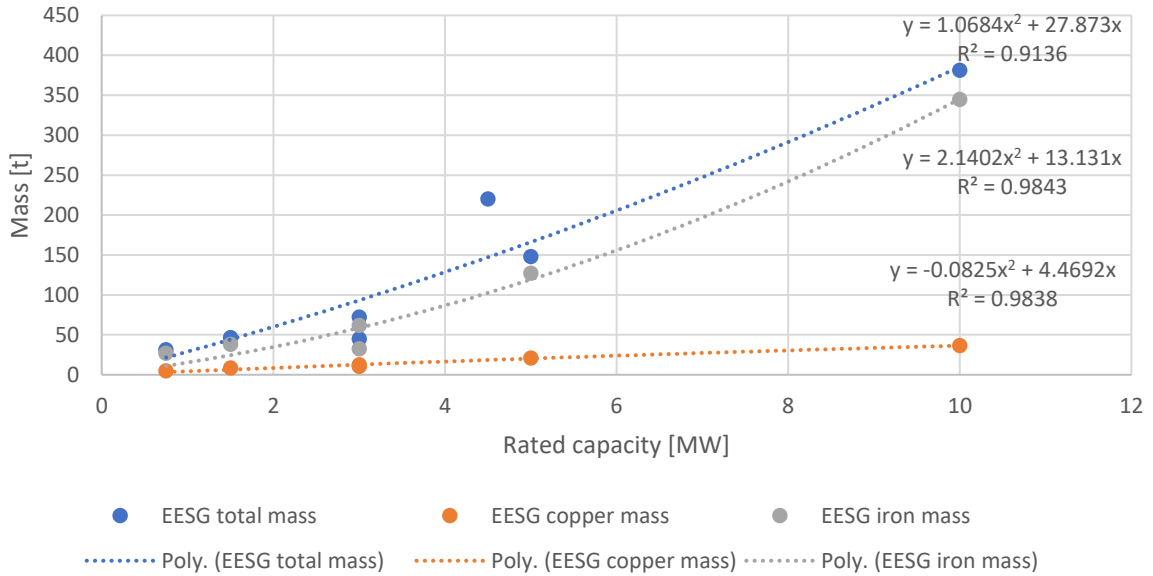


Figure B-19: EESG mass intensity based on NREL scaling studies.

Validating the established equations with a 3MW EESG concept with 32.5t iron and 12.6t copper (Polinder, 2006) shows 58.65t iron and 12.67t copper. Although iron is, like DDPMG, a factor 1.8 overestimated, copper estimates are very similar.

Material	Material by weight	Material by weight %
Iron	32.5	72.1
Copper	12.6	27.9

Geared configurations require no or partial power electronics converters, whereas direct drive configurations always require full power electronics converters. Generator design determines efficiency and quality of the generated electric power. Quality requirements for grid connection have driven the development of power electronics. Tiegna (2012) discuss various drivetrain configurations, including their power electronics converters. The mass and material composition of these converters is largely unknown. Therefore, these are not included in this analysis.

B.4 Tower

Figure B-20 shows a correlation seems to exist for rated capacity and tower mass for smaller turbines, however this correlation becomes very weak for larger turbines due to two reasons. First, distinctions between steel tubular and hybrid concrete/steel appear. Secondly, the relation between rated capacity and tower cannot be assumed to be linear as mass is dependent on various load related aspects.

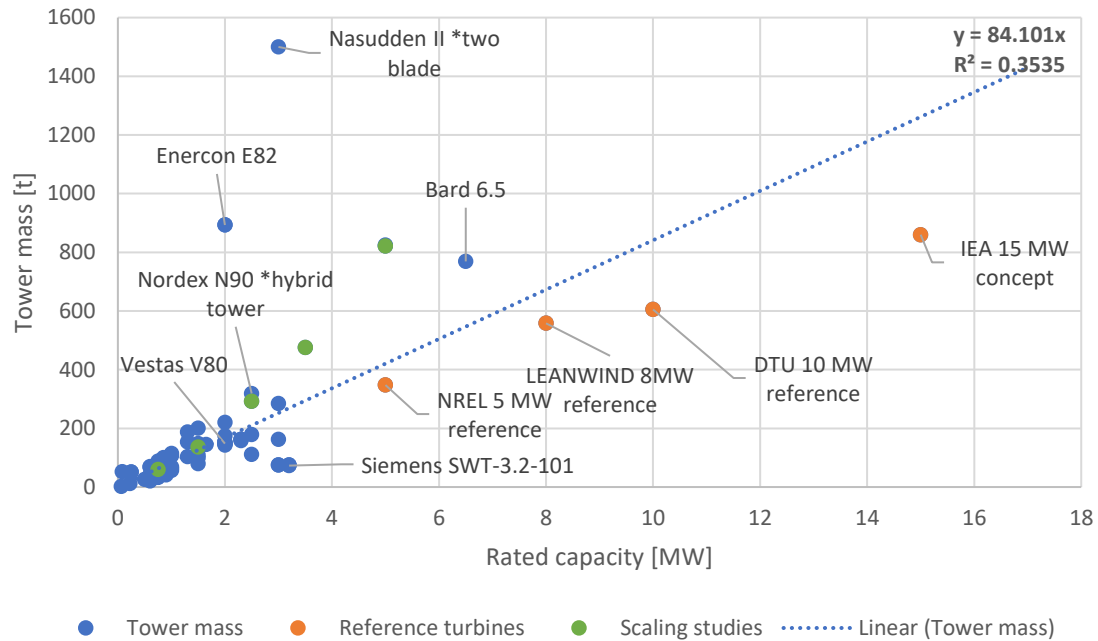


Figure B-20: Tower mass [t] and rated capacity [MW]. Data for 77 turbines from various sources including Wind-turbine-models (2020) and concept designs.

Therefore, a relation between tower height and tower mass would be more accurate. This is confirmed by improved R^2 -values for both linear as polynomial trend lines. However as indicated by red outlined areas in Figure B-21 the distinction between tower types remains an issue (concrete hybrid towers used in Nasudden II, Enercon and Bard turbines and segmented steel towers used in Siemens turbines).

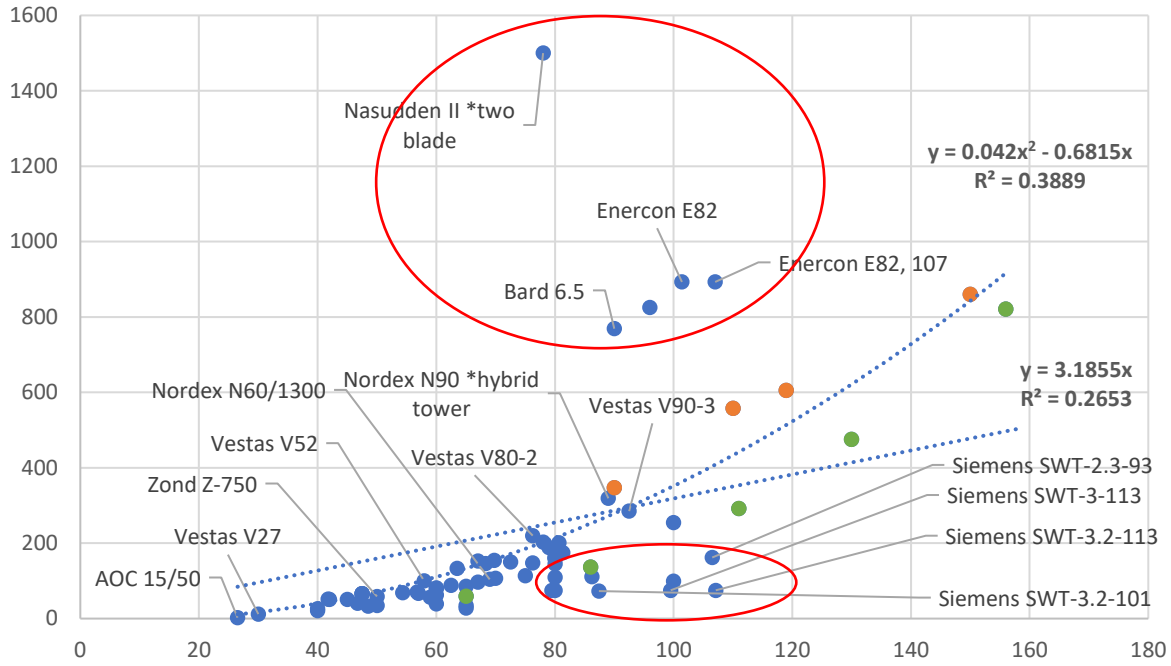


Figure B-21: Tower mass [t] and hub height [m]. Data for 77 turbines from various sources including Wind-turbine-models (2020) and concept designs.

Therefore, Figure B-22 mostly considers tubular steel towers by excluding the identified turbines that use alternative technologies. This results in improved R^2 -values for both trendlines, with the polynomial as best fit.

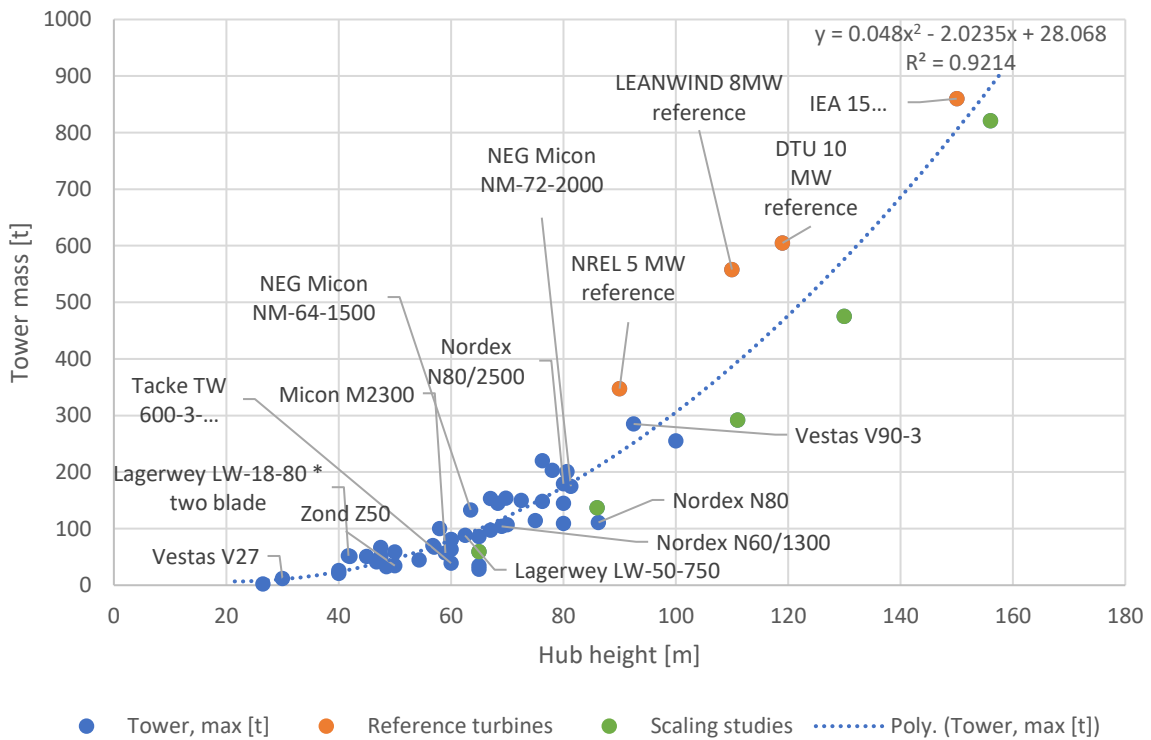


Figure B-22 Tower mass [t] and hub height [m]. Data for 61 turbines from various sources including Wind-turbine-models (2020) and concept designs.

This means for conventional, tubular steel towers, the following equation can be used to determine the mass of construction steel (S355).

$$M_{tower,steel} = 0.048h^2 - 2.0235h + 28.068$$

Given an elemental composition of S355 of 1.6% Mn, 0.05% Si, 0.23% C, 0.05% P and 0.05% S the elemental equations become $M_{tower, i} = c_i \cdot (0.048h^2 - 2.0235h + 28.068)$ for element i and percentage c_i in the base material.

Similarly, for Siemens segmented steel towers a different equation is needed. Various segmented designs (Bolted Steel Shell (BSS) towers Siemens, Large Diameter Steel (LDS) towers Vestas, Lagerwey. However, it is unlikely these towers are used commonly in the Netherlands as they are costly and their major advantage lies in easier transportation for remote and difficult terrains (Personal communication TNO) that are not common in the Netherlands.

Like segmented steel towers, concrete towers offer advantages in transportation. For a concrete tower, used by Enercon, a different equation is needed. However, tower mass data for concrete towers is limited. A 101 m tower has a mass of 2240.38 t, 124 m tower has a mass of 2500 t and a tower of 135 m has a mass of 2800 t. A linear trend ($R^2=0.84$) of $m = 20.872 \cdot h$ can be obtained.

Above a hub height of 80m, a segmented concrete design can be necessary due to transportation and construction restrictions (ASME, 2013). Enercon uses steel tubular towers and concrete towers. By analysing data from wind-turbine-models.com for Enercon turbines, indicators for the choice between steel and hybrid(concrete) towers are determined. Up to 1 MW and 89m hub height exclusively steel towers are used, above 4.5 MW and 124 m hub height, exclusively concrete hybrid towers are used. There is a large range between where no strong trend is present. As for the Netherlands advantages for segmented designs only occur above 80 m hub height, it is assumed all tower heights below 80 m will be steel tubes. This leaves a gap between 80m and 124 m. Closer inspection of the installed capacity in the Netherlands reveals that 48% of Enercon wind turbines (248 out of 517) are in this range. For the model 40% of Enercon turbines is assumed to use hybrid towers.

The uncertainties for concrete tower mass and market share create a very high uncertainty for material flows in concrete and hybrid towers. In addition to this, material compositions can differ substantially as concrete rings are combined with tubular steel top sections in varying configurations. Zimmerman (2013) considers for Enercon E82 E2 tower a material composition of 11.5 Wt% steel and 88.5% concrete. This provides the following formulas material flows:

$$m_{hybrid\ tower} = 20.872 \cdot h$$

$$m_{hybrid\ tower, concrete} = 0.885 \cdot 20.872 \cdot h$$

$$m_{hybrid\ tower, steel} = 0.115 \cdot 20.872 \cdot h$$

B.4.1 Tower internals

Among wind turbine tower internals, lighting, electrical tower internals and infrastructure internals, such as ladders, entrance, door platform (aluminium/steel). Among these electrical tower internals are of most interest as they contain the power cables. Besides power cables, data cables, cable trays and junction boxes are present. (SteelWindTower, 2020).

To prevent diving into too much detail, only power cables are considered. Ghenai et al. (2012) give a bill of materials for a generalized 2 MW wind turbine where copper and aluminium in power

transmission are 0.254t and 0.072t respectively. The length of the cable is assumed to be the major factor in cable mass, the effect of capacity on cable mass is unknown. Assuming an 80m hub height, $3.175 \cdot 10^{-3}$ t/m copper and $9 \cdot 10^{-4}$ t/m aluminium are derived.

B.5 Foundation

Foundations account for a large share in bulk materials. Major differences can be found depending on the location of the turbine. Onshore turbine foundations are dependent on soil stability, whereas offshore turbine foundations depend on the water depth.

B.5.1 Onshore foundation

Various types of onshore foundations exist. Figure B-23 shows various designs for gravity-based foundations. Here, a reinforced concrete slab is used to stabilise the wind turbine and keep it upright. This method is mostly used when the soil can carry the load without sagging.

Bottom-fixed foundations (Figure B-24) are needed to stabilize the wind turbine in less firm soil. These bottom-fixed foundations include concrete piles that support the gravity-based foundation (a), solid pile and hollow pile.

As onshore foundations are dependent on soil-type and online databases and literature report little on their mass, accurate estimations for its mass intensity are difficult.

It can be assumed that the mass of the foundation for gravity-based structures is dependent on the turbine mass, wind power and height as they create the momentum to potential overturn the wind turbine (Busby, 2012; Veritas, 2002). Wilburn (2011) estimates that 30- 65% total turbine weight is the foundation. Therefore, the sum of the nacelle-, rotor- and tower mass should account for 35-70% of the total mass. This results in the following formula for estimating foundation mass, with W being the mass percentage for the foundation.

$$m_{foundation} = W * \frac{m_{rotor} + m_{nacelle} + m_{tower}}{1 - W}$$

$$W * \frac{23.512P + 45.054P + 0.048h^2 - 2.0235h + 28.068}{1 - W} \text{ or } W * \frac{23.512P + 45.054P + 20.872h}{1 - W}$$

Martinez et al. (2008) mention a foundation consisting of a footing and ferrule. The footing consists of 700 tonne concrete and 25 tonne iron. The ferrule consists of 15 tonne steel. 2 MW 70 m height gives a range of 111-604t, indicating an underestimation using the highest mass percentage from Wilburn (2011). Reasons might include an underestimated total turbine weight.

Validating this, using the Enercon E82 E2 (Zimmerman, 2013) and assuming a tower height of 60m, yields a range of 595 – 3242t with 1142 being the correct number. This would indicate for

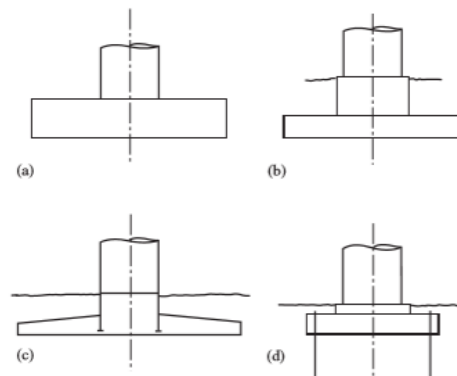


Figure B-23: Gravity based foundations. Image Adapted from Burton et al (2011)

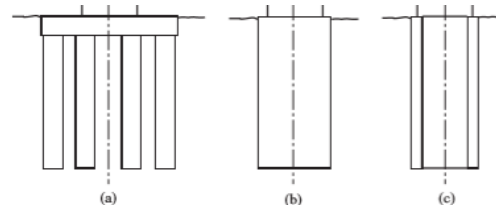


Figure B-24 Bottom fixed foundations. Adapted from Burton et al (2011)

concrete towers a mass percentage of 45 would be more accurate. With a heavier tower and therefore a lower centre of gravity, a lighter foundation makes sense. A distinction between mass percentage is therefore assumed for concrete and steel tower foundations of 45% and 70%. Although using this one instance for validation might result in an overestimation of foundation mass, it suffices as an approximation. Using 61% foundation mass yields:

$$2.33 * (68.566 P + 0.048h^2 - 2.0235h + 28.068) \text{ or } 0.818 * (68.566P + 20.872 h)$$

(possible to extend validation with Yang et al. (2020) and Vestas (2006) estimate of 475 m3 reinforced concrete.)

B.5.2 Offshore support structures

Multiple offshore foundation types exist, e.g. monopiles, jackets, gravity based and floating foundations. For the Dutch offshore wind turbines, currently only monopiles are being used. Given the relative shallowness of the Dutch North Sea (Figure B-25) monopiles are and will be preferred as they have advantages over other foundation types up to 30 m depth (Igwemezie et al., 2019). Designated wind parks do not include very shallow areas, which excludes gravity-based foundations and given the limited depth there is no need for floating foundations. The only alternative to monopiles that could be used in the future would be jackets, but currently no reason exists to assume this. As there is no strong correlation between turbine capacity and foundation weight, it is assumed the depth of the seafloor is a large factor in foundation weight.

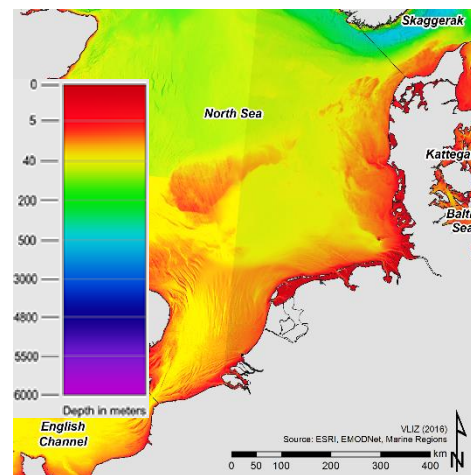


Figure B-25: Bathymetric chart North Sea.

Therefore, this value becomes location dependent. As exact locations for future turbines are unknown, it is assumed the average value of current monopile foundations is a good proxy.

With data obtained from monopile manufacturers SIF and EEW and installation companies Jumbo and Boskalis, estimations for Dutch monopile mass are made. While the range of monopile mass extends from 800 t to 2000 t and for transition pieces from 300 t to 500 t (Jumbo, personal communication, April 8, 2020), data suggests that Dutch monopiles are in the lower end of this range (Mat_comp_data.xlsx, sheet: Monopile). Therefore, a monopile mass of 850 t per turbine and transition piece mass of 300 t per turbine is assumed. Both are assumed to be S355 structural steel, although the transition piece might contain small amounts of other materials.

Sources specific to this appendix

- Adaramola, M. (Ed.). (2014). *Wind turbine technology: Principles and design*. CRC Press.
- Albers, H., Greiner, S., Seifert, H., & Kühne, U. (2009). Recycling of Wind Turbine Rotor Blades—Fact or Fiction?(Recycling von Rotorblättern aus Windenergieanlagen—Fakt oder Fiktion?). *DEWI Mag*, 34, 32-41.
- ASME (2013). Concrete key to taller wind turbines. Accessed July 14th 2020 at: <https://www.asme.org/topics-resources/content/concrete-key-taller-wind-turbines>
- Bak, C., Zahle, F., Bitsche, R., Kim, T., Yde, A., Henriksen, L. C., ... & Natarajan, A. (2013). The DTU 10-MW reference wind turbine. In *Danish Wind Power Research 2013*.
- Bang, D., Polinder, H., Shrestha, G., & Ferreira, J. A. (2009). Possible solutions to overcome drawbacks of direct-drive generator for large wind turbines. EWEC 2009: Europe's Premier Wind Energy Event, Marseille, France, 16-19 March 2009.
- Bonfiglioli. (2020). *Product range wind*. Accessed on July 14th 2020 at: https://www.bonfiglioli.com/Product-Range-Wind_ENG_R04_0.pdf
- Bonifiglioli. (2020). *Product range slew drives*. Accessed on July 14th 2020 at: https://www.bonfiglioli.com/Product-Range-Wind_ENG_R04_0.pdf
- Burton, T., Jenkins, N., Sharpe, D., & Bossanyi, E. (2011). *Wind energy handbook*. John Wiley & Sons.
- CompositesWorld. (2020) <https://www.compositesworld.com/articles/the-making-of-glass-fiber>
- Dellner. (2020a) *Datasheet dellner brakes*. Accessed on July 14th 2020 at: https://www.dellner-brakes.com/wp-content/uploads/2018/10/datasheet_dellnerbrakesjhs_jhs-16.pdf
- Dellner. (2020b) *Datasheet dellner brakes* https://www.dellner-brakes.com/wp-content/uploads/2018/10/datasheet_dellnerbrakesjhs_jhs-16-ls-2018.pdf
- Elsam Engineering A/S. (2004). *Life cycle assessment of offshore and onshore sited wind farms*.
- Ghenai, C. (2012). Life cycle analysis of wind turbine. *InTech: Melbourne, FL, USA*.
- Grande, J.A. Wind Power Blades Energize Composites Manufacturing. *Plast. Technol.* 2008, 54, 68–75.
- Griffin, D. A. (2001). Windpact turbine design scaling studies technical area 1-composite blades for 80-to 120-meter rotor (No. NREL/SR-500-29492). National Renewable Energy Lab., Golden, CO (US).
- ICPwind. (2020). https://www.icpwind.com/media/catalog/product/k/t/ktr_emb_brakes_4_1.pdf
- IFM. (2020) *Wind energy*. Accessed on July 14th 2020 at: <https://www.ifm.com/us/en/applications/060/wind-energy.html#!/content/documents/en-us/shared/applications/060/1020/1020>
- Igwemezie, V., Mehmanparast, A., & Kolios, A. (2019). Current trend in offshore wind energy sector and material requirements for fatigue resistance improvement in large wind turbine support structures—A review. *Renewable and Sustainable Energy Reviews*, 101, 181-196.
- Kühn, M., Cockerill, T. T., Harland, H., Harrison, R., Schöntag, C., van Bussel, G. J. W., & Vugts, J. H. (1998). Methods Assisting the Design of Offshore Wind Energy Conversion Systems. *Opti-OWECS Final Report volume 2, EU JOULE III Project JOR3-CT95*, 87.
- Martínez, E., Sanz, F., Pellegrini, S., Jiménez, E., & Blanco, J. (2009). Life cycle assessment of a multi-megawatt wind turbine. *Renewable energy*, 34(3), 667-673.

Polinder, H. (2011, July). Overview of and trends in wind turbine generator systems. In 2011 IEEE Power and Energy Society General Meeting (pp. 1-8). IEEE.

Polinder, H., Dubois, M. R., & Sloomweg, J. G. (2003). Generator systems for wind turbines. *Proceedings PCIM'03*, 6.

Resor, B. R. (2013). Definition of a 5MW/61.5 m wind turbine blade reference model. *Albuquerque, New Mexico, USA, Sandia National Laboratories, SAND2013-2569, 2013*.

Sethuraman, L., & Dykes, K. L. (2017). GeneratorSE: A Sizing Tool for Variable-Speed Wind Turbine Generators (No. NREL/TP-5000-66462). National Renewable Energy Lab.(NREL), Golden, CO (United States). Schubel, P. J., & Crossley, R. J. (2012). Wind turbine blade design. *Energies*, 5(9), 3425-3449.

Sif-group. (2020). Data on monopile and transition piece mass. Obtained April 2020 from: <https://sif-group.com/nl/wind/fundaties>

SteelNumber (2020). *Elemental composition alloy steel*. Accessed on July 14th 2020 at: http://www.steelnumber.com/en/steel_composition_eu.php?name_id=662

SteelWindTower. (2020). Different types of wind turbine tower internals. Accessed on July 14th 2020 at: <http://www.steelwindtower.com/different-types-of-wind-turbine-tower-internals/>

Teng, W., Zhang, X., Liu, Y., Kusiak, A., & Ma, Z. (2017). Prognosis of the remaining useful life of bearings in a wind turbine gearbox. *Energies*, 10(1), 32.

Tiegna, H., Amara, Y., Barakat, G., & Dakyo, B. (2012, November). Overview of high power wind turbine generators. In *2012 international conference on renewable energy research and applications (ICRERA)* (pp. 1-6). IEEE.

Veritas, N. (2002). Guidelines for design of wind turbines. Det Norske Veritas: Wind Energy Department, Ris, National Laboratory.

Vestas. (2005). Life cycle assessment of offshore and onshore sited wind power plants based on Vestas V90–3 MW turbines.

Wilburn, D. R. (2011). Wind energy in the United States and materials required for the land-based wind turbine industry from 2010 through 2030. US Department of the Interior, US Geological Survey.

Wind-Turbine-Models (2020) Data on various wind turbines obtained April, 2020 from: <https://en.wind-turbine-models.com/turbines>

Yang, J., Zhang, L., Chang, Y., Hao, Y., Liu, G., Yan, Q., & Zhao, Y. (2020). Understanding the material efficiency of the wind power sector in China: A spatial-temporal assessment. *Resources, Conservation and Recycling*, 155, 104668.

C. FUTURE INSTALLED CAPACITY

In this Appendix the scenarios for developments in Dutch wind energy will be created. Several sources for scenarios on wind energy capacity have been identified and compiled. The estimations in total-, offshore- and onshore capacity are shown in Table C-1.

Table C-1: Estimates for future installed capacity in the Netherlands, based on various sources listed below.

Year	Total capacity [MW]	Capacity offshore [MW]	Capacity onshore [MW]
2019	4400	1000 ³	3400 ³
2020	5457 - 5683	957 ¹	4500 ³ , 4700 ¹⁰ 4726 ² , 4750 ⁷
2023	11938	4450 ⁷ , 4750 ¹	5400 ⁷ , 5600 ¹⁰ , 7188 ²
2025	11900	5900 ³ , 10000 ¹⁰ , 12000 ⁹ , 17000 ⁹	6000 ³ , 6000 ⁹ , 6000 ⁹ , 6100 ¹⁰
2030	18500 - 19500	11300 ³ , 11424 ⁵ , 11450 ⁸ , 11552 ¹ , 11700 ⁶	7200 ⁶ , 7800 ³
2035	-	15000 ⁷	-
2050	45000 - 76800 10000-67000 24000 -31000 38000-72000	25450 ⁸ , 28200 ⁶ , 35000 ⁶ -60000 ⁴ 5000 ⁸ , 6000 ⁸ , 26000 ⁸ , 53000 ⁸ 18000 ⁹ , 23000 ⁹ 28000-52000 ¹¹	16800 ⁶ 5000 ⁸ , 5000 ⁸ , 16000 ⁸ , 14000 ⁸ 6000 ⁹ , 8000 ⁹ 10000-20000 ¹¹

1. RVO (2020a)
2. RVO (2020b)
3. Tennet (2019)
4. Klimaatakkoord (2019b)
5. Exter et al. (2019).
6. Klimaatakkoord (2018).

7. PBL & ECN (2017)
8. Alfman & Rooijers (2018)
9. Den Ouden et al. (2018)
10. CBS & TNO (2019)
11. Berenschot (2020)

For the year 2050 estimations seem to diverge significantly and require further explanation. In the following subsections, each scenario source is discussed, put into context and visualised for comparison. Linear development is assumed between data points for the plots, unless stated otherwise. Furthermore, to give additional context, historical data is added to these scenarios. By combining the available scenarios to obtain extremes, averages and valuing their intended purpose insight is gained into probable capacity developments. This section concludes with three scenarios for minimum, maximum and most likely capacity growth towards 2050.

C.1.1 Towards 2050: system choices and dependencies in the energy transition (Berenschot)

In a report from consultancy Berenschot in 2018 titled: "Towards 2050: system choices and dependencies in the energy transition"* , Den Ouden et al. (2018) determine minimal installed capacity according to various explorative studies**. For offshore wind energy, they estimate a current installed capacity of 1 GW, 12-17 GW in 2030 and 18-23 GW in 2050. For onshore wind, they estimate a current installed capacity of 3 GW, 6 GW in 2030 and 6-8 GW in 2050. As minimal installed capacity is considered, these values can serve as baselines when current government policy is considered

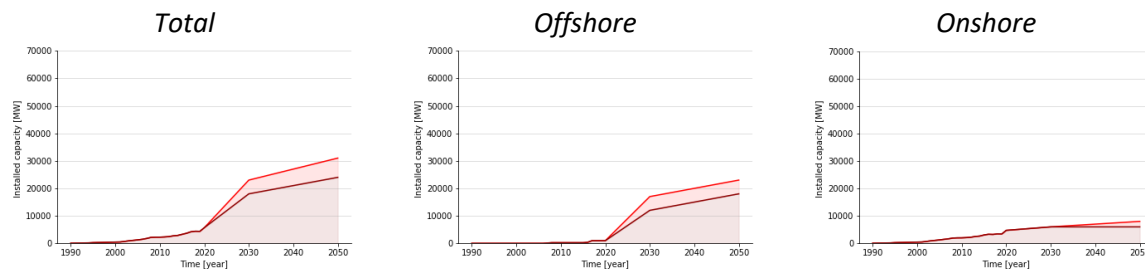


Figure C-1: Berenschot scenarios for future wind energy development.

* Translated from: "Richting 2050: systeemkeuzes en afhankelijkheden in de energietransitie"

** Studies likely include the following:

- PBL & ECN (2017). Nationale Energieverkenning 2017.
- PBL (2017). Verkenning van Klimaatdoelen.
- N&M: Natuur & Milieu (2016). Energievisie 2035
Energietransitie in de hoogste versnelling.
- Berenschot (2018). Elektronen en/of Moleculen: Twee transitiepaden voor een CO₂-neutrale toekomst
- KIVI (2017). The future Dutch full carbon -free energy system
- RLI (2015). Rijk zonder CO₂

C.1.2 Net voor de toekomst (CE Delft)

Alfman & Rooijers (2018) described four scenarios in a report from CE Delft and Netbeheer NL. These four scenarios indicate among others a growth in offshore and onshore wind energy for 2050 based on political and societal choices for governance in the energy transition. Regional governance ("Regie Regionaal") is governed by provinces and municipalities and local energy production. Regional governance sees 26 GW offshore and 16 GW onshore installed capacity for 2050. National governance ("Regie Nationaal") is governed nationally and focuses on an energy autonomous Netherlands, mainly by offshore wind. The National governance scenario sees 53 GW offshore and 14 GW onshore installed capacity. International governance ("Internationaal") shows a more global orientation with import of renewable energy. The international governance scenario sees 6 GW offshore and 5 GW onshore installed capacity. Generic guidance ("Generieke sturing") implies no government intervention, but developments based on organic development and CO₂ pricing. The Generic guidance scenario sees 5GW offshore and 5 GW onshore installed capacity. Compared to Berenschot and other scenarios, the CE scenarios seem to provide extremes. National governance seems to be most in line with other scenarios.

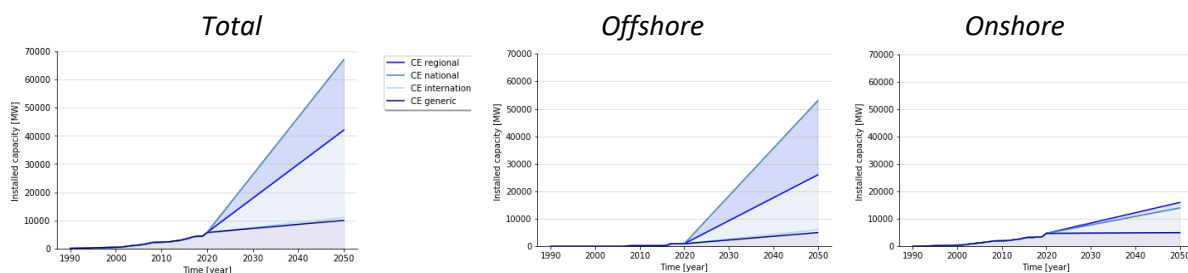


Figure C-2: CE Delft scenarios for future wind energy development under various policies.

C.1.3 Dutch climate accords

In the Dutch Climate Accords from 2018 and 2019, general goals for the Dutch climate policy are set. Both reports aggregate onshore wind and solar as potential for renewable energy production on land. Therefore, no clear estimations can be taken from this for onshore wind. In the 2018 climate accord a minimum of 35 GW and maximum of 75 GW is mentioned for offshore wind capacity in 2050. The 2019 climate agreement mentions no minimum but does mention a 60 GW maximum installed capacity in 2050. Therefore, it is assumed that this indicates a 35 – 60 GW range for offshore wind in

2050. The lower and upper goals wind can serve as guidelines for offshore wind under current government policy.

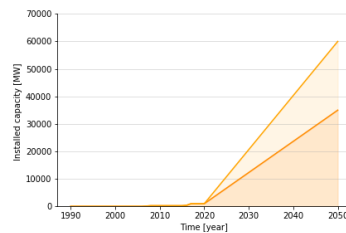


Figure C-3: Climate accord scenarios for future offshore wind energy.

C.1.4 Exter et al.

In a report by Exter et al. (2019) metal requirements for renewable electricity generation in the Netherlands are described. Wind energy is considered here to develop to 11.7 GW and 7.2 GW for offshore and onshore respectively in 2030 and 28.2 and 16800 in 2050. The values for onshore wind seem high compared to other scenarios and the offshore estimate is conservative. For the total this levels out to an average current policy scenario.

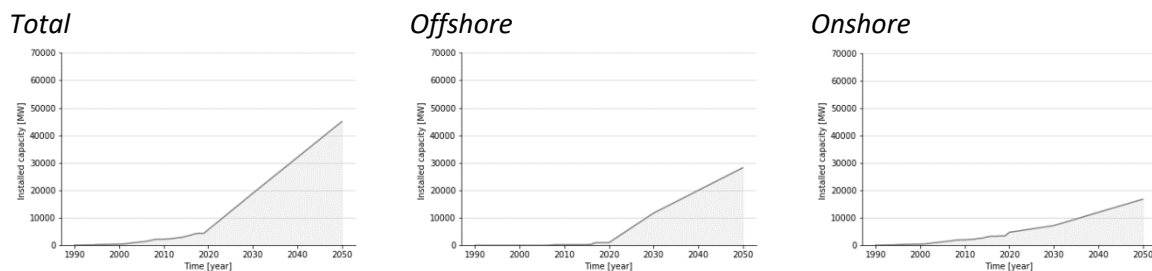


Figure C-4: Exter et al. (2019) scenario for future wind energy development.

C.1.5 National energy exploration (NEV)

PBL and ECN explored the range of possibilities of wind energy development in a 2017 report on National Energy Exploration (“Nationale Energie Verkenningen”). Predictions for 2023 in offshore wind are 4.45 GW with a minimum of 3.05 GW and a maximum of 5.45 GW. Onshore wind is predicted to be 5.4 GW with a minimum of 4.65 GW and a maximum of 6 GW. Further developments for offshore wind towards 2030 are a 1 GW installed capacity annual and after 2030 a 0.7 GW installed capacity annually. This means in 2035 a 15 GW installed capacity can be expected offshore. In the report it is stated that onshore wind is developing slower than expected and could remain difficult due to public issues. Therefore, it is expected to develop towards 6 GW. The NEV scenarios have a small range and give average expectations for total and offshore development. Onshore expectations are low and seem to level off.

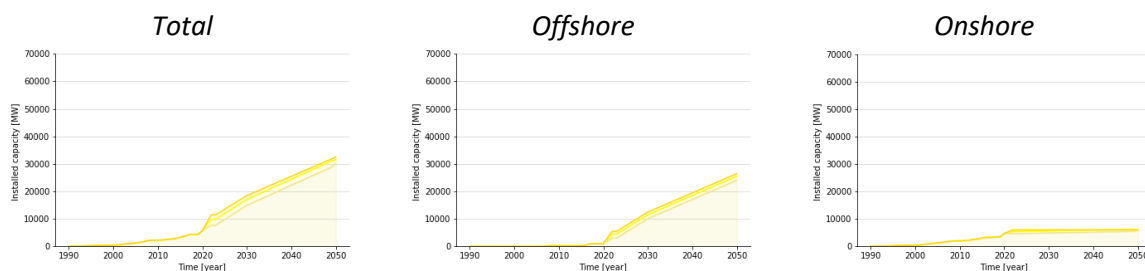


Figure C-5: National energy exploration (NEV) scenarios (low-mid-high) for future wind energy development.

C.1.6 Government publications (RVO)

On the RVO offshore wind (wind op zee) and onshore wind (wind op land) webpages and documents, data can be found for current installed, in preparation and planned installation. For the offshore sector in 2023 this leads to very accurate prediction as currently these wind parks are under development. Current installed capacities are 0.96 GW offshore and 4.73 onshore. An offshore installed capacity of 4.75 GW is expected for 2023 and 11.55 GW in 2030. Onshore, a 7.19 GW installed capacity is expected for 2023.

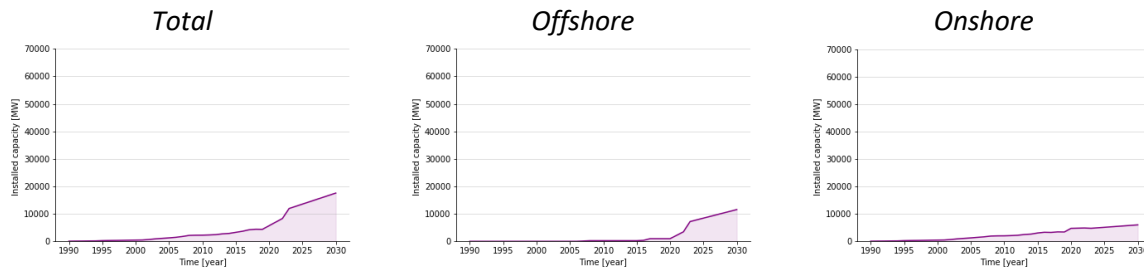


Figure C-6: RVO (government) publications on planned (and approved) installed capacity until 2030.

C.1.7 Monitor supply reliability (TenneT)

TenneT (a Dutch grid provider) published predictions for wind energy towards 2030 in a report on supply reliability (monitor leveringszekerheid 2018-2034). In this report a 5.9 GW and 6 GW installed capacity are predicted for offshore and onshore in 2025 respectively. In 2030, an 11.3 GW and 7.8 GW Installed capacity are estimated.

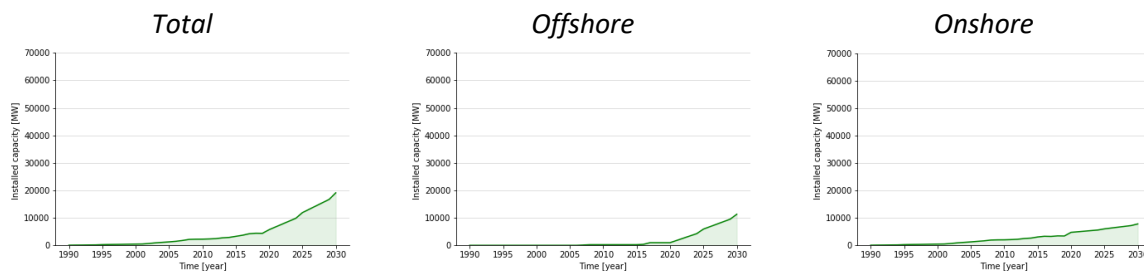


Figure C-7: TenneT scenario for wind energy development towards 2030.

C.1.8 Climate and energy exploration (KEV)

In a 2019 report from government institutions, statistics bureau (CBS) and TNO on Climate and energy exploration (klimaat en energieverkenning) likely developments for onshore and offshore wind energy are described according to government plans. A 5.6 GW onshore installed capacity is expected for 2023 and 6.1 GW in 2030. Offshore is described roughly using a current installed capacity of 1GW, 0.7 GW yearly installed capacity between 2020 and 2026 and 1 GW yearly installed capacity between 2027 and 2030, resulting in roughly 10 GW installed capacity in 2030.

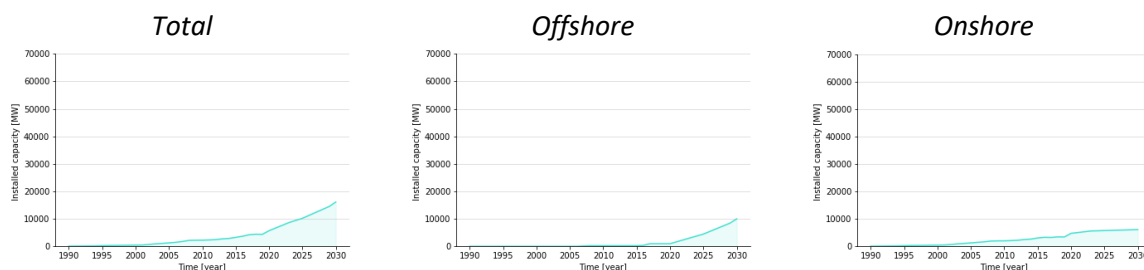


Figure C-8: Climate and energy explorations (KEV) scenarios for wind energy development.

C.1.9 Climate neutral energy scenarios (Berenschot)

In a recent report on climate neutral energy scenarios, Den Ouden et al. (2020) develop scenarios similar to previously discussed CE Delft scenarios. The scenarios (onshore + offshore) consist of regional (20 GW + 31 GW), national (20 GW + 52 GW) and international guidance (10 GW + 28 GW), as per CE Delft scenarios. However, the generic guidance scenario is left out and an EU guidance scenario (10 GW + 30 GW) is added. The International and generic guidance scenarios represent the lower estimates in the CE Delft study, whereas the more recent Berenschot study sees much larger installed capacity under international guidance than the CE Delft study.

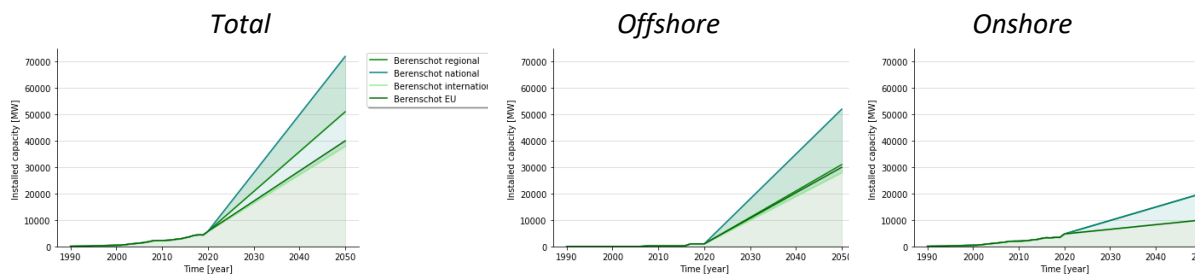


Figure C-9: Berenschot scenarios for wind energy development under different policy scenarios.

C.1.10 Scenario development

Compiling the scenarios creates a range within which the scenarios used in this study can be created. Figure C-10 shows all scenarios for total capacity development in single graph. It seems most scenarios closely resemble each other, with exception of the extremes from CE Delft and Berenschot scenarios. The reason for this is that these scenarios consider varying governance approaches whereas the other scenarios are built on government plans and in some cases one or more of the other scenarios. Most conservative estimations are represented by CE generic guidance and CE international guidance. Under similar assumptions, Berenschot international guidance shows much higher expectations. The recent developments in the offshore wind sector in levelized cost of electricity, could explain this discrepancy.

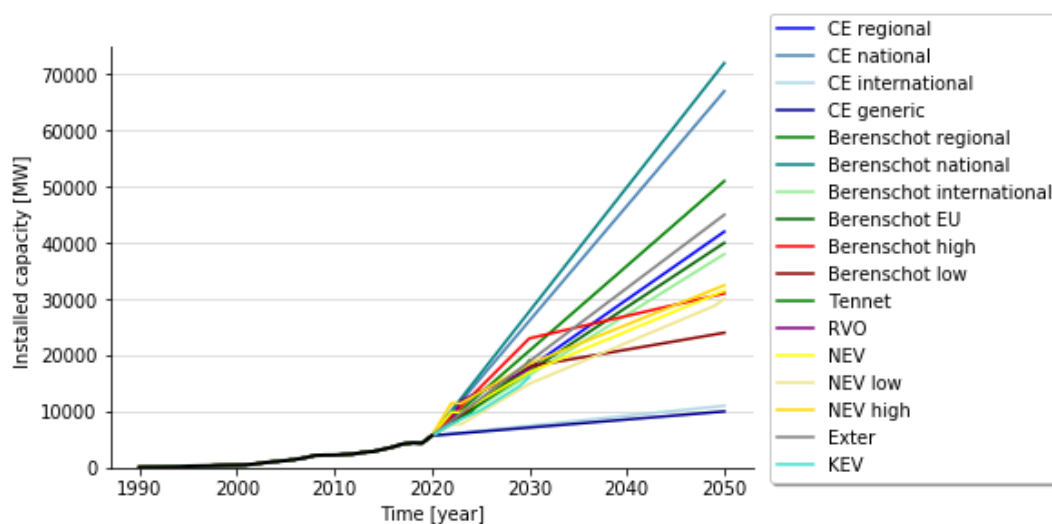


Figure C-10: All scenarios for total wind energy development.

Figure C-11 a and b show these scenarios for onshore- and offshore wind separately. Figure C-11 a shows most scenarios are 'pessimistic' on onshore wind energy development. Underlying reasons include the strong public opposition in the Netherlands and the governments reaction to this (TNO, 2020). Offshore wind capacity developments shown in Figure C-11 a include the Climate Accord

estimates, which are more optimistic than most estimations, but are considered 'goals' and there perhaps will not be reached. As most developments will occur offshore, these developments closely resemble the total capacity.

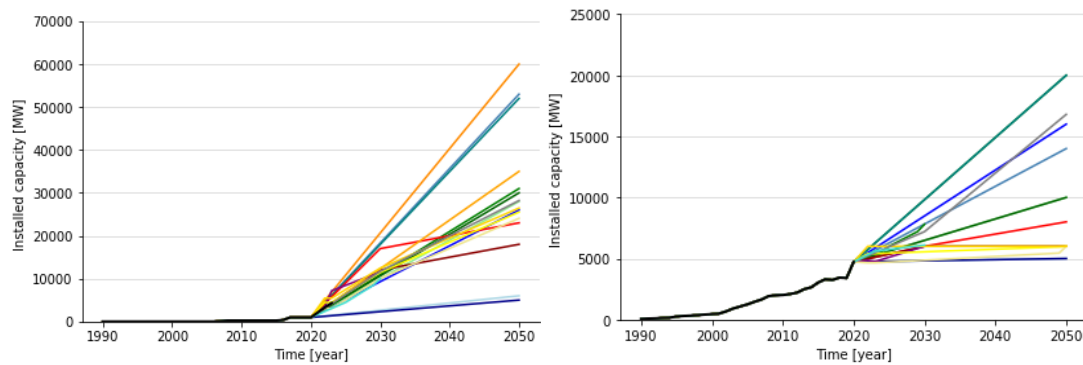


Figure C-11: Offshore and onshore scenarios for wind energy development.

From the given scenarios a minimum-, maximum- and average pathway can be identified. This leads to a range of expected development. It must then follow that there is relative certainty the minimum capacity will be reached, some certainty on the average scenario and a potential for further development towards the maximum scenario. Considering the intended goal of this study, this is useful for the final result of expected material flows. Although this range of expectations is interesting, a smaller divergence of scenarios more in line with government plans might be desirable. Therefore Figure C-12 and Figure C-13 show the minimum- and maximum development excluding the CE scenarios with dotted lines. Furthermore, it is noted the NEV scenarios closely resemble the average

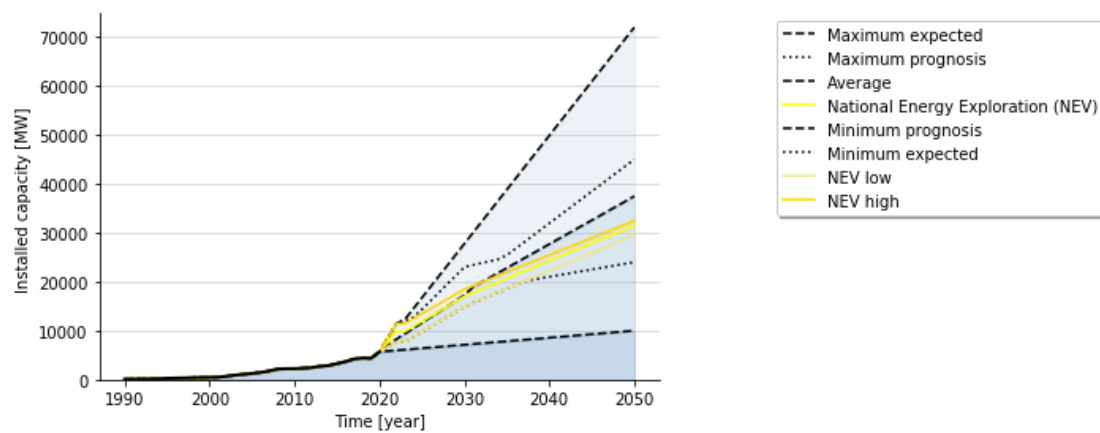


Figure C-12: Future installed capacity scenarios. Dashed lines indicate minimum and maximum expected installed capacity under different policy scenarios. Under the current policy, a range is indicated by the dotted lines. Within this range the average from the examined studies is shown as dashed-dotted line and the predictions based on the National Energy Exploration (NEV) study is shown in yellow. The NEV is used as prognosis and minimum and maximum expected as range.

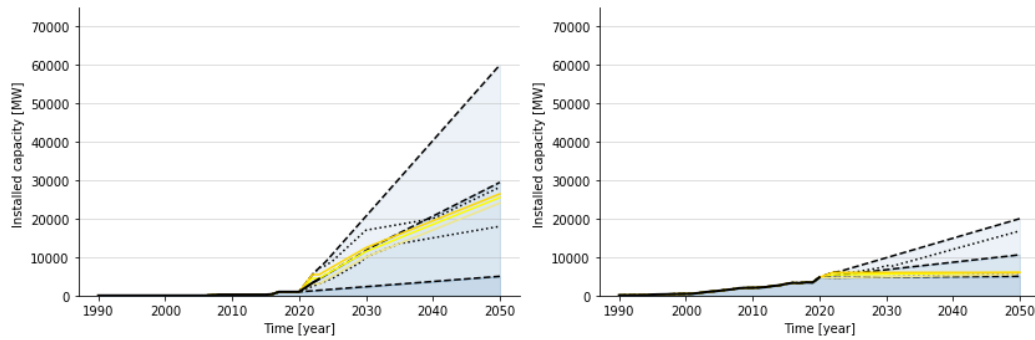


Figure C-13: Resulting scenarios for offshore and onshore wind energy development. Legend from the total scenarios can be used.

As the various scenarios show some strong differences, these outcomes are discussed with wind energy market development at TNO to get an expert opinion. It followed that onshore capacity growth faces uncertainty due to public issues. A 6 GW installed capacity would be a realistic estimation. Offshore wind has a roadmap for 11.5 GW in 2030 and after that an ambition for 50-60 GW, which is reflected by the scenarios. It must also be noted that developments after 2030 are inherently uncertain and therefore its realism remains debatable.

Sources specific to this appendix

Berenschot. (2020). *Klimaatneutrale energiescenario's*

CBS & TNO (2019) *Klimaat en energieverkenning*

Klimaatakkoord (2018). *Dutch climate accord: section 2.1. The Hague.*

Klimaatakkoord (2019b) *Dutch climate accord 2019: section C5-3. The Hague.*

PBL & ECN (2017). *Nationale Energieverkenning 2017*

Tennet. (2019). *Monitoring leveringszekerheid 2019 (2018-2034)*

D. SENSITIVITY CHECKS

Several variables have been further examined as sensitivity checks. First, generator market share scenarios and results are presented. Next concrete and steel flows are examined for normal hybrid tower/steel tower ratios and only steel towers. Default (6%) and increasing blade carbon fibre content is then analysed. Results for composite tower are shown and finally the effect of a static versus dynamic lifespan is shown.

Generator market share -

Generator market share scenarios (Figure D-1) lead to variation in permanent magnet and copper stocks and flows. The results of these various scenarios are presented in Figure D-2 .

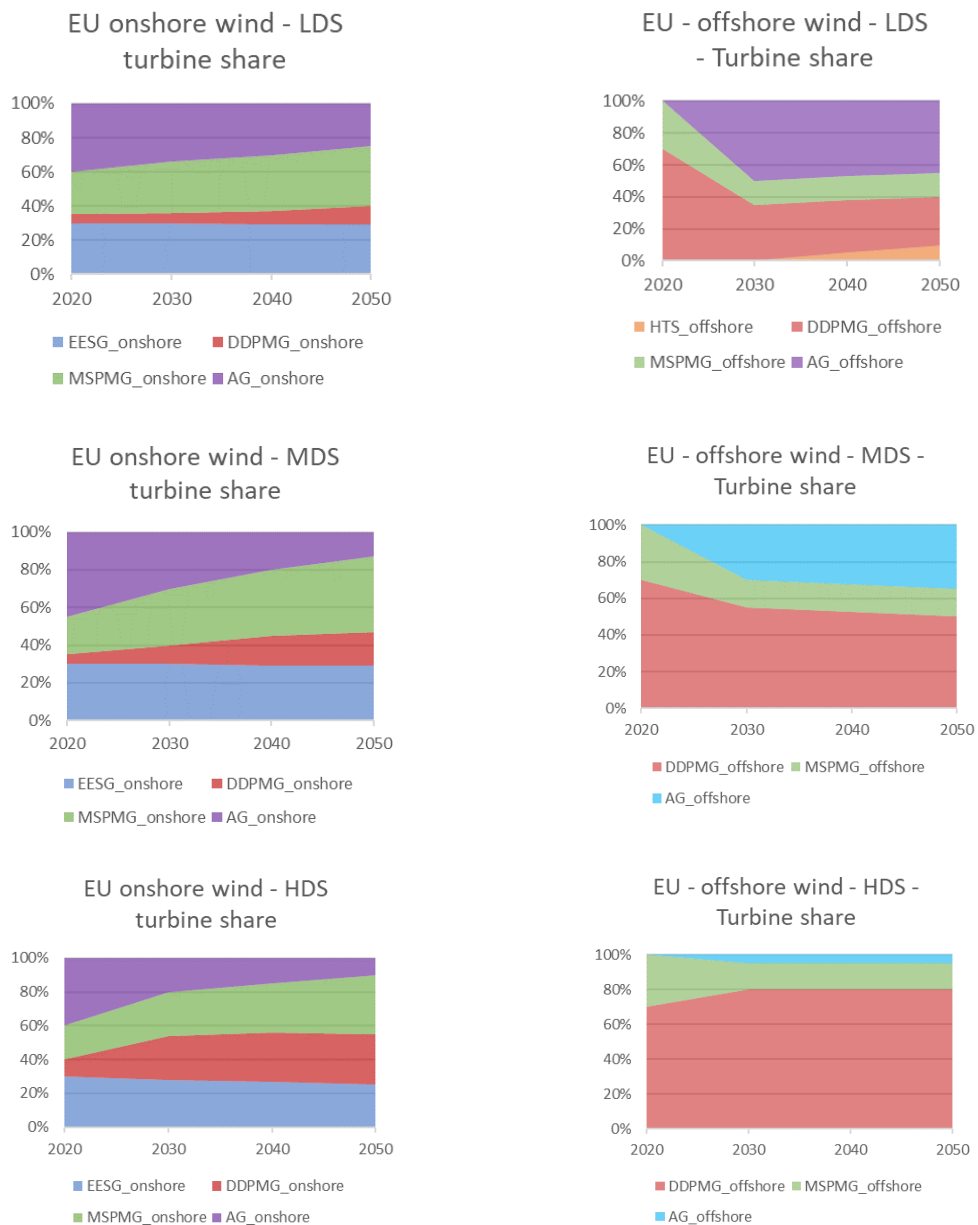
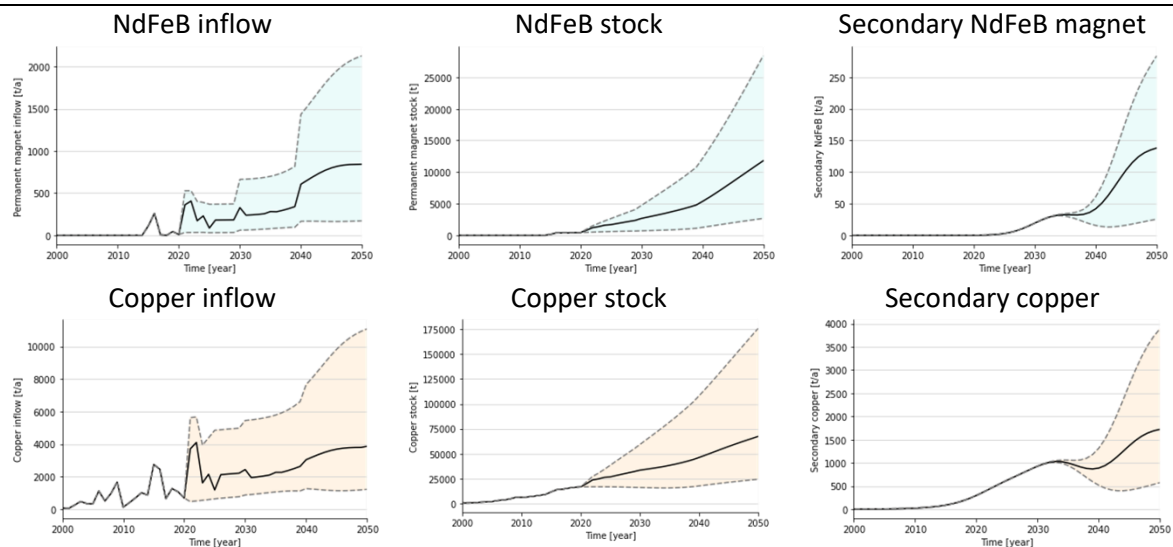
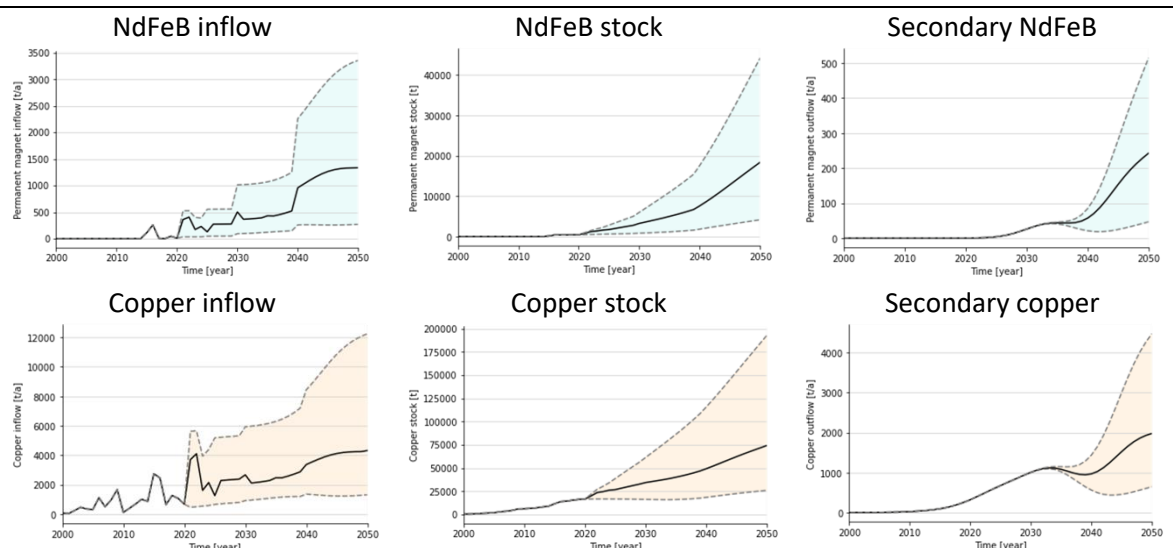


Figure D-1: Generator market share scenarios based on Carrara et al. (2020)

LDS



MDS



HDS

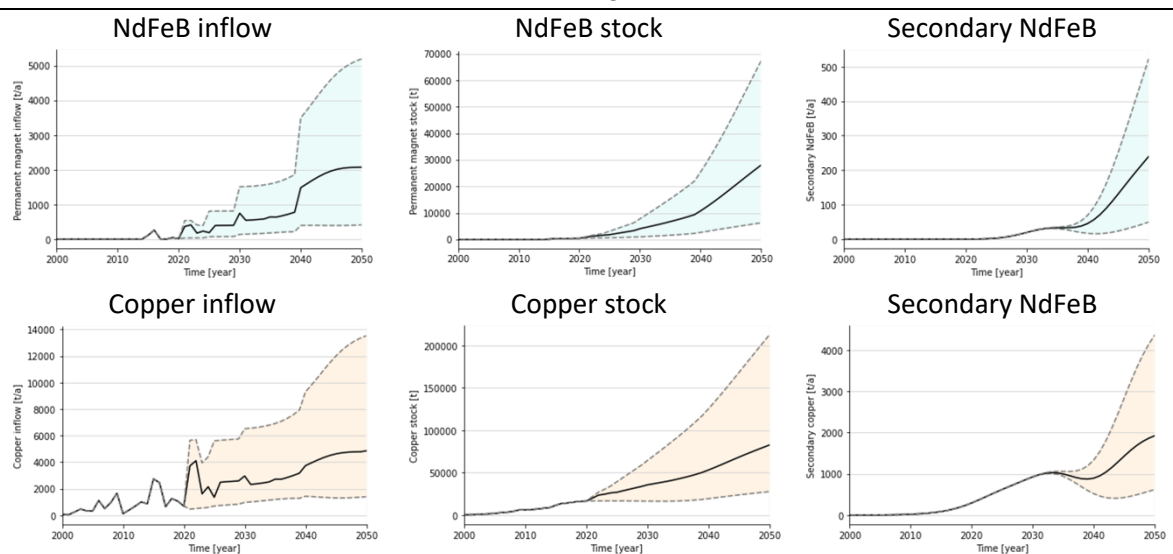


Figure D-2: Results for NdFeB and Copper based on generator market share scenarios.

Tower type

To deepen the understanding of the concrete flows, the assumption of 60% steel towers for onshore wind turbines is changed to 100% steel towers. This entails only concrete in foundations is now considered. The concrete inflows, stock, outflows and recovered materials then follow as shown in Figure D-3.

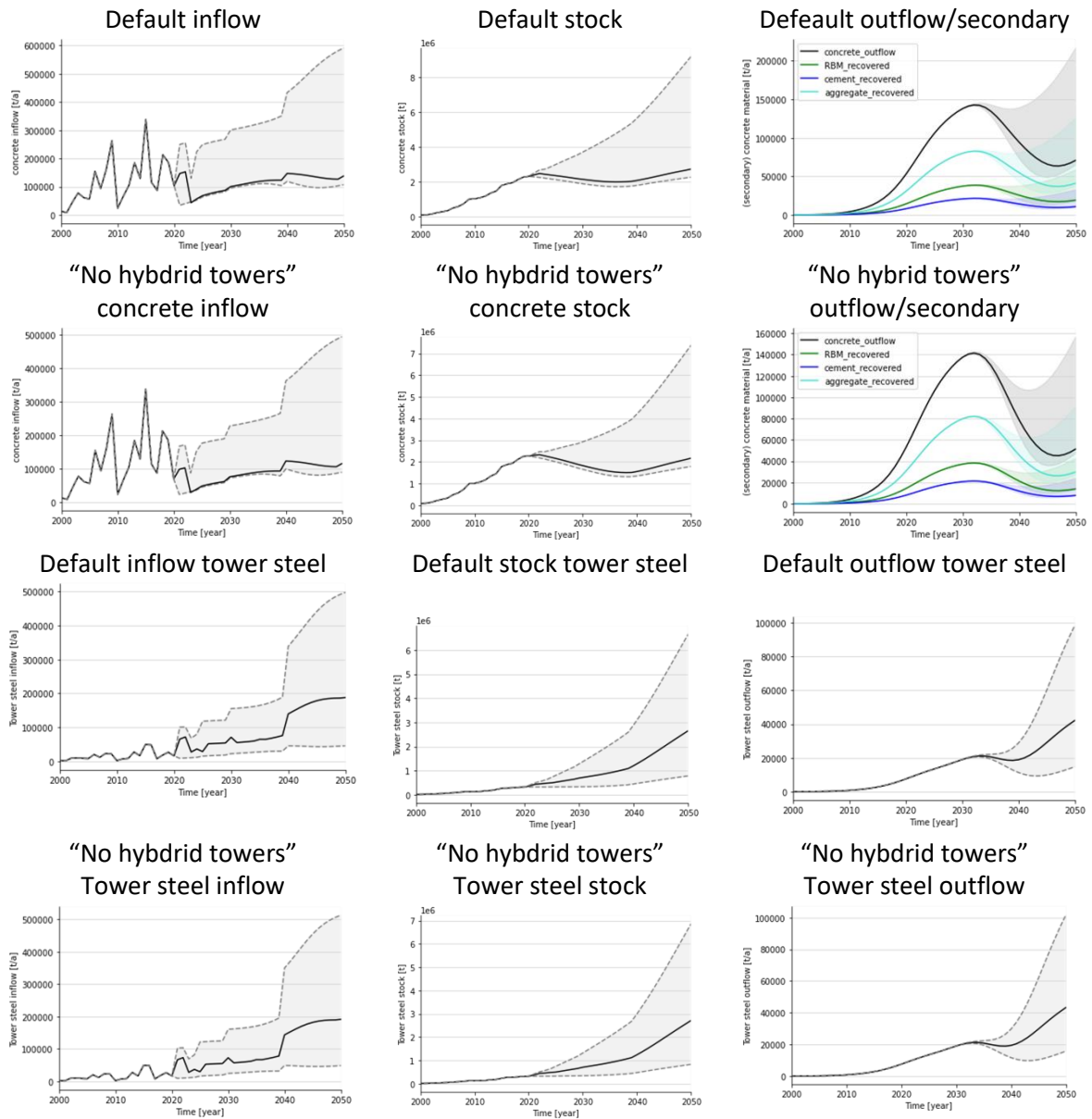


Figure D-3: Results for concrete and steel from variations in tower type.

Blade CF content

Default 6% carbon fibre content for blades after 2010 and above 2MW is compared with an increasing CF content of 6%, Up to 10 % in Figure D-4

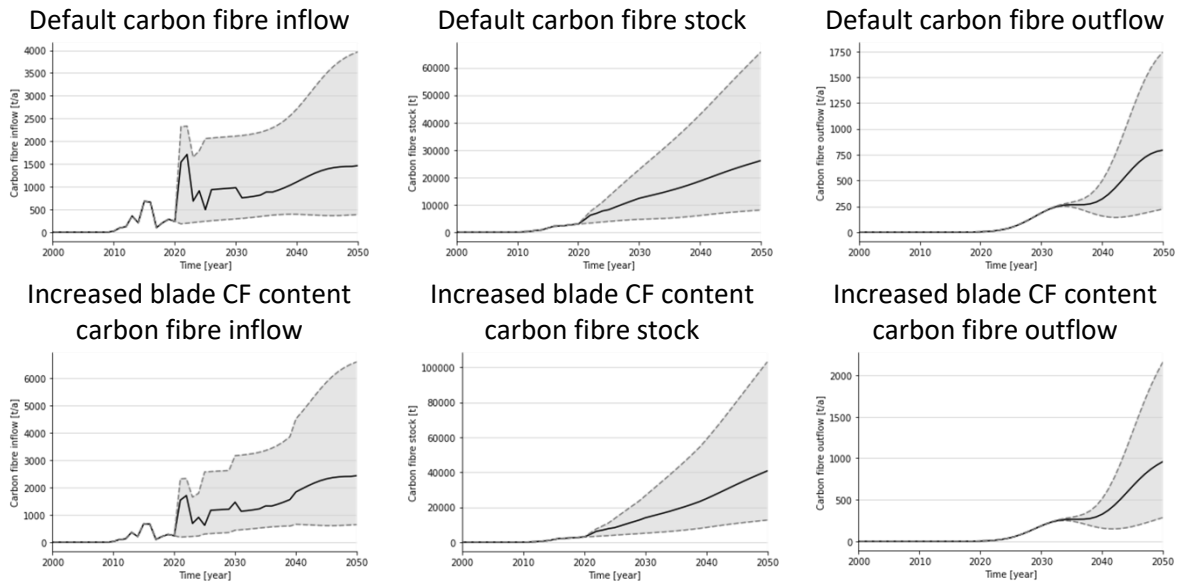


Figure D-4: Results for varying carbon fibre content in blades.

Composite towers

The effect of composite towers is analysed in Figure D-5.

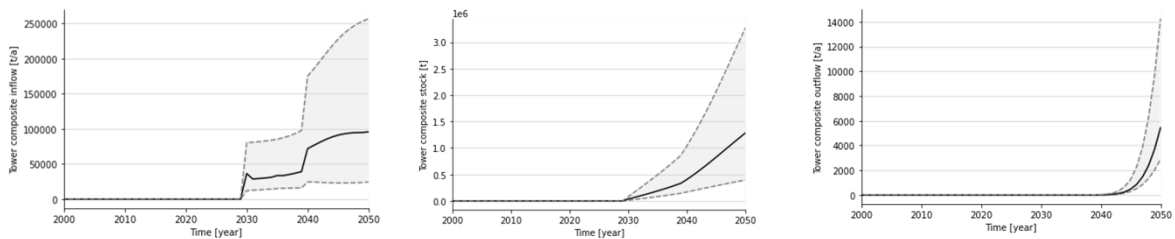


Figure D-5: Results of implementing composite towers.

Lifespan

Variations in lifespan modelling are considered. Figure D-6 and Figure D-7 show dynamic 22-24 onshore and 24-25 offshore versus static 20 onshore 22 offshore

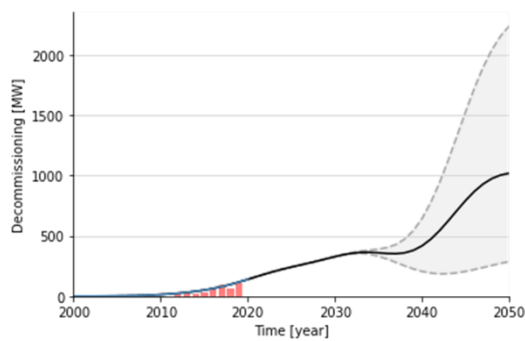


Figure D-6: Outflows variations in lifespan: default dynamic lifespan.

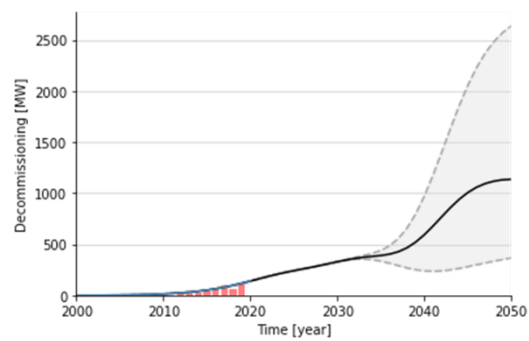
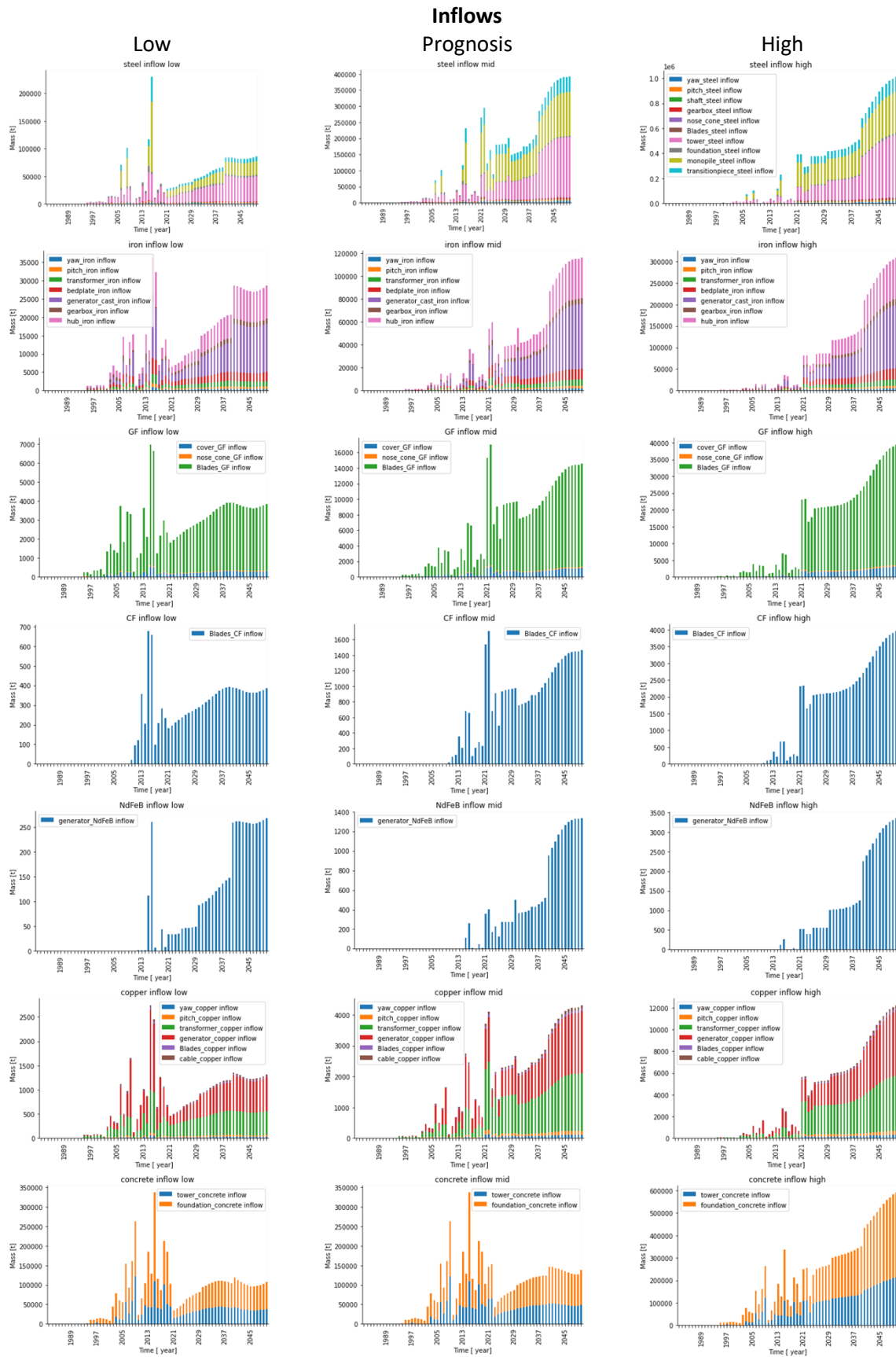


Figure D-7: Outflows variations in lifespan: static lifespan

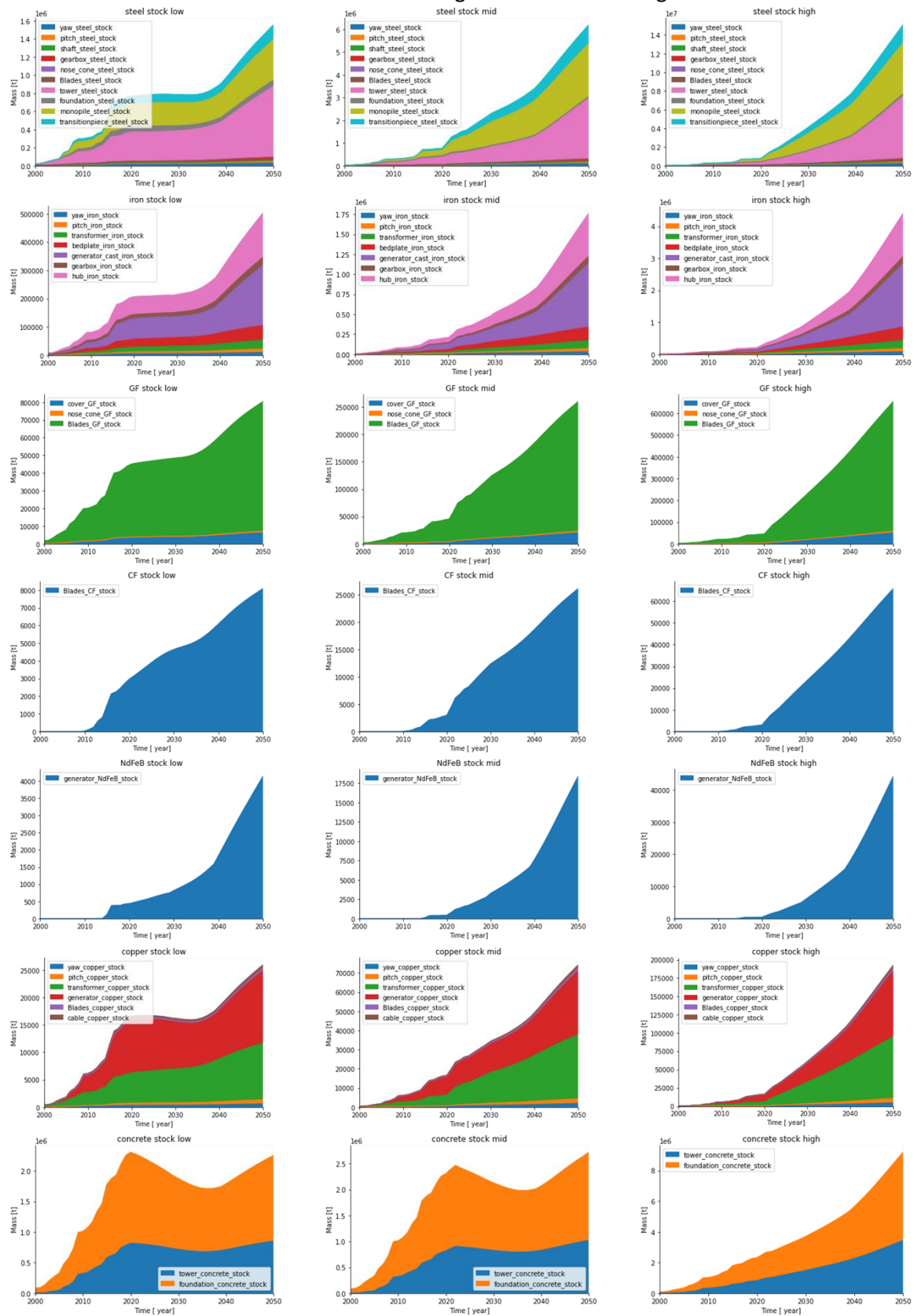
E. STACKED RESULTS



Stock Prognosis

Low

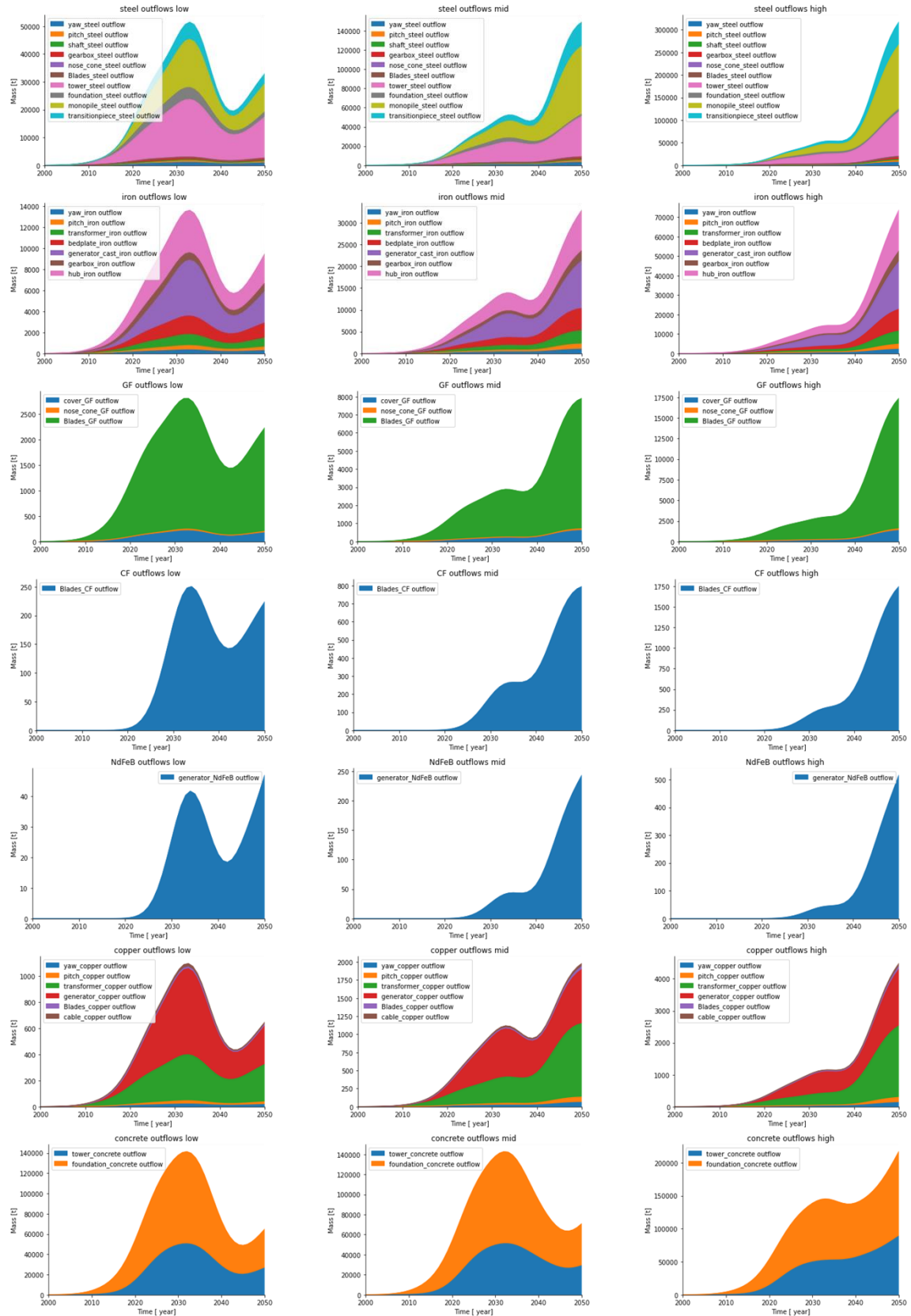
High



Outflows Prognosis

Low

High



F. ADDITIONAL RESULTS

Yttrium flows

As outlined in the inflows, yttrium is potentially interesting. Therefore, the potential stock under the LDS generator type scenario is calculated. Under this scenario, the stock of yttrium in the Netherlands is estimated to be 0.987113- 1.416833 tonne in 2050.

Although highly uncertain due to its late application and relatively low TRL level, outflows of Yttrium can be estimated at 0.00075 - 0.0098 t. This indicates most outflows (considering implementation after 2030) would occur after 2050.

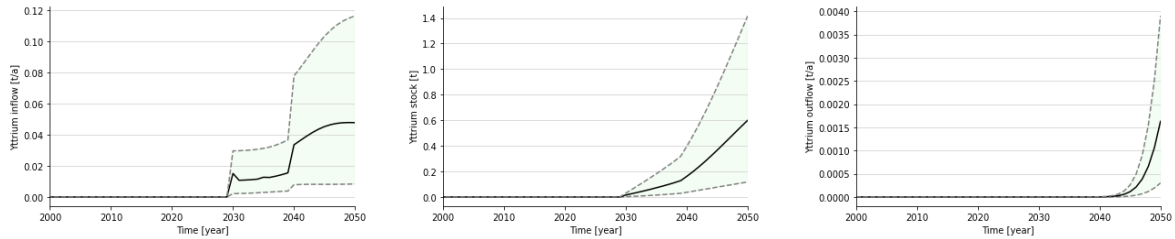


Figure F-1: Inflow, stock and outflow of Yttrium.

Individual alloying elements stock

iron

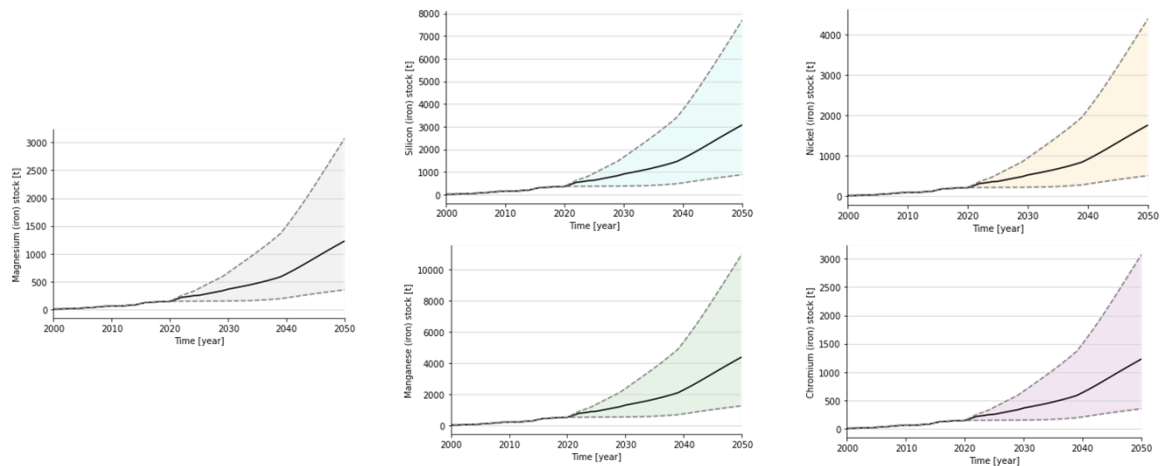


Figure F-2: Stocks of Individual alloying elements for Iron.

Alloy steel

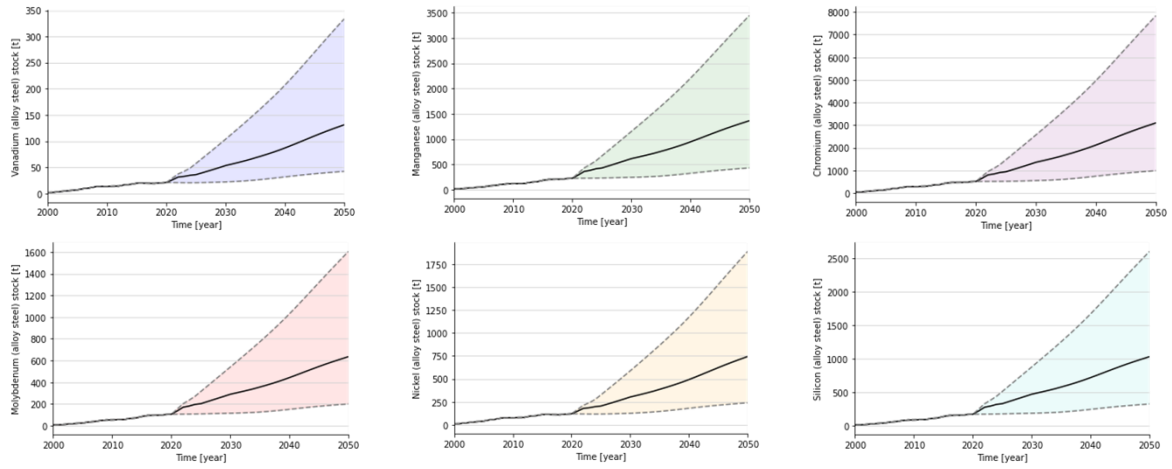


Figure F-3 Stocks of Individual alloying elements for alloy steel.

Structural steel

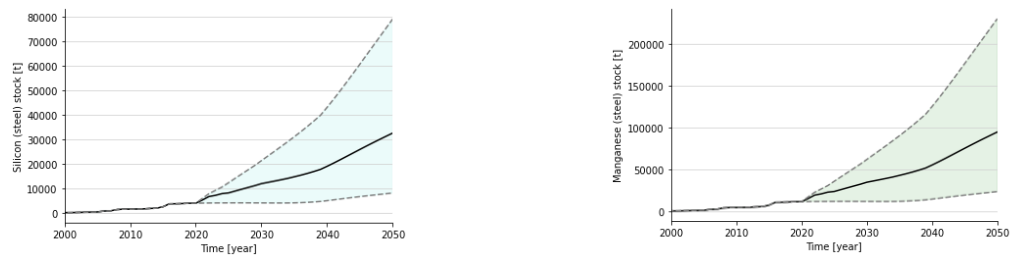


Figure F-4 Stocks of Individual alloying elements for structural steel.

Onshore and offshore peaks in outflows

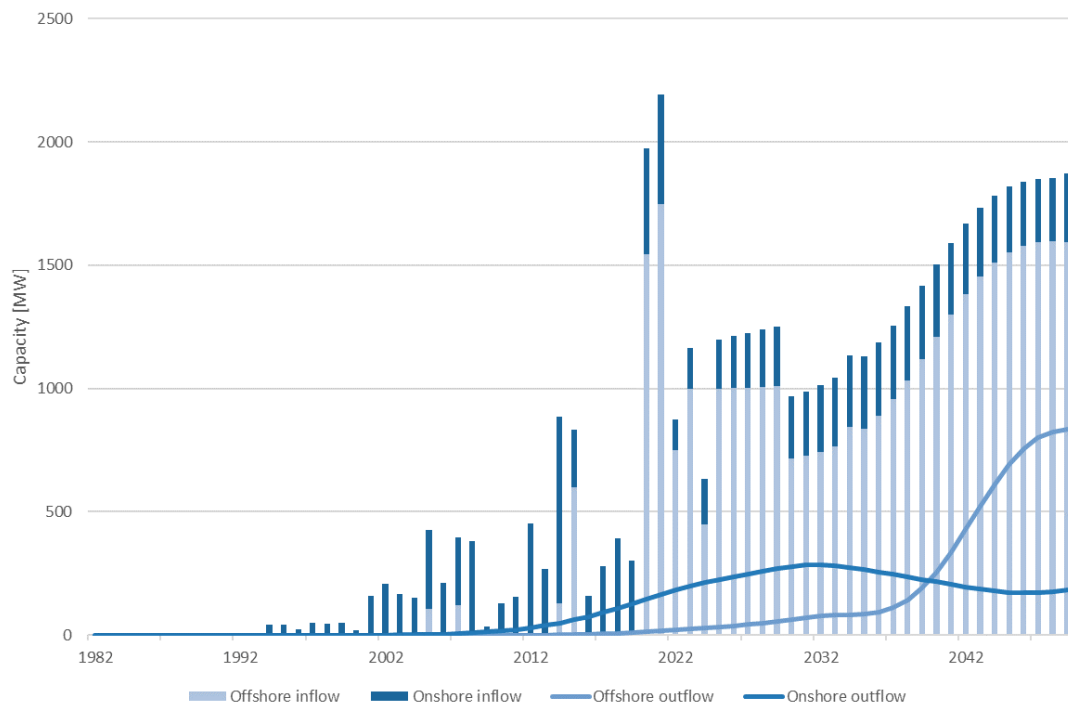


Figure F-5: Onshore and offshore peaks in outflows

Individual alloying elements outflow

Iron

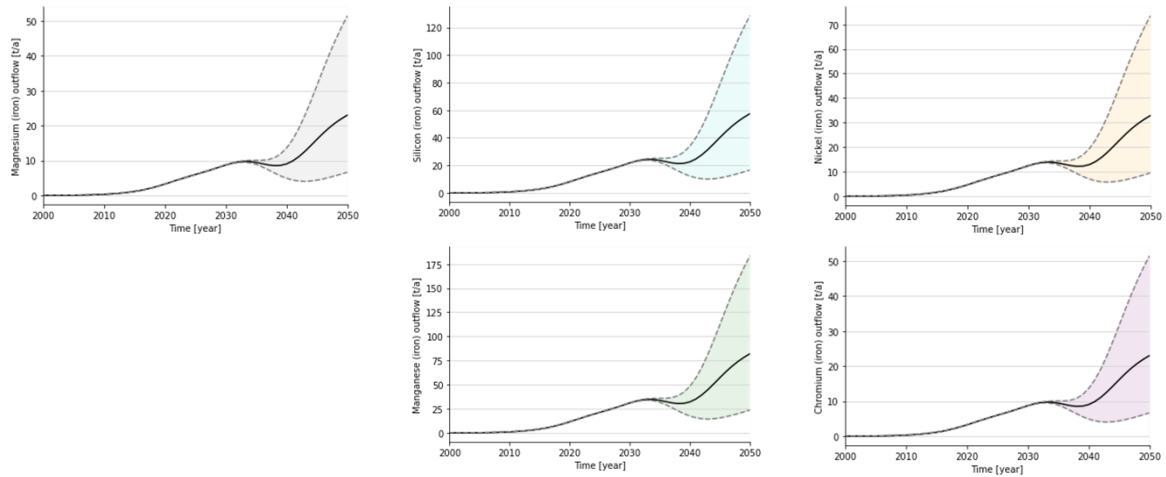


Figure F-6 Individual alloying elements outflow Iron

Alloy steel

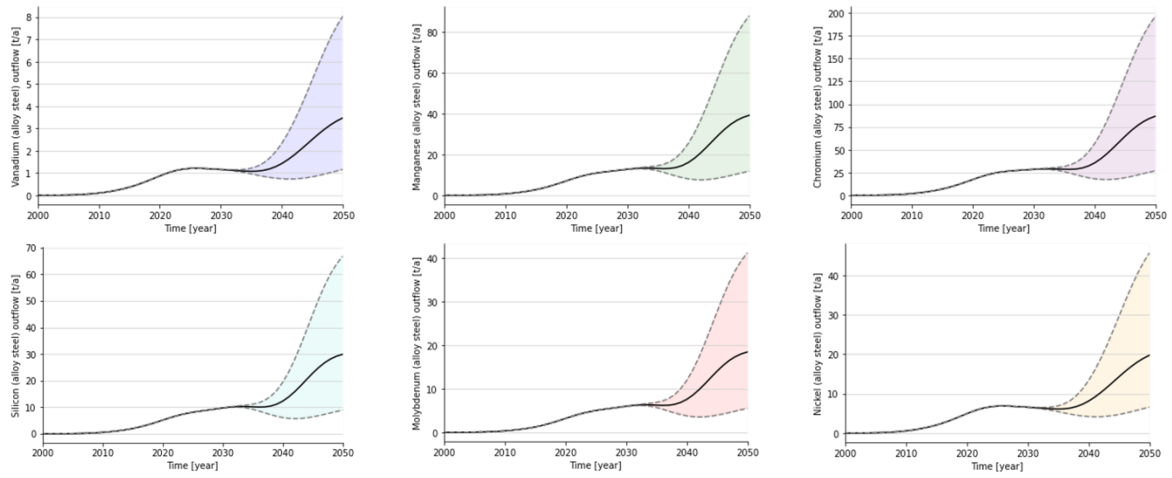


Figure F-7 Individual alloying elements outflow Alloy steel

Structural steel

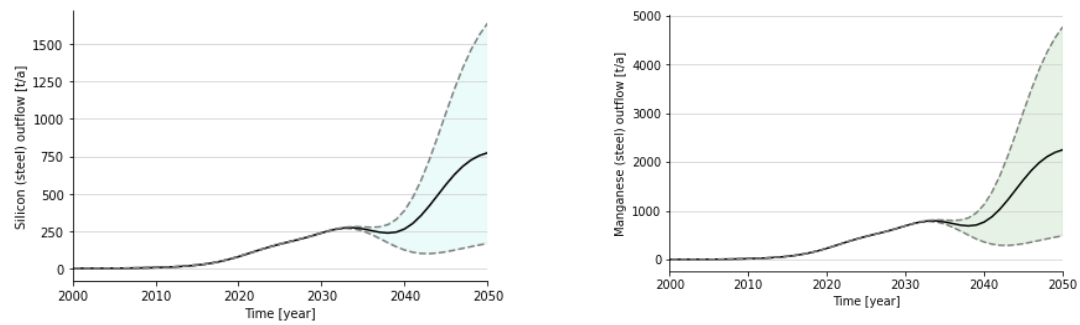


Figure F-8 Individual alloying elements outflow Structural steel

Individual alloying elements recovery

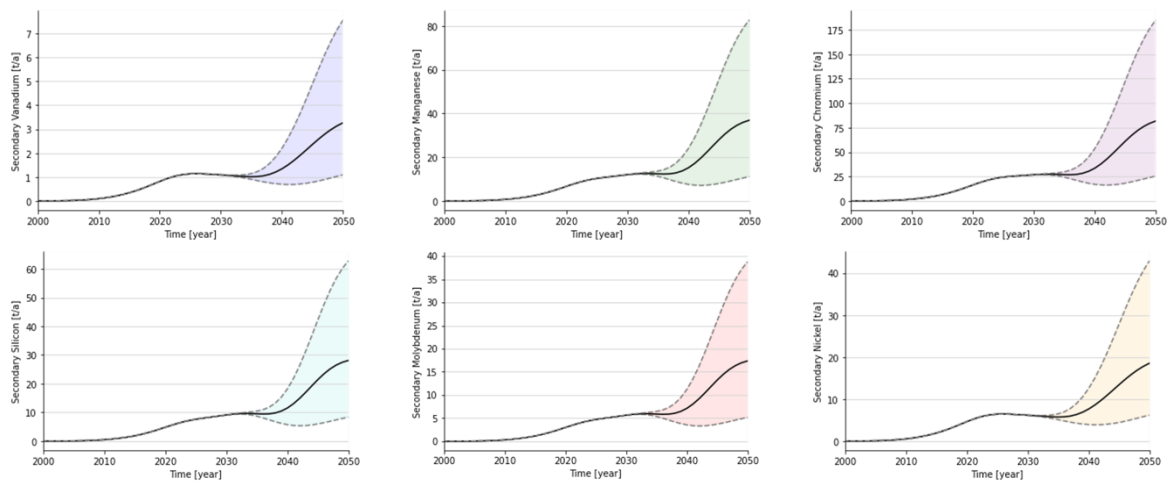


Figure F-9 Individual alloying elements recovery alloy steel

G. PYTHON MODEL

To obtain the results, the python model is used in combination with the Input file and DSM module. Google Colab is used to reduce runtime, which requires uploading the Input and DSM module.

Python model:

https://colab.research.google.com/drive/1QzFtRm8r8v5hmQeJp17lQtaXt_o1Hzbi?usp=sharing

Input data file (*Input_data.xlsx*): <https://drive.google.com/file/d/1ZJmGXaTimYQkUNT4RxJkd3-p8iQU4c1L/view?usp=sharing>

DSM module:

https://drive.google.com/file/d/1Q6lP1ph2Z_jZRp95P8rU9RUxBvHKx54j/view?usp=sharing

Or for full documentation: <https://github.com/stefanpauliuk/pyDSM>

H. BACKGROUND MATERIAL RECOVERY

This appendix supplements the material recovery section with more information on general waste management and processing.

General waste management

According to the European Waste Framework Directive (2008/98/EC) several waste management concepts can be distinguished. The framework puts these in order of preference as shown in the waste hierarchy in Figure H-1.

First, prevention of waste through longer use or reducing initial material requirement would be ideal. This is reflected in this study by increasing average life spans and trends in material composition. Lifetime extension is a common end-of-life strategy in wind energy (Skelton, 2017; WindEurope, 2020a, WindEurope, 2020b). There is no further relevance considered for this recycling background appendix.



Figure H-1: Waste management hierarchy. Image obtained from WindEurope (2020a).

Recycling entails the recovery of secondary materials from end of life components. This category is the last option for actual material recovery, but often requires many processing steps and variation in material quality. Hence, recycling is associated with economic and environmental burdens. Other waste management strategies also have environmental burdens in varying degree. The recycling route is largely determined by the component and material that is to be recycled. This section describes these recycling routes for copper, steels & iron, aluminium, composites, permanent magnets (REE) and concrete. Energy recovery from waste often implies incineration, where the energy of combustion is used to generate electricity and heat. This study only touches energy recovery in fibre recycling from composites as part of the pyrolysis process is energy recovery from matrix material. Disposal often implies landfilling (section cover image), which is the least preferred option in the waste directive framework and not always allowed³¹, yet often cheap and simple. Practical implementation of these strategies reveals the preferred hierarchy is not always true as functional recycling could potentially provide more economic value and reduce environmental impact further than some less functional repurposing strategies. Furthermore, the lines are somewhat blurred as some concepts fall in multiple categories. Examples include pyrolysis where material and energy are recovered, but also some repurposing options where processing is needed to an extent that it could be seen as recycling.

General recycling

Depending on the material and component composition different recycling routes can be optimal for value and material recovery. In general, the recovery of material from end of life products can be described by collection, processing and refining. As recycling is mostly governed by economics, scale of recycling operations and material value are important factors. This recycling section therefore exceeds the primary geographical scope of this study in some cases as recycling plants will likely

³¹ In the Netherlands landfilling is banned, therefore forcing the use of preferred waste management concepts. However, exemptions exist for materials that require alternative methods that cost more than 200 euro per tonne (WindEurope, 2020).

operate on an international level due to required volumes for profitable recycling. The availability of secondary material will therefore be on a global or regional market.

The collection rate is determined by geographical distribution, economic and technical feasibility of collection. Wind turbines are relatively concentrated (compared to consumer electronics, municipal waste, etc) and removal is required by law in the Netherlands. Which means collection should be close to 100%. However, technical and logistical limitations occur due to size and location of the turbines. Large components are often segmented on site to enable easier transport. Furthermore, offshore foundations (monopiles) remain partly on site as they are cut 1-2m below the sea floor (Topham et al., 2019). Processing and refining are generally more material specific and is discussed in the following subsections and in more detail in the material specific sections.

Processing

To enable material recovery from complex products/components, homogenized streams of materials are required. This requires liberation and separation of materials in the product. Processing can also entail only size reduction of for example already homogenous components to increase surface area or decrease component size. Liberation processes include mostly mechanical cutting, crushing and grinding. Separation (where needed) becomes more component and material specific. Depending on the composition of the material stream various steps are needed to separate a targeted material. These separation methods rely on physical properties, such as density, magnetism, conductivity, particle size/shape, colour and opacity. Specific processing steps will be discussed in the material specific sections.

As collection of outflows is now discussed, Figure H-2 shows hibernating stock. The only hibernation that is expected is from monopile collection where part is left in the sea floor. This aspect is discussed in structural steel recovery. For the individual materials secondary material potential is estimated and shown in context with its outflow. For new recycling technologies, minimum throughputs are required for a recycling plant to operate. These necessary flows for dedicated recycling facilities are indicated where relevant. For critical materials a share of material demand is estimated to see in what degree secondary material can alleviate criticality and finally for degraded materials, potential secondary markets are discussed and visualised in contrast to secondary material flows.

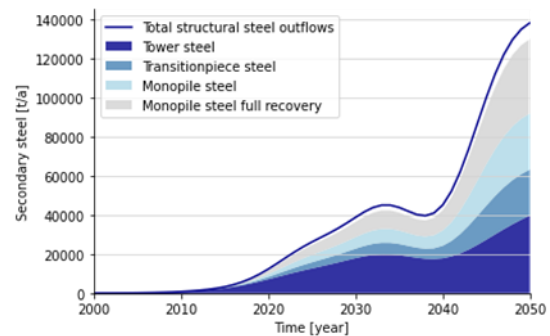


Figure H-2: Stacked structural steel outflows, potential recovery (including full monopile recovery) and estimated secondary material under the prognosis scenario.